UNIVERSITY OF CALIFORNIA, SAN DIEGO

Adenovirus proteins regulate nuclear sumoylation and hijack the chromatin remodeling complex PRC1 to mediate silencing of anti-viral genes

A dissertation submitted in partial satisfaction of the requirements for the degree Doctor of Philosophy

in

Biomedical Sciences

by

Jennifer Marie Higginbotham

Committee in charge:

Professor Clodagh O'Shea, Chair
Professor Arshad Desai, Co-Chair
Professor Tony Hunter
Professor Dong Wang
Professor Jing Yang
Professor Gene Yeo

2015

The Dissertation of Jennifer Marie Higginbotham is approved, and it is acceptable in quality and form for publication on microfilm and electronically.

_____

_____

_____

_____

_____

_____
Co-Chair

_____
Chair

University of California, San Diego

2015

DEDICATION

To my parents Joseph and Monica
To my siblings Joseph, Joshua, Claire, Elizabeth, and Caleb
To my husband Sebas
To my son Lucas

EPIGRAPH

You look at science…as some sort of demoralizing invention of man, something apart from real life, and which must be cautiously guarded and kept separate from everyday existence. But science and everyday life cannot and should not be separated.

Rosalind Franklin

TABLE OF CONTENTS

LIST OF FIGURES

LIST OF TABLES

ACKNOWLEDGEMENTS

The five chapters of my thesis are focused on two projects that truly captivated me through out these past years as a graduate student. The first relates to the role of the post-translational modification of sumoylation in adenovirus infection and encompasses Chapters 2, 3, and 4 and outlined below. The second project investigated the role of the PRC1 complex in mediating adenovirus-induced gene silencing at anti-viral promoters and is discussed in Chapter 5.

Chapter 2 is based on the Journal of Virology publication "Adenovirus E4-ORF3 targets PIAS3 and Together with E1B-55K Remodels SUMO Interactions in the Nucleus and at Virus Genome Replication Domains." Chapter 3 represents a working manuscript entitled "Adenovirus targets SUMO proteases and utilizes SUMO interactions to assemble viral genome replication domains." Chapter 4 represents a working manuscript entitled "Sumoylation and SIMs of E2A DNA binding protein." I would like to thank members of the O'Shea laboratory, Kristen Espantman, and J. Sebastian Gomez-Cavazos for their support, insights, and helpful comments. We thank Huaiyu Sun and Tony Hunter for discussions and for contributing the GFP-4xSUMO2AA construct.

Chapter 5 is based on the working manuscript entitled "Adenovirus mediates chromatin remodeling and gene silencing at antiviral promoters." I would especially like to thank Jason DeHart and Horng Ou for support and

discussion and for teaching me many of the techniques discussed in this chapter. This work was supported by R01CA137094 and P30CA014195 from the National Cancer Institute. C.C.O. is supported by The Leona M. and Harry B. Helmsley Charitable Trust grant #2012-PG-MED002, the Marshall Legacy Foundation, the William Scandling Trust and the Price Family Foundation. J.H. was supported by the T32 GM008666 Genetics Training Program.

I would not be here writing these words if it was not for the help and generosity of many people, not only through out my Ph.D., but during my whole life. First, I would like to thank my thesis advisor Clodagh O'Shea for the guidance and opportunity she provided me during my stay at The Salk Institute. Her training and mentorship will always remain with me as I go on in my scientific career. I also would like to thank current and former members of the O'Shea lab, whose advice and assistance in the lab gave me the confidence and experience to approach scientific questions comprehensively. I will never forget their support, scientific ideas, stupid jokes, extracurricular activities, and sincere friendship during my doctorate. I am indebted to my committee for their support and valuable advice over the years. I am especially grateful for Arshad Desai, for helping to guide my career and for helping me establish critical collaborations on the Mesa, and for Tony Hunter, for giving expert advice particularly in my sumoylation project.

Finally, I am lucky and filled with gratitude to be part of a loving and supportive family. I am eternally thankful for having my parents Joseph and Monica, my siblings Joseph, Joshua, Claire, Elizabeth, and Caleb, my sister-in-law Lauren, and my brother-in-law Kyle. I am especially grateful for my husband Sebastian, my son Lucas, and my dog Odie. I owe them everything for who I am as a person. I am infinitely grateful for their constant motivation, encouragement, care, enjoyment, support and love. My success is part of their success, which is easier to obtain having this family next to me.

VITA

Education

2015 Doctor of Philosophy, Biomedical Sciences, University of California, San Diego

2008 Bachelors in Biology, Xavier University

Publications

Higginbotham JM, O'Shea CC. 2015. Adenovirus E4-ORF3 targets PIAS3 and together with E1B-55K remodels SUMO interactions in the nucleus and at virus genome replication domains. J Virol 89:10260-10272

Hoskins EE, Morreale RJ, Werner SP, Higginbotham JM, Laimins LA, Lambert PF, Brown DR, Gillison ML, Nuovo GJ, Witte DP, Kim MO, Davies SM, Mehta PA, Butsch Kovacic M, Wikenheiser-Brokamp KA, Wells SI. 2012. The fanconi anemia pathway limits human papillomavirus replication. J Virol 86:8131-8138.

Hoskins EE, Morris TA, Higginbotham JM, Spardy N, Cha E, Kelly P, Williams DA, Wikenheiser-Brokamp KA, Duensing S, Wells SI. 2009. Fanconi anemia deficiency stimulates HPV-associated hyperplastic growth in organotypic epithelial raft culture. Oncogene 28:674-685.

Kiselyuk A, Lee SH, Farber-Katz S, Zhang M, Athavankar S, Cohen T, Pinkerton AB, Ye M, Bushway P, Richardson AD, Hostetler HA, Rodriguez-Lee M, Huang L, Spangler B, Smith L, Higginbotham J, Cashman J, Freeze H, Itkin-Ansari P, Dawson MI, Schroeder F, Cang Y, Mercola M, Levine F. 2012. HNF4alpha antagonists discovered by a high-throughput screen for modulators of the human insulin promoter. Chem Biol 19:806-818.

ABSTRACT OF THE DISSERTATION

Adenovirus proteins regulate nuclear sumoylation and hijack the chromatin remodeling complex PRC1 to mediate silencing of anti-viral genes

by

Jennifer Marie Higginbotham

Doctor of Philosophy in Biomedical Sciences

University of California, San Diego, 2015

Professor Clodagh O'Shea, Chair
Professor Arshad Desai, Co-Chair

Adenovirus E4-ORF3 and E1B-55K converge in subverting critical overlapping cellular pathways to facilitate virus replication. Here, we show that E1B-55K and E4-ORF3 induce sumoylation and the assembly of SUMO2/3 viral genome replication domains. Using a conjugation-deficient SUMO2 construct, we demonstrate that SUMO2/3 is recruited to E2A viral genome replication domains through noncovalent interactions. E1B-55K and E4-ORF3 have critical functions in inactivating MRN and ATM to facilitate viral genome replication. We show that

ATM kinase inhibitors rescue ΔE1B-55K/ΔE4-ORF3 viral genome replication and that the assembly of E2A domains recruits SUMO2/3 independently of E1B-55K and E4-ORF3. However, the morphology and organization of SUMO2/3-associated E2A domains is strikingly different from that in wild-type Ad5-infected cells. These data reveal that E1B-55K and E4-ORF3 specify the nuclear compartmentalization and structure of SUMO2/3-associated E2A domains, which could have important functions in viral replication. We show that E4-ORF3 specifically targets and sequesters the cellular E3 SUMO ligase PIAS3 and the SUMO proteases SENP1 and SENP2. The assembly of E4-ORF3 into a multivalent nuclear matrix is required to target PIAS3, SENP1, and SENP2. In contrast to MRN, PIAS3, SENP1, and SENP2 are targeted by E4-ORF3 proteins from disparate adenovirus subgroups. Our studies reveal that PIAS3, SENP1, and SENP2 are novel and evolutionarily conserved targets of E4-ORF3 in human adenovirus infections. Furthermore, we reveal that viral proteins not only disrupt but also usurp SUMO2/3 to transform the nucleus and assemble novel genomic domains that could facilitate pathological viral replication. We also show that adenovirus protein E2A, which is paramount for viral genome replication, is itself sumoylated and has SUMO-interacting motifs, which may play a role in adenovirus replication.

The Polycomb Repressive Complex 1 (PRC1) has been shown to be required to maintain the transcriptionally repressive state of many genes, acting via both chromatin remodeling and modification of histones. We have identified PRC1 complex members CBX2, CBX4, and Ring1b as novel cellular targets

mislocalized with E4-ORF3 into the nuclear scaffold that specifies heterochromatin silencing of p53 and antiviral target genes. These studies help to understand how transcription of cellular genes is misregulated in adenovirus infected cells and which viral proteins are responsible.

Chapter 1

Introduction

1.1 Using adenovirus to interrogate critical cellular processes.

The study of DNA virus-host protein interactions has revealed cellular proteins critical for cell growth and survival. Small DNA tumor viruses have evolved proteins that target the critical cellular pathways that regulate cell growth and survival. For example, the discovery of mouse polyoma virus in the 1950's opened the door for researchers to explore the role of DNA viruses as cancer-inducing agents which led to the discovery of numerous significant insights into the mechanisms underlying human cancer (1). The group of small DNA tumor viruses include polyomaviruses, adenoviruses, and the papillomaviruses; some herpesviruses (Epstein-Barr Virus and Kaposi's Sarcoma Herpesvirus) and the hepadnaviruses (Hepatitis B virus) are also associated with human cancers (2). For these DNA viruses to effectively reproduce, they must first initiate cellular

DNA replication, while simultaneously blocking apoptosis and dampening the body's immune response. To successfully hijack the host cell, DNA viruses encode proteins that manipulate host cell proteins and DNA in order to turn on and off the desired pathways (3). Therefore, virology is fundamentally interconnected with the study of the human host cells. The discovery of viral protein interactions with cellular proteins has and will continue to reveal critical proteins that regulate cell growth and survival.

1.2 Adenovirus genome replication.

Our studies focus on the DNA tumor virus adenovirus, a ubiquitous human pathogen (4). Adenovirus has a 36 kbp linear double strand DNA genome that encodes genes that are divided into early (E1, E2, E3, and E4) and late transcriptional units that mediate different stages of the viral replication cycle (L1, L2, L3, L4, L5)(Fig. 1.1). The late proteins comprise viral capsid and packaging proteins that encase the newly replicated viral genome, while the early proteins usurp and subvert cellular factors to commandeer the host DNA and protein machinery to for viral replication. Adenovirus binds to specific cellular receptors such as Car to enter the cell through endocytosis. Adenovirus capsid proteins actively lyse the endocytic vesicles and deliver the viral genome directly to the nucleus through the nuclear pore (5). Adenovirus serotype 5 normally infects quiescent airway epithelial cells, in which early viral proteins activate E2F transcription of cellular and viral genes to drive concomitant cellular and viral DNA replication within the nucleus (6). Adenovirus genome replication can be

reconstituted *in vitro* with precursor Terminal Protein (pTP), the E2B viral DNA polymerase and the E2A single strand DNA binding protein (7). The first rounds of adenovirus genome replication are semi-conservative (initiated from double stranded DNA genomic substrates), similar to eukaryotic genome replication. Subsequent rounds can be initiated from displaced single strand DNA that accumulates at high concentrations in specialized nuclear domains with E2A (8). Viral capsid assembly and genome packaging occurs in the host cell nucleus starting 20 to 24 hours post infection. Two to three days post infection, the cells begin to lyse and release virions.

1.3 Adenovirus subgroups.

Adenovirus type 5 (Ad5) from Subgroup C is the most widely studied adenovirus due to its seroprevalence and use in viral vectors (9); however, there are 68 distinct adenoviruses within 7 disparate subgroups (A-G) based on sequence homology (10, 11), biophysical, and biochemical criteria (12, 13). Comparing and contrasting the conserved and non-conserved functions and sequences of disparate early adenovirus proteins can reveal the precise residues required for their various separate functions.

1.4 Adenovirus early proteins.

With a minimum proteome, viral proteins have evolved to be extraordinarily efficient and often perform multiple functions. Upon forcing the host cell into replicative S phase to drive DNA replication, early adenovirus

proteins concurrently inactivate tumor suppressors to evade cell cycle arrest and apoptosis (3). Adenovirus E1A is the first gene to be transcribed and its protein products play a major role in the transcriptional regulation of viral and cellular genes (14). E1A binds to RB, blocking the RB-checkpoint and inducing E2F activity (15). E2F activity induces S-phase and DNA replication, yet also provokes a host immune response. Therefore, other early viral proteins must suppress the immune response.

To counteract the host cell's defenses, E4-ORF3 and E1B-55K target cellular pathways such as MRE1/RAD50/NBS1 (MRN) complex and p53 through distinct mechanisms. E1B-55K binds and inactivates cellular targets, most famously p53. E1B-55K binds to the p53 transactivation domain and suppresses p53 transactivation of target genes. In viral infection, E1B-55K forms a complex with another viral protein E4-ORF6 that recruits a cellular ubiquitin ligase complex. Together, the E1B-55K/E4-ORF6 ubiquitin ligase complex targets p53 for ubiquitination and degradation in the proteasome (16) (17-19). E1B-55K also binds to MRE11 and together with E4-ORF6 targets it for ubiquitination and degradation in the proteasome (19, 20). In addition, E1B-55K has also been proposed to function as an E3 SUMO ligase towards p53 (21, 22) and to interact with the E2 SUMO ligase UBC9 (23).

An adenovirus lacking E1B-55K, which inactivates p53, was theorized to be complemented for replication in cancer cells with an inactivated p53 pathway. This premise was the basis for an oncolytic adenovirus coined ONYX-015. ONYX-015 is an adenovirus that lacks the ability to express E1B-55K. Cells

infected with ONYX-015 induce high levels of p53, which was expected to limit viral replication in normal cells, but not p53 mutant tumors. On this basis, ONYX-015 was tested in patients as a p53 tumor-selective oncolytic viral therapy and is now approved in several countries (known as Oncorine). However, the loss of E1B-55K functions in viral RNA export, rather than p53 inactivation, is the major determinant of ONYX-015 tumor selectivity (24, 25). Contrary to expectations, although p53 accumulates to high levels in the nucleus of ONYX-015 infected normal cells, p53 transcriptional targets are not induced (24). The failure of p53 stabilization to activate transcriptional targets is not a tissue-specific effect and occurs in multiple primary cell types and tumor cell lines. This revealed a fundamental gap in our understanding of not only adenovirus biology, but also p53 activation as it was previously believed that high p53 levels were tantamount to its transcriptional activation.

Our lab revealed that another early adenovirus protein, E4-ORF3, shares the function of blocking transcriptional activation of p53 target genes with E1B-55K. E4-ORF3 is a 13kDa protein that assembles a multivalent scaffold in the nucleus that disrupts cellular protein interactions. E4-ORF3 weaves through the nucleus of infected cells forming irregular fibers that polymerize via reciprocal and non-reciprocal swapping of E4-ORF3 C-terminal tails (26), disrupting PML bodies (27) and mislocalizing MRN, TRIM24, and TRIM33 (28-30). Mutation of the conserved N82 residue of E4-ORF3 prevents the higher order assembly of E4-ORF3 dimer subunits, inactivates its functions in viral replication, and renders it no longer able to mislocalize its targets (26, 28, 31). Like E1B-55K, E4-ORF3

blocks transcriptional activation of p53 target genes; only when E1B-55K and E4-ORF3 are both deleted are p53 target genes turned on during viral replication (32).

1.5 Hijacking and compartmentalizing the nucleus.

Adenovirus genome replication occurs in the nucleus, a highly crowded yet structured space. Understanding the structure of the nucleus and how adenovirus modulates nuclear architecture during infection is essential for understanding how the virus is able to overwhelmingly hijack the host cell. The nucleus contains chromatin and interchromatin compartments and various nuclear bodies. Non-membrane bound nuclear bodies are a way to spatially control local concentrations of molecules involved in chromatin remodeling, transcription initiation, and RNA processing (33). These structures could also play a role in functioning as biophysical switches, responding to local signals when concentrations achieve a certain threshold (33). In short, nuclear bodies function as the ‘sub-organelles’ of the nucleus.

Viral genomes are miniscule compared to the host nucleus; they must navigate a nucleus thousands of times its own size for genome replication. This problem, while seemingly daunting for adenovirus, can be overcome by locally compartmentalizing viral parts to avoid diffusion. To ensure replicative success, early adenovirus proteins must modulate subnuclear spaces and maintain discrete subcompartments, similar to cellular nuclear bodies. Adenovirus replication induces de novo subnuclear viral genome replication domains

demarcated by the adenovirus protein E2A. The roles of the post-translational modification of sumoylation in creating these domains and the cellular SUMO enzymes that are targeted by adenovirus will be discussed in Chapters 2, 3, and 4.

A second mechanism used by viruses to ensure their replicative success is to control transcription of host genes. Our lab discovered a novel function of adenoviral protein E4-ORF3 in preventing p53 activation independent of p53 protein levels. E4-ORF3 induces de novo heterochromatin formation at p53 and anti-viral target promoters, preventing transcription factor binding and consequently, transcription of these targets. The ability of E4-ORF3 to induce repressive histone methylation and heterochromatin compaction at a known set of targets makes it an ideal instrument for elucidating the initiating signals, histone modifiers, and chromatin remodeling complexes that orchestrate heterochromatin formation and transcriptional regulation (32). These results suggest that early adenovirus proteins such as E1B-55K and E4-ORF3 regulate key cellular programs. The role of early adenovirus proteins in shutting down the host immune response through the inactivation of anti-viral genes will be discussed more in Chapter 5.

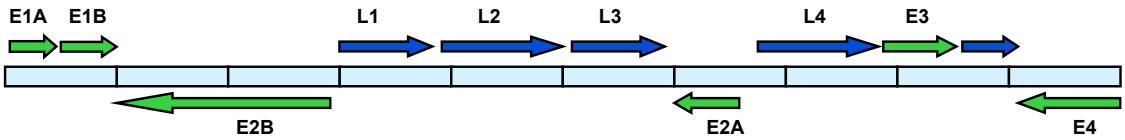

Figure 1.1 Schematic of adenovirus genome. Early transcriptional units are shown in green; late transcriptional units are shown in blue.

Chapter 2

Adenovirus E4-ORF3 targets PIAS3 and together with E1B-55K remodels SUMO interactions in the nucleus and at virus genome replication domains

2.1 Introduction.

Viruses usurp and trigger cellular signaling cascades that have dynamic and systems-wide consequences for host-pathogen interactions. Protein post-translational modifications have the power to alter the functions, structural interactions, and localization of cellular and viral proteins to determine the outcome of infection. For example, studies with polyomavirus middle T antigen and v-Src associated kinase activities led to the discovery of protein tyrosine phosphorylation (34, 35). Phosphorylation was subsequently found to be a critical signaling nexus that is deregulated in response to viral and cellular oncogenes (36). Interferon signaling cascades and the induction of ISGylation, ubiquitination, or sumoylation can also be triggered by viral infection as critical host anti-viral signaling defenses that engage innate and systemic immunity (37-41).

Sumoylation—the conjugation of a small ubiquitin-like modifier—can affect a protein's activity, intracellular localization, stability, and interaction partners. Changes in SUMO levels and conjugation can be triggered by the cell cycle (42), differentiation (43), as heat shock (44), DNA damage (45), and viral infection (39, 40). Regulation of sumoylation can occur at the level of transcription, translation, or degradation of different SUMO pathway components (46). In vertebrates, there are two SUMO subfamilies, SUMO1 and SUMO2/3. SUMO1 and SUMO2/3 share only about 50% sequence identity, while SUMO2 and SUMO3 share 97% sequence similarity and appear to be functionally indistinguishable. SUMO1 is predominantly conjugated with target proteins, while SUMO2 and SUMO3 are found in a larger pool of free, unconjugated SUMO, which is readily available for responding to external stimuli (47). SUMO conjugated proteins are recognized and bound by proteins containing SUMO interacting motifs (SIMs) (46). The interactions between sumoylated proteins and SIM-containing proteins can act as a scaffold to promote the self-assembly of large multi-protein complexes. For example, PML is conjugated to SUMO and contains SIM motifs that drive PML assembly into nuclear bodies (48). Sumoylation is critical for the assembly of PML nuclear bodies and the recruitment of additional SUMO-SIM proteins such as DAXX and Sp100 (49-51). SUMO-SIM driven assembly creates subnuclear compartments that are physically distinct from the surrounding nucleoplasm, despite the lack of a defining membrane. SUMO-SIM nuclear bodies can function as hubs for a particular activity such as transcription or induce the local concentration of components within the nucleoplasm (52). Thus, sumoylation is a

means to induce the dynamic structural organization and compartmentalization of molecular interactions.

The potential for controlling transcriptional regulation and immunity makes it unsurprising that many viral proteins usurp the SUMO pathway (39, 40). For example, to evade the immune response, some viral proteins target the PIAS family of E3 SUMO ligases, which are associated with suppression of innate immune signaling through inhibition of STAT proteins, interferon-regulatory factors, and NF-κB (53, 54). There is also mounting evidence for viruses targeting the SUMO pathway to promote nuclear reorganization. One well-characterized example of viruses modulating nuclear organization is the disruption of nuclear PML bodies, which are targeted by many DNA tumor virus proteins via SUMO-mediated mechanisms (40). Thus, an interesting question is if viral proteins utilize SUMO to assemble new nuclear bodies such as viral genome replication domains.

Many viruses utilize cytoplasmic membranes and cytoskeletal components to create a physical boundary to concentrate components involved in viral genome replication (55, 56). Adenovirus is a small double strand DNA tumor virus that replicates in the cell nucleus. After the initial rounds of DNA replication, single and double strand virus genomes assemble with the viral E2A DNA-Binding Protein (DBP) to form specialized replication compartments that concentrate viral genomes, proteins, and RNA (57). E2A viral replication domains change in morphology and size at different stages in the viral lifecycle (58). Therefore, an interesting question is if sumoylation and/or SUMO-SIM

interactions are associated with the assembly of adenovirus replication centers in the nucleus.

In adenovirus infection, the early viral proteins E1B-55K and E4-ORF3 have overlapping cellular targets and functions in viral replication. E1B-55K and E4-ORF3 converge in disrupting the MRE11/RAD50/NBS1 (MRN) complex and preventing p53 activated transcription via independent mechanisms (28, 32). E1B-55K targets p53 and MRE11 for ubiquitination and degradation in the proteasome (19, 20). E4-ORF3 assembles a multivalent nuclear scaffold that sequesters MRN and induces repressive heterochromatin silencing at p53 target gene (28, 32). In addition to their overlapping roles in inactivating MRN and p53, E1B-55K and E4-ORF3 have also been implicated in the SUMO pathway (Fig. 2.1A). E1B-55K has been shown to function as an E3 SUMO ligase towards p53 (21, 22) and to interact with the E2 SUMO ligase UBC9 (23). E4-ORF3 forms a nuclear polymer that disrupts PML bodies (27) and mislocalizes TRIM24 and TRIM33 (28-30), all of which are sumoylated. Recently, E4-ORF3 was reported to modulate the sumoylation of MRN and other substrates (59, 60). The crystal structure of E4-ORF3 indicates that it is not a structural homolog of cellular proteins involved in sumoylation (26). Thus, a key question is if E4-ORF3 targets cellular SUMO enzymes to modulate SUMO conjugation and interactions in viral infection (Fig. 2.1A).

Here we show that E1B-55K and E4-ORF3 are required for the induction of sumoylation and the assembly of SUMO2/3 associated viral genome replication domains in Ad5 infected cells. We show that the assembly of E2A viral

genome replication domains is sufficient to recruit SUMO2/3 independently of E1B-55K/E4-ORF3 and SUMO2/3 conjugation. However, E1B-55K/E4-ORF3 determines the structure and nuclear organization of SUMO2/3 associated E2A domains. We show that E4-ORF3 specifically targets and mislocalizes the cellular E3 SUMO ligase PIAS3 into a nuclear scaffold but not related protein family members PIAS1, 2, or 4. In contrast to MRN, we show that PIAS3 is a target of E4-ORF3 proteins from disparate human adenovirus subgroups, indicating that it is an important and conserved target in virus evolution.

2.2 Results.

2.2.1 In Ad5 infected cells SUMO2/3 is mislocalized by E4-ORF3 and recruited to E2A viral genome replication centers.

Adenovirus infection and replication transforms the cell nucleus and remodels nuclear protein complexes, including PML bodies and MRN, both of which are targeted by sumoylation (27, 28, 59). We reasoned that adenoviral proteins could subvert SUMO conjugation and localization to reorganize cellular proteins and compartments within the nucleus to facilitate virus replication. SUMO2 and SUMO3 are the predominant SUMO conjugates that modify proteins in response to external stimuli and cell stress (47). SUMO2 and SUMO3 share 97% sequence homology and cannot be distinguished using endogenous cellular antibodies. Therefore, to analyze SUMO2 and SUMO3 in adenovirus infection, we transfected U2OS cells with either Flag-SUMO2 or Flag-SUMO3 and examined SUMO localization over the time course of wild type (WT) Ad5

infection. In uninfected cells, Flag-SUMO2 and Flag-SUMO3 are distributed throughout the nucleus and PML bodies. At early times, 12 hours post infection (h.p.i.), E4-ORF3 colocalizes with Flag-SUMO2 and Flag-SUMO3 associated nuclear bodies. The latter is consistent with the well-established role of E4-ORF3 in targeting and disrupting sumoylated proteins at PML nuclear bodies (27). However, as the viral life cycle progresses, Flag-SUMO2 and Flag-SUMO3 are induced at viral genome replication domains demarcated by the viral E2A protein (24 h.p.i. and 36 h.p.i.) (Fig. 2.1B). Flag tagged SUMO2 and SUMO3 have indistinguishable localization patterns. Therefore, for the remainder of these studies we used SUMO2, as it appears to be interchangeable with SUMO3. Furthermore, we confirmed that endogenous SUMO2/3 localizes to viral genome replication domains using an antibody that recognizes both SUMO2 and SUMO3 (Fig. 2.1C). We conclude that Ad5 infection mislocalizes sumoylated proteins into the E4-ORF3 nuclear matrix and induces SUMO2/3 at E2A viral genome replication domains, suggesting a larger role for SUMO2/3 in adenovirus infection than was previously appreciated.

2.2.2 SUMO2/3 is recruited to E2A viral genome replication domains independently of SUMO conjugation.

The modulation of SUMO2/3 localization in viral infection could be due to covalent SUMO2/3 conjugation or non-covalent SUMO2/3 interactions with cellular or viral SIM containing proteins. To distinguish between these possibilities, we used a GFP construct that has four SUMO2 tandem repeats that

can interact with SIM-containing proteins but cannot be conjugated to target proteins (GFP-4xSUMO2AA). In uninfected cells, GFP-4xSUMO2AA is nuclear diffuse and does not form nuclear bodies (Fig. 2.1D). The latter likely represents the failure of GFP-4xSUMO2AA to be conjugated to proteins at PML bodies. In WT virus infected cells, GFP-4xSUMO2AA does not co-localize with E4-ORF3 but is induced at E2A viral genome replication domains (Fig. 2.1D and E). Furthermore, we show that E4-ORF3 does not mislocalize GFP-4xSUMO2AA in co-transfected cells (Fig. 2.1F and G). We conclude that SUMO2/3 localization at E2A viral genome replication domains does not require covalent SUMO conjugation and can be mediated through non-covalent SUMO interactions with cellular and/or viral components.

2.2.3 E1B-55K and E4-ORF3 determine the morphology and nuclear organization of SUMO2/3 associated E2A viral genome replication domains.

We hypothesized that SUMO localization at E2A viral genome replication domains is modulated by early viral oncoproteins. E1B-55K has been reported to have SUMO ligase activity (21, 22) and to interact with the cellular E2 SUMO ligase UBC9 (23). E4-ORF3 has been recently reported to modulate sumoylation of MRN and other substrates (59, 60), although the mechanism remains unknown. To determine if E1B-55K and E4-ORF3 modulate SUMO localization at E2A domains, we analyzed Flag-SUMO2 localization in cells infected with WT Ad5 or mutant viruses in which E1B-55K and/or E4-ORF3 sequences are deleted. In WT, ΔE1B-55K, and ΔE4-ORF3 virus infected cells, Flag-SUMO2 is induced at

E2A viral genome replication domains. However, ΔE1B-55K/ΔE4-ORF3 viruses fail to induce E2A and SUMO2 associated viral genome replication domains (Fig. 2.2A). Similar results were observed with endogenous SUMO2/3 (data not shown).

E1B-55K or E4-ORF3 is required to inactivate a critical early MRN-ATM checkpoint to viral genome replication (61). Therefore, the lack of SUMO2 at E2A domains could be an indirect consequence of an upstream block in viral genome replication in ΔE1B-55K/ΔE4-ORF3 infected cells. Alternatively, it could reflect a direct role of E1B-55K/E4-ORF3 in regulating SUMO2 localization and organization at E2A domains. To distinguish between these possibilities, we used the ATM kinase inhibitor KU-55933 (62) to rescue viral genome replication in ΔE1B-55K/ΔE4-ORF3 infected cells (61). We also analyzed ΔE1B-55K/ΔE4-ORF3 superinfected cells (MOI of 250) as previous studies have shown that high MOIs can rescue the replication defect of E4 deleted viruses (63-65).

KU-55933 has no effect on virus genome replication or the localization and morphology of SUMO2 associated viral genome replication domains in WT virus infected cells. However, KU-55933 rescues viral genome replication by 15-fold in ΔE1B-55K/ΔE4-ORF3 infected U2OS cells (Fig. 2.2B). Similar to KU-55933, high MOIs also rescue viral genome replication and the assembly of SUMO2 associated E2A domains (Fig. 2.2C and D). We conclude that the assembly of E2A viral genome replication domains is sufficient to recruit SUMO2 independently of E1B-55K/E4-ORF3. However, the morphology of SUMO2/E2A domains in ΔE1B-55K/ΔE4-ORF3 infected cells is strikingly different to that in WT

virus infected cells (Fig. 2.2D). In contrast to WT virus infected cells, the SUMO2 associated E2A domains are globular and amorphous in ΔE1B-55K/ΔE4-ORF3 infected cells treated with KU-55933 or infected at high MOI. The SUMO associated E2A domains are fewer in number and larger in size in the absence of E1B-55K/E4-ORF3 and appear to be fused together into giant clusters as opposed to distinct compartments. These data indicate that E1B-55K and E4-ORF3 have important roles in determining the architecture and compartmentalization of SUMO2 associated E2A viral genome replication domains.

2.2.4 Ad5 infection induces SUMO2/3 modified proteins.

To determine if adenovirus infection induces SUMO2/3 levels and conjugation, we first used a dot blot analysis. There is almost a 5-fold increase in total SUMO2/3 levels in protein lysates from Ad5 infected cells relative to uninfected control U2OS cells (Fig. 2.3A). SUMO2 and SUMO3 share 97% sequence homology but their transcription is differentially regulated (66). For example, the transcription of SUMO3, but not SUMO2, is down-regulated in response to oxidative stress (67). To determine if adenovirus infection induces the transcription of SUMO2 or SUMO3, we compared mRNA levels of SUMO2 and SUMO3 in infected versus uninfected U2OS cells. SUMO2 and SUMO3 mRNA levels are similar in both infected and uninfected cells (Fig. 2.3B).

Unconjugated forms of SUMO2 and SUMO3 are 8 kDa. However, SUMO2 and SUMO3 form higher molecular weight bands on SDS PAGE gels when they

are covalently attached to protein substrates (68). In WT Ad5 infected U2OS cells, there is a substantial increase in the levels of high molecular weight SUMO2/3 conjugated proteins compared to uninfected cells (Fig. 2.3C). Taken together, these data demonstrate that WT adenovirus infection induces SUMO2/3 conjugation of cellular and/or viral proteins.

2.2.5 E1B-55K and E4-ORF3 induce SUMO2/3 conjugated proteins in Ad5 infected cells.

We hypothesized that E1B-55K and E4-ORF3 are required to induce sumoylation as well as SUMO nuclear organization in Ad5 infected cells. To determine if SUMO2/3 levels and conjugated proteins are induced in WT versus ΔE1B-55K/ΔE4-ORF3 infected cells, we performed dot blot and Western blot for SUMO2/3. Total SUMO2/3 levels are induced 3-4 fold in WT, ΔE1B-55K, and ΔE4-ORF3 infected cells. However, in ΔE1B-55K/ΔE4-ORF3 infected cells, SUMO2/3 levels are only nominally increased relative to uninfected cells (1.6-fold relative to uninfected) (Fig. 2.4A). By Western blot analysis, we show that compared to uninfected and ΔE1B-55K/ΔE4-ORF3 virus infected cells, there is an increase in the levels of high molecular weight SUMO2/3 conjugated proteins in WT, ΔE1B-55K, and ΔE4-ORF3 infected cells (Fig. 2.4B). We conclude that either E1B-55K or E4-ORF3 is required to induce SUMO2/3 conjugated proteins in Ad5 infected cells.

2.2.6 E4-ORF3 does not mislocalize or destabilize the E2 SUMO ligase

UBC9.

Our data demonstrate that E1B-55K and E4-ORF3 modulate SUMO2/3 localization and conjugation during Ad5 infection. E1B-55K has been reported to have SUMO ligase activity itself (21, 22) and to interact with cellular E2 SUMO ligase UBC9 (23). The recent crystal structure of an Ad5 E4-ORF3 dimer indicates that it is not a structural homolog of sumoylation enzymes (26). Therefore, to determine if E4-ORF3 targets cellular proteins that regulate sumoylation, we conducted a candidate screen. Conjugation of SUMO proteins requires processing by a SUMO protease to reveal a digycline motif, followed by conjugation by the E1 ligase SAE1/SAE2 and the E2 SUMO ligase UBC9. From here, SUMO can be conjugated directly to a substrate or be targeted through one of about a dozen E3 SUMO ligases such as the PIAS protein family (Fig. 2.5A). The single E2 SUMO ligase UBC9 is a particularly compelling candidate due its central role in the SUMO pathway. Some viral proteins modulate sumoylation by regulating UBC9 protein levels, such as the avian adenovirus protein Gam1 (69). To determine if UBC9 protein levels are modulated by E1B-55K or E4-ORF3 during adenovirus infection, we infected U2OS cells with WT Ad5, ΔE1B-55K, ΔE4-ORF3, or ΔE1B-55K/ΔE4-ORF3 viruses (Fig. 2.5B). UBC9 protein levels are not changed upon infection. To determine if E4-ORF3 mislocalizes UBC9, we co-transfected U2OS cells with Flag-UBC9 and E4-ORF3. Flag-UBC9 is not mislocalized by E4-ORF3 (Fig. 2.5C). We conclude that E4-ORF3 does not target the central E2 SUMO ligase UBC9.

2.2.7 E4-ORF3 specifically targets PIAS3 from the E3 SUMO ligase family of proteins.

E3 SUMO ligases determine the substrate specificity of sumoylation (70). The PIAS family of E3 SUMO ligases, which include PIAS1, PIAS2 (PIASx), PIAS3, and PIAS4 (PIASy), has important roles in regulating transcription and immunity (71). To determine if the PIAS E3 SUMO ligases are targeted by E4-ORF3, we created epitope tagged cDNA constructs of the four human PIAS family members and co-transfected them with E4-ORF3. E4-ORF3 fails to mislocalize Flag-PIAS1, Flag-PIAS2, and Flag-PIAS4 into nuclear track structures (Fig. 2.6A). In contrast, E4-ORF3 specifically targets and mislocalizes Flag-PIAS3 (Fig. 2.6B and C).

We also determined if PIAS3 is mislocalized by E4-ORF3 in the context of viral infection. Consistent with the conclusions of E4-ORF3 transfection experiments, PIAS3 is mislocalized by E4-ORF3 in WT and ΔE1B-55K virus infected cells. PIAS3 is not mislocalized in ΔE1B-55K/ΔE4-ORF3 virus infected cells and has a similar localization pattern as uninfected cells. Interestingly, in ΔE4-ORF3-infected cells, although PIAS3 is not mislocalized by E4-ORF3, it appears to form larger, more fibrillar structures in the nucleus compared to uninfected and ΔE1B-55K/ΔE4-ORF3 virus infected cells. These data suggest that virus infection and proteins could modulate PIAS3 distribution in the absence of E4-ORF3 (Fig. 2.6D). We conclude that PIAS3, but not other PIAS family members, is targeted and mislocalized by E4-ORF3.

2.2.8 E4-ORF3 higher order assembly is required to mislocalize PIAS3 and is independent of binding to MRN.

E4-ORF3 assembles an insoluble nuclear polymer that makes conventional biochemical and structural analyses challenging. However, the structure of Ad5 E4-ORF3 was recently solved using N^{82} point mutations (28, 72, 73) that prevent the higher order assembly of dimer subunits (26). E4-ORF3 forms a dimer with a central β-core that is sealed at the front and back by the 'C-terminal tail' (residues 99 to 116) containing a short β4 strand (Fig. 2.7A and B). Multiple lines of evidence support a model in which N^{82} residue mutations lock the β-core into a 'closed' conformation that prevent the further assembly of dimer subunits through C-terminal swapping (Fig. 2.7A) (26). E4-ORF3 higher order assembly is required for interactions with PML, TRIM24, MRN, and inactivation of p53 target genes (26, 28, 29, 72, 73). To determine if the higher order assembly of E4-ORF3 dimers is also required for targeting PIAS3, we co-transfected U2OS cells with Flag-PIAS3 and either wild type (WT) E4-ORF3 or E4-ORF3 N82A. In contrast to WT E4-ORF3, E4-ORF3 N82A mutants do not assemble a higher order polymer and exhibit a diffuse nuclear and cytoplasmic localization. Furthermore, we show that E4-ORF3 N82A dimers fail to mislocalize PIAS3 (Fig. 2.7C). We conclude that the higher-order assembly of E4-ORF3 dimer subunits is required for targeting and mislocalizing PIAS3.

The higher order assembly of E4-ORF3 dimers creates avidity-driven interactions with PML and an emergent interface between residues V^{101} to D^{105} in the C-terminal tail that is required for mislocalizing MRN (Fig. 2.7D) (26). MRN

mislocalization has been suggested to be a pre-requisite for MRN sumoylation by E4-ORF3 (59). Therefore, we hypothesized that residues in the E4-ORF3 C-terminal tail required for mislocalizing MRN are also required to target PIAS3. To test this, we determined if WT E4-ORF3, E4-ORF3 V101A, and E4-ORF3 D105A/L106A mislocalize PIAS3 in co-transfected U2OS cells. Consistent with previous studies, E4-ORF3 V101A and E4-ORF3 D105A/L106A point mutants fail to mislocalize NBS1, which is part of the MRN complex (26, 72). However, E4-ORF3 V101A and D105A/L106A mutants behave analogous to WT E4-ORF3 with respect to their ability to mislocalize PIAS3 (Fig. 2.7E). Thus, the functions of Ad5 E4-ORF3 in mislocalizing MRN and PIAS3 can be biochemically separated. We conclude that Ad5 E4-ORF3 targets and mislocalizes PIAS3 independently of its interactions with MRN.

2.2.9 PIAS3 is a conserved target of E4-ORF3 proteins from disparate human adenovirus subgroups.

There are 68 human adenoviruses that are divided into 7 subgroups (A-G) based on sequence homology, biophysical, and biochemical criteria. There is 37.6% pairwise amino acid identity and 55.2% pairwise similarity between Ad5 E4-ORF3 (Subgroup C) and E4-ORF3 proteins from disparate adenoviral subgroups: Ad9 (Subgroup D), Ad12 (Subgroup A), and Ad34 (Subgroup B) (Fig. 2.8A). The ability of E4-ORF3 to bind and mislocalize MRN appears to be peculiar to Subgroup C virus proteins (74). However, interactions with PML, TRIM24, and TRIM33 are conserved functions of E4-ORF3 proteins across

subgroups (29, 30, 75). To determine if PIAS3 is a conserved target of E4-ORF3 proteins from disparate adenovirus subgroups, we co-transfected Flag-PIAS3 with Myc-tagged Ad5, Ad9, Ad12, or Ad34 E4-ORF3 constructs. We show that E4-ORF3 proteins from Ad5, Ad9, Ad12, and Ad34 all target and mislocalize PIAS3 (Fig. 2.8B). We conclude that PIAS3 is an evolutionarily conserved cellular target of E4-ORF3 proteins from disparate human adenovirus subgroups.

2.3 Discussion.

Our studies demonstrate that adenovirus infection induces SUMO2/3 conjugation and remodels SUMO2/3 subnuclear localization. We show that the induction of sumoylation and SUMO2/3 associated E2A viral genome replication centers in the nucleus require the expression of either E1B-55K or E4-ORF3. Furthermore, we identify the E3 SUMO ligase PIAS3 as a novel target of E4-ORF3 proteins from disparate adenovirus subgroups, suggesting a conserved evolutionary role in adenovirus infection.

Our data reveal a striking change in the nuclear distribution of SUMO2/3 at different stages in adenovirus infection (Fig. 2.1B). While the disruption of sumoylated proteins at PML bodies by E4-ORF3 is well established (40), the association of SUMO in E2A viral genome replication domains has not been previously shown. Using conjugation defective SUMO2 constructs, we reveal that SUMO can be recruited to E2A viral genome replication domains though non-covalent interactions with cellular and/or viral proteins (Fig. 2.1D). SUMO2/3 could be recruited through interactions with SIM containing viral and cellular

proteins and/or through novel interactions with DNA, RNA, or other macromolecules concentrated at E2A domains.

In contrast to WT, ΔE1B-55K, and ΔE4-ORF3 viruses, ΔE1B-55K/ΔE4-ORF3 viruses fail to induce SUMO2/3 associated E2A viral genome replication domains (Fig. 2.2A). In addition to modulating sumoylation, E1B-55K and E4-ORF3 have a critical role in inactivating MRN and ATM to facilitate viral genome replication (61, 76-78). We show that the lack of SUMO2 associated E2A domains in ΔE1B-55K/ΔE4-ORF3 infected cells is due to an upstream MRN-ATM mediated checkpoint that prevents viral genome replication. Using ATM kinase inhibitors and high MOIs to rescue ΔE1B-55K/ΔE4-ORF3 viral genome replication, we show that the assembly of E2A domains recruits SUMO2/3 independently of E1B-55K and E4-ORF3 (Fig. 2.2C and D). Thus, the assembly of viral genome replication domains is sufficient to induce the localization and recruitment of SUMO2/3 independently of E1B-55K/E4-ORF3. Taken together, these data reveal that SUMO2/3 is recruited through non-covalent interactions with additional adenoviral/cellular macromolecules concentrated at E2A viral replication domains.

E2A viral replication domains exhibit dramatic morphological differences and variations in size and number over the course of the viral lifecycle (58). The structural basis for these differences in E2A domains and functional consequences is poorly understood. Intriguingly, the structure and nuclear organization of E2A domains in KU-55933 treated ΔE1B-55K/ΔE4-ORF3 infected cells is strikingly different to that in WT virus infected cells. The E2A domains in

KU-55933 treated ΔE1B-55K/ΔE4-ORF3 cells are larger in size and have a more amorphous, uniform morphology compared to WT virus infected cells (Fig. 2.2D). Thus, although viral genome replication is rescued by KU-55933 the E2A domains lack internal structure and are not compartmentalized from each other and the surrounding nucleoplasm in the absence of E1B-55K/E4-ORF3. These data demonstrate that E1B-55K and E4-ORF3 have novel roles in determining the structure and nuclear compartmentalization of E2A viral replication domains. Interestingly, early confocal microscopy studies indicate that the morphologies of E2A domains associated with sites of single strand and double strand viral genome accumulation are distinct (79). In addition, these studies suggested that viral DNA replication and transcription/splicing are spatially and functionally separated by distinct E2A domains at specific sites in the nucleus (79). E1B-55K and E4-ORF3 have overlapping functions in facilitating transcription through late viral mRNA export and splicing (24, 25, 80). Thus, E1B-55K and E4-ORF3 may modulate sumoylation and SUMO-SIM interactions to specify the function and dynamic structural re-organization of viral replication and transcription/splicing centers. This could play an important role in compartmentalizing and catalyzing different activities in the course of the viral lifecycle.

Adenovirus infection induces a global increase in SUMO2/3 conjugates (Fig. 2.3C). Sumoylation has strong links to transcriptional regulation and immunity. Therefore, the induction of sumoylation in Ad5 infected cells could also be a cellular anti-viral response to productive virus replication. Many transcription factors and co-regulators are proteins that are targeted and modulated by

sumoylation, which usually results in transcriptional repression (81). E1B-55K and E4-ORF3 inhibit the interferon-mediated anti-viral response (76). Thus, the induction of SUMO conjugation by E1B-55K and E4-ORF3 could inactivate a cellular anti-viral transcriptional response to virus replication (Fig. 2.4B). For example, adenovirus-induced changes in sumoylation may regulate proteins that are involved in the transcriptional repression of p53 and anti-viral genes (32).

Either E1B-55K or E4-ORF3 is sufficient to mediate changes in SUMO localization and conjugation in infected cells (Fig. 2.2A and Fig. 2.4B). E1B-55K functions as an E3 SUMO ligase that specifically conjugates SUMO to p53, inhibiting its transcriptional activity (21, 22), and likely targets other proteins for sumoylation. We hypothesized that E4-ORF3 usurps cellular SUMO enzymes to modulate the SUMO pathway. E1B-55K has been shown to interact with UBC9 (23). However, E4-ORF3 does not mislocalize UBC9 or modulate UBC9 protein levels in virus-infected cells (Fig. 2.5B and C). Instead, we show that E4-ORF3 specifically targets PIAS3 but not PIAS1, PIAS2 or PIAS4 E3 SUMO ligases (Fig. 2.6A and B).

The PIAS family of proteins share over 40% sequence identity and have an N-terminal SAP domain, a PINIT motif, a RING-type zinc-binding structure, a SIM, and a serine/threonine-rich (S/T) C-terminal tail (53). The least conserved region is in the C-terminal S/T region (82), which may account for the differences in E4-ORF3 specificity in targeting the PIAS family. However, the function of the C-terminal S/T region is poorly understood. The role of PIAS3 mislocalization by E4-ORF3 remains to be determined. One possibility is that E4-ORF3

mislocalizes PIAS3 to facilitate the disruption of sumoylated proteins in PML nuclear bodies and/or nuclear rearrangement, promoting the sumoylation of cellular targets that aid in the formation of E2A viral replication domains. An alternative but not mutually exclusive possibility is that PIAS3 could play a role in gene regulation during Ad5 infection, as it regulates the activity of many transcription factors, including those involved in interferon pathways (53). E4-ORF3 is key to suppressing the anti-viral interferon response (76), but the mechanism is unknown. E4-ORF3 may utilize PIAS3 to overcome the cell's defenses and anti-viral response. Alternatively, mislocalization of PIAS3 could be an indirect consequence of E4-ORF3 targeting a pre-existing cellular protein complex that is associated with PIAS3. For example, if PIAS3 is involved in the formation or maintenance of PML bodies, the entire multi-protein complex could be disrupted by E4-ORF3.

Using oligomerization mutants, we show that the higher order assembly of E4-ORF3 into a multivalent scaffold is required for targeting and mislocalizing PIAS3 (Fig. 2.7C). E4-ORF3 is necessary and sufficient for inducing the sumoylation of the MRN complex (59, 60). However, we show that E4-ORF3 V101A and D105A/L106A mutants that are defective for binding and sumoylating MRN still mislocalize PIAS3 (Fig. 2.7E). Thus, if E4-ORF3 induces MRN sumoylation through PIAS3, it first requires MRN mislocalization and sequestration in the E4-ORF3 nuclear scaffold. Alternatively, E4-ORF3 induced sumoylation of MRN could by mediated through a distinct E3 SUMO ligase or the inhibition of SUMO proteases. Lastly, in contrast to MRN, PIAS3 is a conserved

target of E4-ORF3 proteins from disparate adenovirus subgroups (Fig. 2.8B). PML is also a conserved target of E4-ORF3. It will be interesting to determine if E4-ORF3's functions in targeting PML and PIAS3 can be biochemically or functionally separated. We conclude that PIAS3 is a conserved cellular target of E4-ORF3 that may play an important role in facilitating the productive infection of all human adenoviruses.

Our analysis of sumoylation during adenovirus infection demonstrates that early viral proteins disrupt and induce SUMO2/3 associated nuclear bodies and viral replication domains as well as SUMO conjugation. These data indicate an important role for SUMO2/3 in facilitating and/or responding to adenovirus replication that is targeted and modulated by E1B-55K and E4-ORF3 viral protein interactions. Our results reveal an increasingly important role for SUMO2/3 in orchestrating the assembly of intranuclear compartments and a new function for the SUMO pathway in pathological infection.

2.4 Materials and methods.

2.4.1 Cells, culturing conditions, and viral infections.

U2OS cells were cultured in DMEM supplemented in 10% heat-inactivated FBS without antibiotics. Infection was performed at an experimentally determined multiplicity of infection (MOI) of 30 plaque-forming units (PFU) in DMEM containing 2% heat inactivated FBS. Superinfection was performed at an MOI of 250 PFU.

2.4.2 Viruses.

Viruses were titered on 293/E4/pIX cells, as described previously (24). Wild type (WT) virus is Ad5. The ΔE1B-55K virus (AdSyn-CO124) was created by mutating the start codon of E1B-55K (ATG to GTG) and I90 of E1B-55K to a stop codon (ATT to TAG). The ΔE4-ORF3 virus (AdSyn-CO118) was created by deleting the coding region of E4-ORF3. The ΔE1B-55K/ΔE4-ORF3 virus (AdSyn-CO140) is the same as ΔE1B-55K except the E4-ORF3 coding region is also deleted (26).

2.4.3 Drugs.

KU-55933 (Calbiochem) was used at 10 mM and was added 2 hours post adenovirus infection. DMSO was used as a vehicle control.

2.4.4 Plasmids and transfections.

SUMO2, SUMO3, UBC9, and PIAS family plasmids were first cloned into pDONR221 and then recombined into a CMV expression vector with an N-terminal tag using the Gateway Cloning System (Invitrogen). The GFP-4xSUMO2AA construct was obtained from Dr. Tony Hunter's laboratory. E4-ORF3 constructs were generated as described previously (26). Lipofectamine 2000 (Invitrogen) was used for transfection of U2OS cells according to manufacturer's instructions.

2.4.5 Immunofluorescence.

Cells were fixed in 4% paraformaldehyde for 30 minutes at room temperature, permeabilized in 0.1% TritonX-100 PBS-/-, and stained as described previously (24, 25). Primary antibodies were Flag (F742 from Sigma), E4-ORF3 (6A11), E2A (B6-8), SUMO2/3 (C-terminus from Abgent), and NBS1 (NB 100 from Novus Biologicals). Alexa 488-, 555- and 633-conjugated secondary antibodies (Molecular Probes) were used for detection of primary antibodies. Hoechst-33342 was used to stain DNA. Images were acquired with a Zeiss LSM780 imaging system with a 63x objective. Images are single z-planes.

2.4.6 Quantification of immunofluorescence colocalization and statistics.

Colocalization was measured using Imaris Software, which analyzes the intensity of each fluorescent label. The Pearson correlation coefficient was used as a measure of colocalization with values between -1 and +1, with positive values indicating a positive correlation (83). Statistical analyses consisted of Student's t-test, with significance set at 0.05.

2.4.7. Protein lysates, dot blot analysis, and Western analysis.

Protein lysates were harvested in reducing SDS-PAGE sample buffer containing 50mM Tris pH 8, 2% SDS, 10% glycerol, 100mM dithiothreitol, and 0.1% Bromophenol Blue. Lysates were boiled for 10 minutes and sonicated. For dot blot, samples were spotted onto nitrocellulose membrane. For Western blot, samples were analyzed by SDS-PAGE and transferred to nitrocellulose membranes. The membranes were blocked using 5% milk. Primary antibodies

were SUMO2/3 (8A2 from Abcam) and β-Actin (AC-15 from Sigma). β-Actin expression was used as a loading control. Primary antibodies were detected with secondary antibodies labeled with either IRDye800 (Rockland), or Alexa Fluor 680 (Molecular Probes). Fluorescent antibodies were visualized using a LI-COR-Odyssey scanner. Quantification of dot blots was performed using LI-COR-Odyssey Software (68).

2.4.8 Real-Time Quantitative PCR analysis.

RT-qPCR quantification of SUMO2 and SUMO3 mRNA was performed using the Bio-Rad CFX96 and analyzed using the Bio-Rad CFX Manager 3.0 software. RNA (1 µg) was reverse-transcribed with iScript cDNA synthesis kit (Bio-Rad). Taqman primers and probe sets for SUMO2 and SUMO3 were obtained from Life Technologies. RT-qPCR reactions were set up using Taqman Fast Mix (ABI) and run in triplicate. For 18S rRNA analysis, 10ng input cDNA was used; for SUMO2 and SUMO3 analysis, 40 ng of input cDNA was used. Normalized gene expression (ΔΔCq) was determined using 18S rRNA as a reference gene and fold change was determined by setting gene expression levels of uninfected samples to 1. Error bars represent Standard Error of the Mean of triplicates.

2.4.9 Quantification of viral genome replication.

Total DNA was extracted using the QiaAMP DNA Micro kit (Qiagen) following the manufacturer's protocol. Taqman probes for quantifying adenovirus

DNA were as described previously (84). Q-PCR reactions were set up using Taqman Fast Mix (ABI) and run in triplicate. Input DNA (5 ng) was used for Ad5 genomes and 18S rDNA analysis. Q-PCR quantification of viral genomes was performed using the Bio-Rad CFX96. Viral DNA was quantified relative to 18S rDNA to obtain a ΔC_t for each sample (85). Error bars represent standard deviation of triplicates.

2.5 Acknowledgements

We thank members of the O'Shea laboratory, Kristen Espantman, and J. Sebastian Gomez-Cavazos for their support, insights, and helpful comments. We thank Huaiyu Sun and Tony Hunter for discussions and for contributing the GFP-4xSUMO2AA construct. This work was supported by R01 CA178932 and P30CA014195 from the National Cancer Institute. C.C.O. is supported by The Leona M. and Harry B. Helmsley Charitable Trust, grant 2012-PG-MED002, the Marshall Legacy Foundation, the William Scandling Trust, and the Price Family Foundation. J.M.H. was supported by the T32 GM008666 Genetics Training Program.

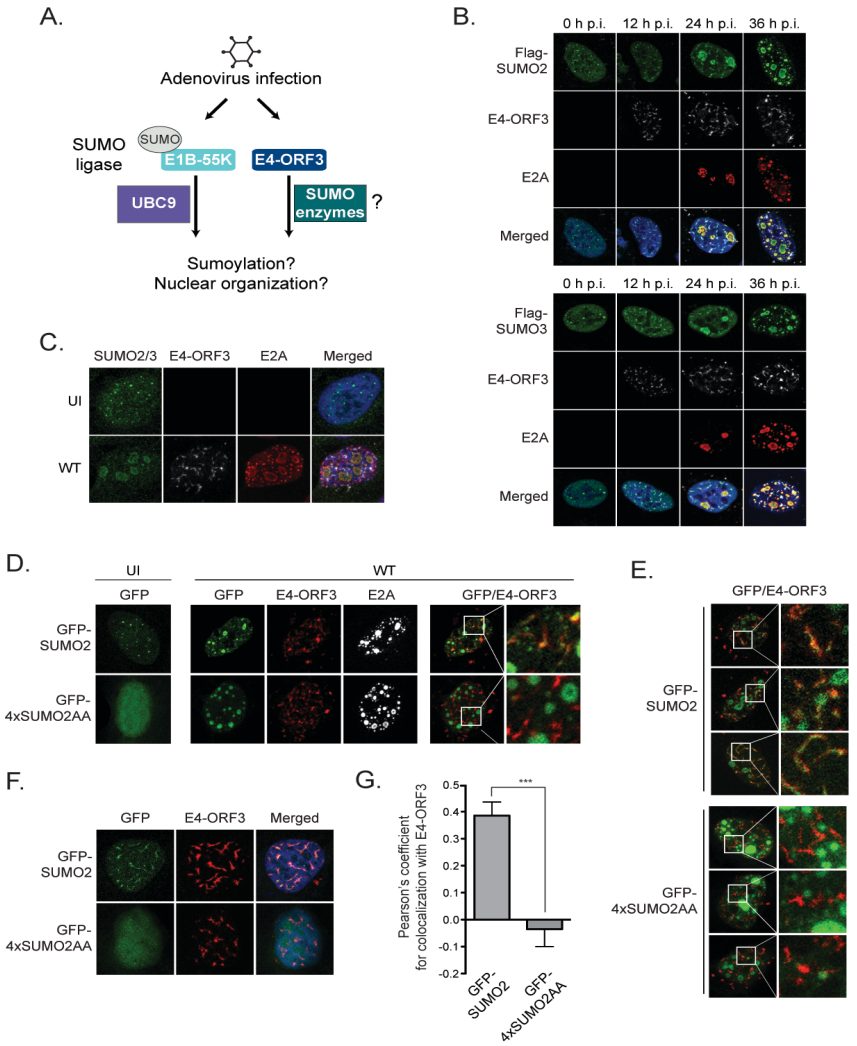

Figure 2.1. In Ad5-infected cells, SUMO2/3 is mislocalized by E4-ORF3 and recruited to E2A viral genome replication centers. (A) Schematic of premise for these studies and role of adenovirus proteins E1B-55K andE4-ORF3in subverting SUMO to facilitate viral replication. (B) U2OS cells were transfected with Flag-SUMO2 or Flag-SUMO3 and then infected with wild-type (WT) Ad5 virus. Cells were fixed at 0, 12, 24, and 36 h.p.i. and immunostained for Flag (green), E4-ORF3 (white), and E2A (red). Nuclei were counterstained with Hoechst-33342. (C) Uninfected (UI) and WT Ad5-infected U2OS cells were fixed at 36 h.p.i. and immunostained for SUMO2/3 (green), E4-ORF3 (white), and E2A (red). Nuclei were counterstained with Hoechst-33342. (D) U2OS cells were transfected with GFP-SUMO2 or GFP-4xSUMO2AA and left uninfected or were infected with WT Ad5. Cells were fixed at 36 h.p.i. and immunostained for E4-ORF3 (red) and E2A (white). Box indicates 4x zoom. (E) Additional images ofWTAd5-infected U2OS cells transfected with either GFP-SUMO2 or GFP-4xSUMO2AA. (F) U2OS cells were cotransfected with either GFP-SUMO2 or GFP-4xSUMO2AAand E4-ORF3 and then fixed 24 hr later and immunostained for E4-ORF3 (red). Nuclei were counterstained with Hoechst-33342. (G) Quantitative analysis of colocalization of transfected E4-ORF3 with GFP-SUMO2 and GFP-4xSUMO2AA. Pearson's correlation coefficients were calculated using Imaris colocalization (see Materials and Methods) (41). Bars represent the means +/- standard errors of the means. ***, P 0.001, which indicates a significant difference between GFP-SUMO2 and GFP-4xSUMO2AA by t test.

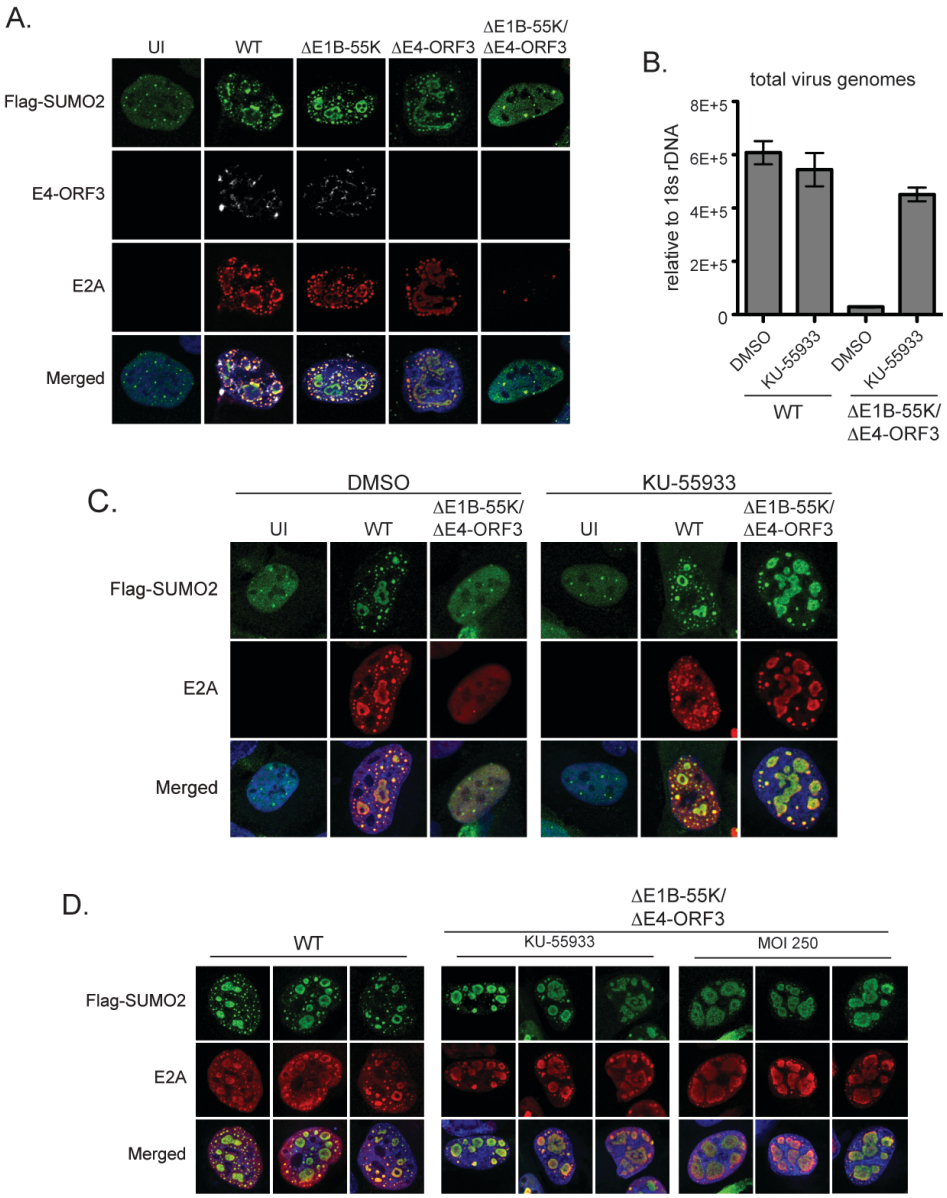

Figure 2.2. E1B-55K and E4-ORF3 determine the morphology and nuclear organization of SUMO2/3 associated E2A viral genome replication domains. (A) U2OS cells were transfected with Flag-SUMO2 and then infected as indicated. Cells were fixed at 36 h.p.i. and immunostained for Flag (green), E4-ORF3 (white), and E2A (red). Nuclei were counterstained with Hoechst-33342. (B) U2OS cells were infected as indicated then treated with DMSO or 10 mM KU-55933 at 2 h.p.i. and harvested at 36 h.p.i. Viral genomes were quantified by Q-PCR and normalized relative to 18s rDNA. Error bars indicate standard deviation of triplicates. (C) U2OS cells were transfected with Flag-SUMO2 and then infected as indicated. Cells were treated with DMSO or 10 mM KU-55933 at 2 h.p.i., fixed 36 h.p.i., and immunostained for Flag (green) and E2A (red). Nuclei were counterstained with Hoechst-33342. (D) U2OS cells were transfected with Flag-SUMO2 and then infected with WT Ad5 or ΔE1B-55K/ΔE4-ORF3 viruses. MOI 250 indicates a multiplicity of infection of 250 PFU. Cells were treated with 10 mM KU-55933 at 2 h.p.i. as indicated, fixed 36 h.p.i., and immunostained for Flag (green) and E2A (red).

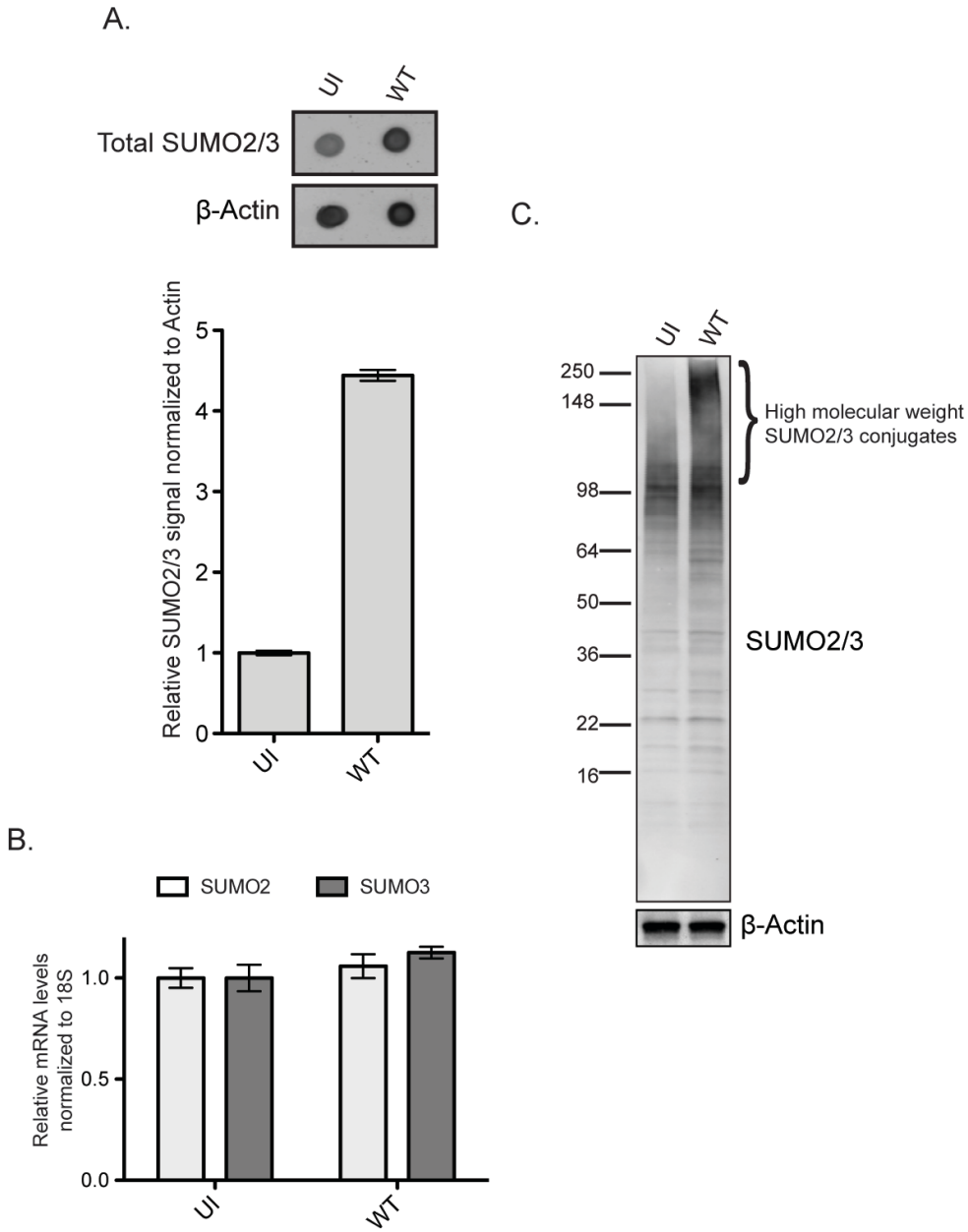

Figure 2.3. Ad5 infection induces SUMO2/3 modified proteins. (A) U2OS cells were infected as indicated then protein lysates were collected at 36 h.p.i. and dot blot for total SUMO2/3 was performed. β-Actin is a loading control. Quantification was performed using LI-COR-Odyssey Software with SUMO2/3 normalized to β-Actin. (B) U2OS cells were infected as indicated and analyzed by RT-qPCR. SUMO2 and SUMO3 transcripts were normalized relative to cellular 18S rRNA. Error bars indicate the Standard Error of the Mean of triplicates. (C) U2OS cells were infected as indicated then protein lysates were collected at 36 h.p.i. and immunoblotted for SUMO2/3. β-Actin is a loading control.

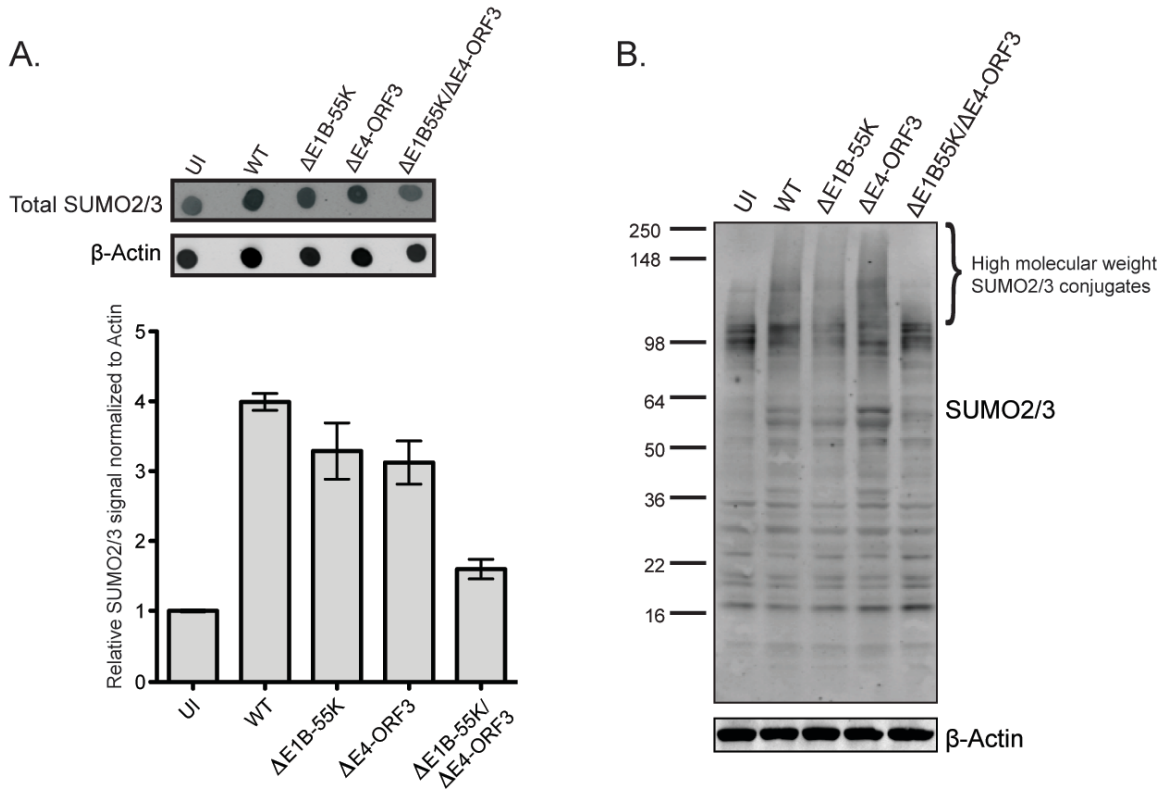

Figure 2.4. E1B-55K and E4-ORF3 induce SUMO2/3 conjugated proteins in Ad5 infected cells. (A) U2OS cells were infected as indicated then protein lysates were collected at 36 h.p.i. and dot blot for total SUMO2/3 was performed. β-Actin is a loading control. Quantification was performed using LI-COR-Odyssey Software with SUMO2/3 normalized to β-Actin. (B) U2OS cells were infected as indicated, then protein lysates were collected at 36 h.p.i. and immunoblotted for SUMO2/3. β-Actin is a loading control.

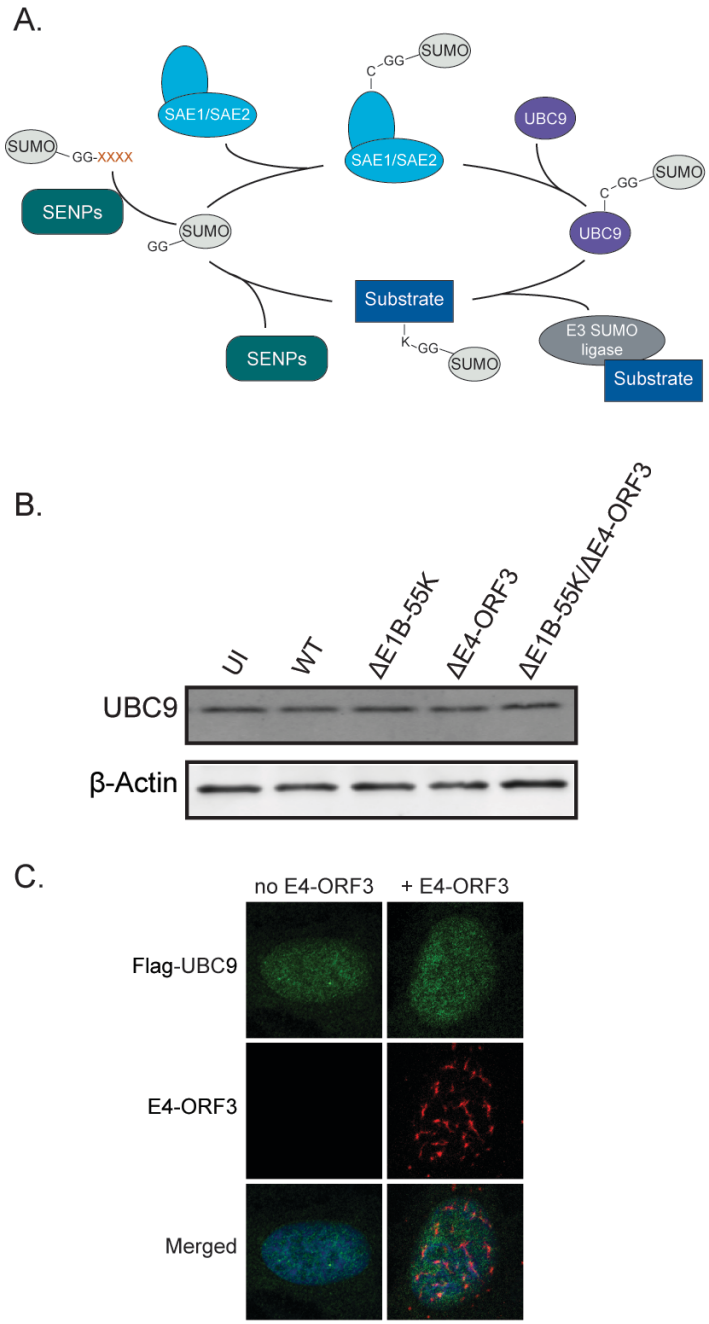

Figure 2.5. E4-ORF3 does not mislocalize or destabilize the E2 SUMO ligase UBC9. (A) Schematic representation of the sumoylation pathway. (B) U2OS cells were infected as indicated. Protein lysates were collected at 36 h.p.i. and immunoblotted for UBC9. β-Actin is a loading control. (C) U2OS cells were co-transfected with Flag-UBC9 and E4-ORF3, fixed 24 hours later, and immunostained for Flag (green) and E4-ORF3 (red). Nuclei were counterstained with Hoechst-33342.

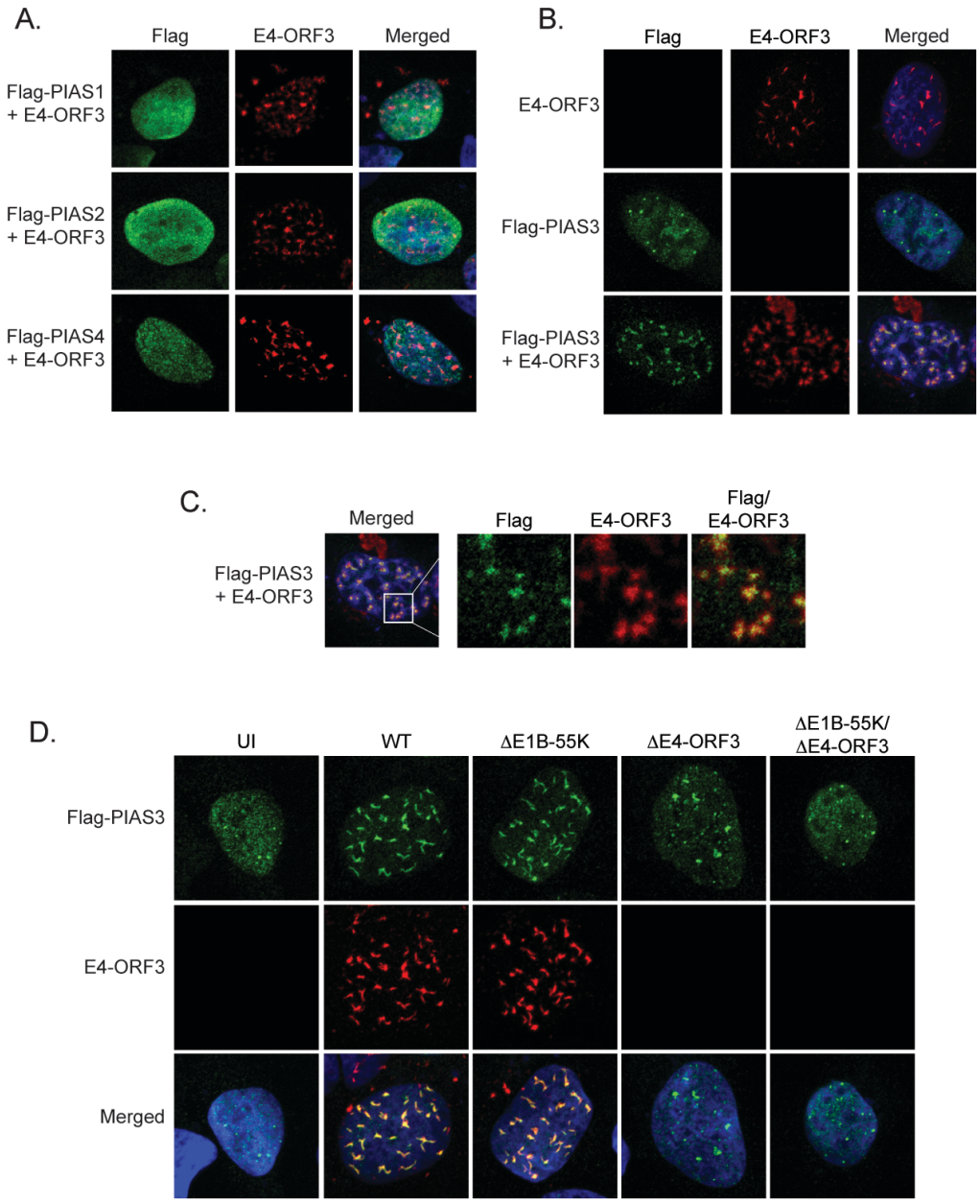

Figure 2.6 E4-ORF3 specifically targets PIAS3 from the E3 SUMO ligase family of proteins. (A) U2OS cells were co-transfected with E4-ORF3 and either Flag-PIAS1, Flag-PIAS2, or Flag-PIAS4 then fixed 24 hours post transfection and immunostained for Flag (green) and E4-ORF3 (red). Nuclei were counterstained with Hoechst-33342. (B) U2OS cells were transfected with E4-ORF3 and Flag-PIAS3 as indicated then fixed 24 hours post transfection and immunostained for Flag (green) and E4-ORF3 (red). Nuclei were counterstained with Hoechst-33342. (C) Zoom (4x) of merged cell in panel B co-transfected with Flag-PIAS3 and E4-ORF3. (D) U2OS cells were transfected with Flag-PIAS3 then infected as indicated. Cells were fixed 36 h.p.i. and immunostained for Flag (green) and E4-ORF3 (red). Nuclei were counterstained with Hoechst-33342.

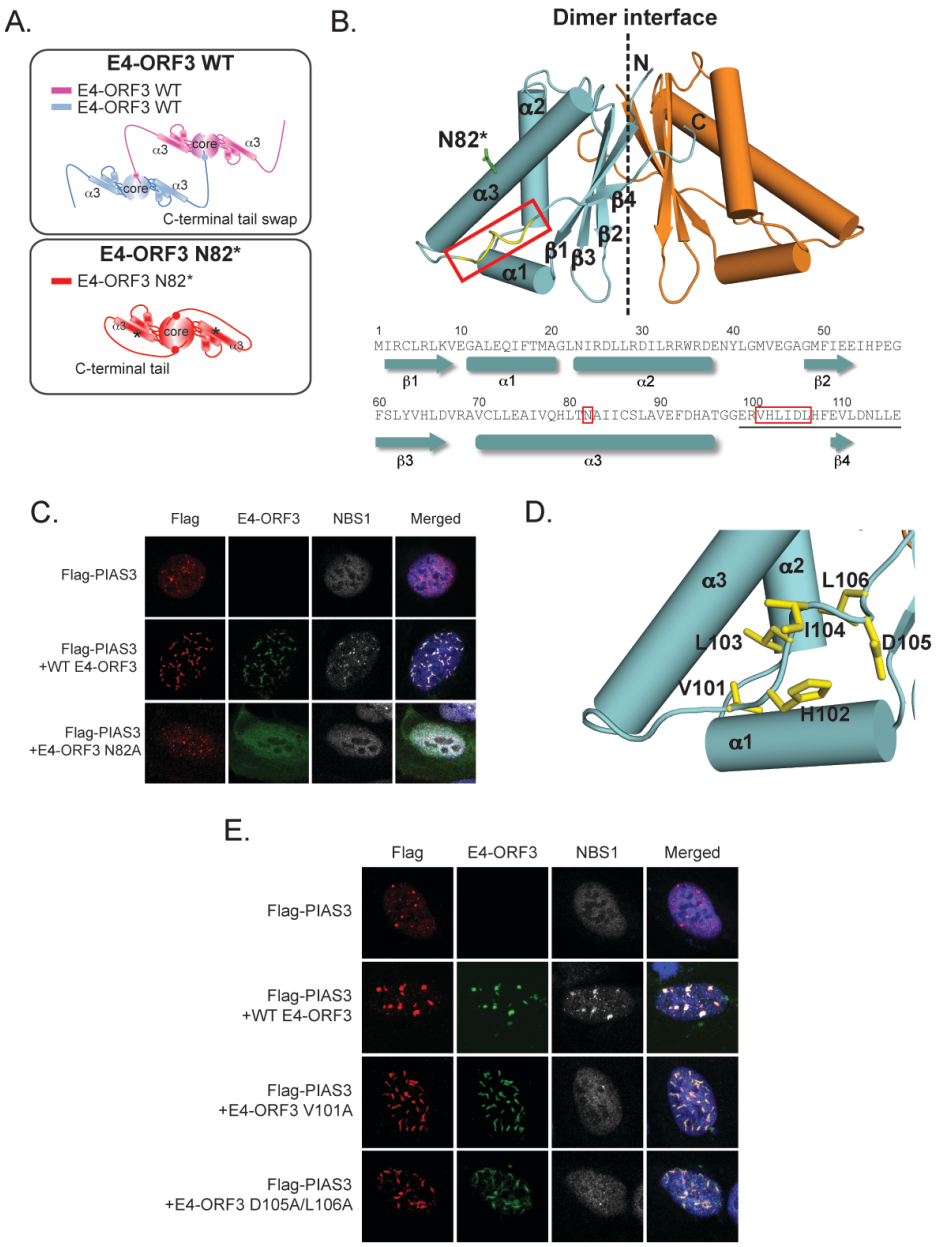

Figure 2.7. E4-ORF3 higher order assembly is required to mislocalize PIAS3 and is independent of binding to MRN. (A) Model showing the assembly of E4-ORF3 dimer subunits through intermolecular exchanges of their C-terminal tails. N82* mutations prevent the further assembly of E4-ORF3 dimer subunits and lock the β-core in a closed configuration. (B) The crystal structure of an E4-ORF3 N82* dimer, highlighting residues N^{82} and $VHLIDL^{101-106}$. (C) U2OS cells were transfected with Flag-PIAS3 and wild type (WT) E4-ORF3 or E4-ORF3 N82A. Cells were fixed 24 hours post transfection and immunostained for Flag (red), E4-ORF3 (green), and NBS1 (white). Nuclei were counterstained with Hoechst-33342. (D) Residues in the E4-ORF3 C-terminal tail required for mislocalizing MRN. (E) U2OS cells were co-transfected with Flag-PIAS3 and either WT E4-ORF3, E4-ORF3 V101A, or E4-ORF3 D105A/L106A. Cells were fixed 24 hours post transfection and immunostained for Flag (red), E4-ORF3 (green), and NBS1 (white). Nuclei were counterstained with Hoechst-33342.

A.

```
          1         10         20         30         40         50
Ad5   MIRCLRLKVEGALEQIFTMAGLNIRDLLRDILRRWRDENYLGMVEGAGMFIEEIHPE-G
Ad9   MKVCLIMKVEGALWELFHMCGVDLHQQFVEIIQGWKNENYLGMVQECNLMIDEIDGP-A
Ad12  MKYCLRMAVEGALTELFNIHGLNLQNQCVQIIQQWKNENYLGMVQSGSLMIEEFHDN-A
Ad34  MRVCLRMVVEGALRDLFVMCGLDLPQELTRIIQGWKAENYLGMVQECNMMIEELENAPS

          60         70         80         90        100        110
Ad5   FSLYVHLDVRAVCLLEAIVQHLTNAIICSLAVEFDHATGGERVHLIDLHFEVLDNLLE
Ad9   FNVILMLDVRVEPLLEATVEHLENRVGFDLAVCFHQHSGGERCHLRDLHFIVLRDRLE
Ad12  FALLLFIEIRAVALLEAVVEHLENRLQFDLAVIFHQHSGGDRCHLRDLRIQILADRLD
Ad34  FGILLFLDVRVEALLEATVEHLENRISFDLAVLFHQHSGGERCHLRDLQFEVLRDRLE
```

B.

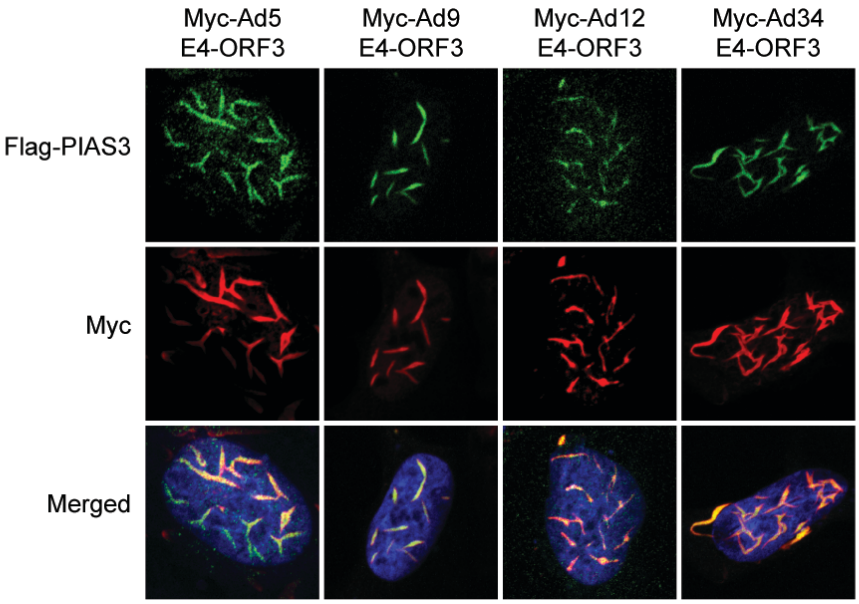

Figure 2.8. PIAS3 is a conserved target of E4-ORF3 proteins from disparate human adenovirus subgroups. (A) Alignment of E4-ORF3 protein sequences from Subgroup A – Ad12, Subgroup B – Ad34, Subgroup C – Ad5, and Subgroup D – Ad9. Blue, orange, and black letters denote conserved, semi-conserved, and non-conserved residues, respectively. (B) U2OS cells were co-transfected with Flag-PIAS3 and Myc-tagged E4-ORF3 from Ad5, Ad9, Ad12, or Ad34. Cells were fixed 24 hours post transfection and immunostained for Flag (green) and Myc (red). Nuclei were counterstained with Hoechst-33342.

Chapter 3

Adenovirus targets SUMO proteases and utilizes SUMO interactions to assemble viral genome replication domains

3.1 Introduction.

The nucleus of the human cell is classically recognized for housing the 3 billion bp genome, which is folded and organized into spatially defined 3D compartments (86). In addition to containing DNA, the cell nucleus contains a multitude of discrete non-membrane bound 'suborganelles' that are essential part of the nuclear landscape (52). These nuclear bodies are a way to spatially control local concentrations of molecules involved in chromatin remodeling, transcription initiation, and RNA processing (33). The functions of nuclear bodies are diverse: ribosome biogenesis in the nucleolus, mRNA editing paraspreckles, and storage and recycling of splicing factors in nuclear speckles (87). PML nuclear bodies have been proposed to have a wide range of functions, including transcription, DNA repair, viral defense, and regulating genome stability (87).

At present, no strictly architectural protein of subnuclear components is known, but protein-protein interactions play a primary role in maintaining the structure of subnuclear bodies (52). Sumoylation is one particularly dynamic means to modulate protein-protein interactions and change the structural organization and compartmentalization of molecular interactions. The interactions between sumoylated proteins and SIM-containing proteins can drive the assembly of large multi-protein complexes and bodies, and changes in SUMO status can change the complexes' structure. For example, PML is conjugated to SUMO and contains SIM motifs that drive PML assembly into nuclear bodies (48). Removal of SUMO from the protein PML affects assembly; desumoylation results in a decrease in the number of PML nuclear bodies, with the remnant PML foci to appear larger (88).

Sumoylation status of a substrate protein is a highly regulated process controlled by both conjugation by a SUMO ligase and deconjugation by a SUMO protease (Fig. 2.5A). The addition of SUMO to a target protein is carried out by SUMO ligases and is reversed by the isopeptidase activity of SENtrin-specific Proteases (SENPs) (89). SENPs are responsible for processing immature SUMO into its mature form, exposing a di-glycine C-terminal motif. In addition, SENPs remove SUMO from substrate proteins through deconjugation. There are six human SENP protein family members, SENP1-3 and SENP5-7 (there is no SENP4) (90).

Many viral proteins have been shown to interfere with the host SUMO pathway. Some viral proteins encode their own SUMO ligases, but there has yet

to be identification of a viral protein that usurps a SUMO protease (91). Post-translational modifications are a means to increase proteomic diversity. Therefore, utilizing both the addition and removal of SUMO modification on target substrates could enrich the proteome and establish a dynamic environment, poising the virus for its changing needs as the life cycle progresses. For example, upon infection, the replication of adenovirus genomes leads to the formation of specialized replication compartments within the nucleus that concentrate viral genomes, proteins, and RNA (57). E2A viral replication domains change in morphology and size at different stages in the viral lifecycle (58), yet the structural basis for these differences in E2A domains and functional consequences is poorly understood. Our studies have shown that adenovirus infection induces SUMO2/3 conjugation and remodels SUMO2/3 subnuclear localization to E2A viral genome replication domains, which changes as the virus life cycle progresses (92). These results indicate a potential role for sumoylation in the compartmentalization of viral genomes.

To determine how adenovirus may be modulating changes in SUMO localization and conjugation in infected cells, we conducted a candidate screen of SUMO enzymes and identified the E3 SUMO ligase PIAS3 as a novel target of adenovirus protein E4-ORF3 (Fig. 2.6). However, to effectively modulate SUMO-SIM-mediated protein-protein interactions and to allow for dynamic changes in nuclear substructures, we hypothesized that adenovirus proteins may target SUMO proteases in addition to the E3 SUMO ligase PIAS3. The dynamics between SUMO conjugation and deconjugation may regulate the

compartmentalization needed to form E2A viral replication domains. Modulating SUMO-SIM interactions could give adenovirus the tools to dynamically and constantly restructure nuclear architecture and various substructures throughout its life cycle.

Here we show that adenovirus protein E4-ORF3 specifically targets and mislocalizes the SUMO proteases SENP1 and SENP2 into its nuclear scaffold, but not related protein family members SENP3, SENP5, SENP6, or SENP7. SENP1 and SENP2 are targets of E4-ORF3 proteins from disparate human adenovirus subgroups, indicating that they are important and conserved targets in virus evolution. Further, our results indicate that the balance of SUMO conjugation and deconjugation must be regulated during adenovirus infection, as overexpression of SENPs and PIASes inhibits the formation of E2A viral genome replication domains.

3.2 Results.

3.2.1 Adenovirus E4-ORF3 targets SUMO proteases SENP1 and SENP2.

We have shown that Ad5 proteins E1B-55K and E4-ORF3 induce SUMO conjugation and interactions to organize viral replication compartments within the nucleus (Fig. 2.3 and 2.4). We also identified the E3 SUMO ligase PIAS3 as a novel target of E4-ORF3 (Fig. 2.6) (92). To determine whether E4-ORF3 targets additional components of the SUMO pathway, we created epitope tagged cDNA constructs of the six human SENP family members and transfected them in U2OS cells. SENPs have varying specificity for SUMO1 or SUMO2/3, their

abilities to process immature SUMO, and their localization (90)(Table 3.1). Consistent with previously published results, SENP1 and SENP2 localize to the nucleoplasm and subnuclear compartments, SENP3 and SENP5 localize to the nucleolus, and SENP6 and SENP7 localize to the neoplasm (Fig. 3.1A). Upon co-transfection with E4-ORF3, we found that E4-ORF3 fails to mislocalize Flag-SENP3, Flag-SENP5, Flag-SENP6, and Flag-SENP7 into nuclear track structures. In contrast, E4-ORF3 specifically targets and mislocalizes Flag-SENP1 and Flag-SENP2 (Fig. 3.1B).

We also determined if SENP1 and SENP2 are mislocalized by E4-ORF3 in the context of viral infection. Consistent with the conclusions of our E4-ORF3 transfection experiments, SENP1 and SENP2 are mislocalized by E4-ORF3 in WT and ΔE1B-55K virus infected cells. SENP1 and SENP2 are not mislocalized in ΔE1B-55K/ΔE4-ORF3 virus infected cells and have a similar localization pattern as uninfected cells (Fig. 3.2A and B). We conclude that SENP1 and SENP2, but not other SENP family members, are targeted and mislocalized by E4-ORF3.

3.2.2 E4-ORF3 higher order assembly is required to mislocalize SENP1 and SENP2 and is independent of binding to MRN.

E4-ORF3 assembles an insoluble nuclear polymer that makes conventional biochemical and structural analyses challenging. However, the structure of Ad5 E4-ORF3 was recently solved using N^{82} point mutations (28, 72, 73) that prevent the higher order assembly of dimer subunits (26). E4-ORF3

forms a dimer with a central β-core that is sealed at the front and back by the 'C-terminal tail' (residues 99 to 116) containing a short β4 strand (Fig. 2.7A and B). Multiple lines of evidence support a model in which N^{82} residue mutations lock the β-core into a 'closed' conformation that prevent the further assembly of dimer subunits through C-terminal swapping (Fig. 2.7A) (26). E4-ORF3 higher order assembly is required for interactions with PML, TRIM24, MRN, and inactivation of p53 target genes (26, 28, 29, 72, 73). To determine if the higher order assembly of E4-ORF3 dimers is also required for targeting SENP1 and SENP2, we co-transfected U2OS cells with Flag-SENP1 or Flag-SENP2 and either wild type (WT) E4-ORF3 or E4-ORF3 N82A. In contrast to WT E4-ORF3, E4-ORF3 N82A mutants do not assemble a higher order polymer and exhibit a diffuse nuclear and cytoplasmic localization. Furthermore, we show that E4-ORF3 N82A dimers fail to mislocalize SENP1 and SENP2 (Fig. 3.3A and B). We conclude that the higher-order assembly of E4-ORF3 dimer subunits is required for targeting and mislocalizing SENP1 and SENP2.

The higher order assembly of E4-ORF3 dimers creates avidity-driven interactions with PML and an emergent interface between residues V^{101} to D^{105} in the C-terminal tail that is required for mislocalizing MRN (Fig. 2.7D) (26). We hypothesized that residues in the E4-ORF3 C-terminal tail required for mislocalizing MRN may also be required to target SENP1 and SENP2. To test this, we determined if WT E4-ORF3, E4-ORF3 V101A, and E4-ORF3 D105A/L106A mislocalize SENP1 and SENP2 in co-transfected U2OS cells. Consistent with previous studies, E4-ORF3 V101A and E4-ORF3 D105A/L106A

point mutants fail to mislocalize NBS1, which is part of the MRN complex (Fig. 2.7E, data not shown)(26, 72). However, E4-ORF3 V101A and D105A/L106A mutants behave analogous to WT E4-ORF3 with respect to their ability to mislocalize SENP1 and SENP2 (Fig. 3.3A and B). Thus, the functions of Ad5 E4-ORF3 in mislocalizing MRN and SENP1 and SENP2 can be biochemically separated. We conclude that Ad5 E4-ORF3 targets and mislocalizes SENP1 and SENP2 independently of its interactions with MRN.

3.2.3. SENP1 and SENP2 are conserved targets of E4-ORF3 proteins from disparate human adenovirus subgroups.

There are 68 human adenoviruses that are divided into 7 subgroups (A-G) based on sequence homology, biophysical, and biochemical criteria. There is 37.6% pairwise amino acid identity and 55.2% pairwise similarity between Ad5 E4-ORF3 (Subgroup C) and E4-ORF3 proteins from disparate adenoviral subgroups: Ad9 (Subgroup D), Ad12 (Subgroup A), and Ad34 (Subgroup B)(Fig. 2.8A). The ability of Ad5 E4-ORF3 to bind and mislocalize MRN appears to be peculiar to Subgroup C virus proteins (74). However, interactions with PML, TRIM24, TRIM33, and PIAS3 are conserved functions of E4-ORF3 proteins across the 4 subgroups (29, 30, 75, 92). To determine if SENP1 and SENP2 are conserved targets of E4-ORF3 proteins from disparate adenovirus subgroups, we co-transfected Flag-SENP1 or SENP2 with Myc-tagged Ad5, Ad9, Ad12, or Ad34 E4-ORF3 constructs from subgroups. We show that E4-ORF3 proteins from Ad5, Ad9, Ad12, and Ad34 all target and mislocalize both SENP1 and

SENP2 (Fig. 3.4A-C). We conclude that SENP1 and SENP2 are evolutionarily conserved cellular targets of E4-ORF3 proteins from disparate human adenovirus subgroups.

3.2.4. Overexpression of PIAS3, SENP1, and SENP2 inhibit the formation of E2A viral genome replication domains.

Our analyses of sumoylation during adenovirus infection and identification of three SUMO enzymes—PIAS3, SENP1, and SENP2—that are targeted by adenovirus protein E4-ORF3 suggest an increasingly important role for SUMO2/3 in orchestrating the assembly of intranuclear compartments and a function for the SUMO pathway in pathological infection (92). Modulating sumoylation and desumoylation may be critical in forming the compartmentalization necessary for viral genome replication. We hypothesized that perturbations in the SUMO pathway may abrogate adenovirus-induced remodeling of SUMO2/3 subnuclear localization, particularly in viral replication centers. To test this, we overexpressed SUMO ligases and SUMO proteases to disrupt normal levels of SUMO conjugation. We used PIAS1 and SENP3, which are not known targets of any adenovirus proteins, as well as targets of adenovirus protein E4-ORF3: PIAS3, SENP1, and SENP2. U2OS cells were first transfected with each SUMO enzyme then infected with WT Ad5 to observe the consequences on the formation of E2A viral genome replication domains. To control for potentially adverse effects on viral replication from use of a transfection reagent, we compared the formation of E2A viral replication domains of transfected U2OS

cells to those transfected with Flag-GFP.

We found that no matter which SUMO ligase or SUMO protease was expressed, there was a defect in the formation of viral E2A genome replication domains when compared to the GFP control (Fig. 3.5A). We quantified differences in E2A formation by categorizing nuclear E2A staining into four groups. Bin #1 includes nuclei with a diffuse pattern of E2A and/or very small foci and have the least formed domains; Bin #2 includes nuclei with mostly diffuse E2A but with many (>5) large foci; Bin #3 includes nuclei containing mostly large foci and very little diffuse E2A; Bin #4 includes nuclei full of large foci and domains of E2A (Fig. 3.5B). Quantification of the Bins in Flag-GFP transfected cells at 36 h.p.i. in WT Ad5 infected U2OS cells reveals that about 75% of infected cells are in Bins #3 or #4, indicating that E2A domains are maturely formed. However, in Flag-SENP1, Flag-SENP2, Flag-SENP3, Flag-PIAS1, or Flag-PIAS3 transfected cells, only 10-35% of nuclei fall into Bins #3 or #4 (Fig. 3.5C). These data indicate that overexpression of SUMO ligases or SUMO proteases inhibits efficient formation of E2A viral genome replication domains.

3.3 Discussion.

Our studies identify the SUMO proteases SENP1 and SENP2 as novel targets of E4-ORF3 proteins. E4-ORF3 specifically targets family members SENP1 and SENP2, as SENP3, SENP5, SENP6, and SENP7 are not mislocalized into E4-ORF3 tracks (Fig. 3.1B). The specificity E4-ORF3 has in targeting only SENP1 and SENP2 may lie in their ability to equally modulate

SUMO1 and SUMO2/3, as these are the only two SENPs that seem to show equal preference for each. We have shown that adenovirus infection induces SUMO2/3 conjugation and remodels SUMO2/3 subnuclear localization (92), but have not yet characterized SUMO1. In general, SUMO1 participates mainly in normal cell physiology and maintenance whereas SUMO2/3 is predominantly involved in the stress response (47). E4-ORF3 may play a currently unknown role in modulating SUMO1 conjugation through SENP1 and SENP2. Alternatively, E4-ORF3 may target SENP1 and SENP2 based on their location within the nucleoplasm. For example, it is unsurprising that E4-ORF3 does not target SENP3 or SENP5, as these SUMO proteases are primarily located within the nucleolus (Fig. 3.1A), and E4-ORF3 weaves around these nuclear domains (26).

We have shown that E4-ORF3 targets PIAS3, which also colocalizes with PML bodies by immunofluorescence and may be involved in their formation or maintenance. Surprisingly, E4-ORF3 does not target the SUMO protease characterized to localize with and regulate sumoylation of PML bodies, SENP6 (Fig. 3.1B)(93). This suggests that E4-ORF3 may target PIAS3 to facilitate the disruption of sumoylated proteins in PML nuclear bodies, but is targeting SENP1 and SENP2 SUMO proteases for a novel function independent of the disruption of PML bodies (94).

Using oligomerization mutants, we show that the higher order assembly of E4-ORF3 into a multivalent scaffold is required for targeting and mislocalizing SENP1 and SENP2 (Fig. 3.3A and B). E4-ORF3 is necessary and sufficient for inducing the sumoylation of the MRN complex (59, 60). We show that E4-ORF3

V101A and D105A/L106A mutants that are defective for binding and sumoylating MRN still mislocalize SENP1 and SENP2 (Fig. 3.3A and B). If MRN is a constitutive target of SENP1 or SENP2 for removal of SUMO, E4-ORF3 may induce sumoylation of MRN through the inhibition of the protease activity of SENP1 and SENP2. Furthermore, in contrast to MRN, SENP1 and SENP2 are conserved targets of E4-ORF3 proteins from disparate adenovirus subgroups (Fig. 3.4B and C).

It is very interesting to speculate why both a SUMO ligase and SUMO proteases are targets of the same adenovirus protein E4-ORF3. Post-translational modification by SUMO can induce distinct physiological consequences, yet its primary function is to control interactions of the modified protein with other proteins. The addition of SUMO to some substrates and the removal of SUMO to others does not have a zero net effect; rather, it is a means to regulate protein-protein interactions and help mediate compartmentalization. This model is supported by our results that show that overexpression of both SUMO ligases (PIAS1 and PIAS3) and SUMO proteases (SENP1, SENP2, and SENP3) inhibit the formation of E2A viral genome replication domains (Fig. 3.5A – C).

An alternative, but not mutually exclusive possibility is that E4-ORF3 mislocalizes PIAS3, SENP1, and SENP2 to modulate transcription. For example, PIAS3 regulates the activity of many transcription factors, including those involved in interferon pathways (53), and SENP2 regulates the p53/MDM2-stress

response (95). Targeting SUMO enzymes may be a means to regulate transcription and suppress the immune response that is triggered during infection.

Our findings, together with our previously published results (92), indicate that the adenovirus protein E4-ORF3 targets at least three SUMO enzymes: PIAS3, SENP1, and SENP2 (Fig. 3.1 and 3.2)(92). Furthermore, misregulation of SUMO enzymes by inducing overexpression inhibits the formation of E2A viral genome replication domains (Fig. 3.5). Together, these data indicate that sumoylation is highly regulated during Ad5 infection and that cellular SUMO enzymes may play an important role in facilitating the productive infection for all human adenoviruses.

3.4 Materials and methods.

3.4.1 Cells, culturing conditions, and viral infections.

U2OS cells were cultured in DMEM supplemented in 10% heat-inactivated FBS without antibiotics. Infection was performed at an experimentally determined multiplicity of infection (MOI) of 30 plaque-forming units (PFU) in DMEM containing 2% heat inactivated FBS.

3.4.2 Viruses.

Viruses were titered on 293/E4/pIX cells, as described previously (24). Wild type (WT) virus is Ad5.

3.4.3 Plasmids and transfections.

SENP family plasmids and Ad5 E2A were first cloned into pDONR221 and then recombined into a CMV expression vector with an N-terminal tag using the Gateway Cloning System (Invitrogen). E4-ORF3 constructs were generated as described previously (26). Lipofectamine 2000 (Invitrogen) was used for transfection of U2OS cells according to manufacturer's instructions.

3.4.4 Immunofluorescence.

Cells were fixed in 4% paraformaldehyde for 30 minutes at room temperature, permeabilized in 0.1% TritonX-100 PBS-/-, and stained as described previously (24, 25). Primary antibodies were Flag (F742 from Sigma), E4-ORF3 (6A11), Myc (71D10 from Cell Signaling Technology), and E2A (B6-8). Alexa 488-, 555- and 633-conjugated secondary antibodies (Molecular Probes) were used for detection of primary antibodies. Hoechst-33342 was used to stain DNA. Images were acquired with a Zeiss LSM780 imaging system with a 63x objective. Images are single z-planes.

3.4.5 Quantification of E2A viral genome replication domains.

Data binning was used to qualitatively measure the degree of assembly of E2A viral genome replication domains. E2A staining was divided into four groups. Bin #1 includes nuclei with a diffuse pattern of E2A and/or very small foci; Bin #2 includes nuclei with mostly diffuse E2A but with many (>5) large foci; Bin #3 includes nuclei containing mostly large foci and very little diffuse E2A; Bin #4 includes nuclei full of large foci and domains of E2A.

Table 3.1. Functions and localization of each SENP SUMO protease.

SENP	Specificity	Processing	Localization
SENP1	SUMO1 and SUMO2/3	maturation and deconjugation	nuclear pore and sub-nuclear compartments
SENP2	SUMO1 and SUMO2/3	maturation and deconjugation	nuclear pore and sub-nuclear compartments
SENP3	favors SUMO2/3	deconjugation	nucleolus
SENP5	favors SUMO2/3	maturation and deconjugation	nucleolus
SENP6	favors SUMO2/3	deconjugation and editing of SUMO2/3 chains	nucleoplasm; PML bodies
SENP7	favors SUMO2/3	deconjugation and editing of SUMO2/3 chains	nucleoplasm

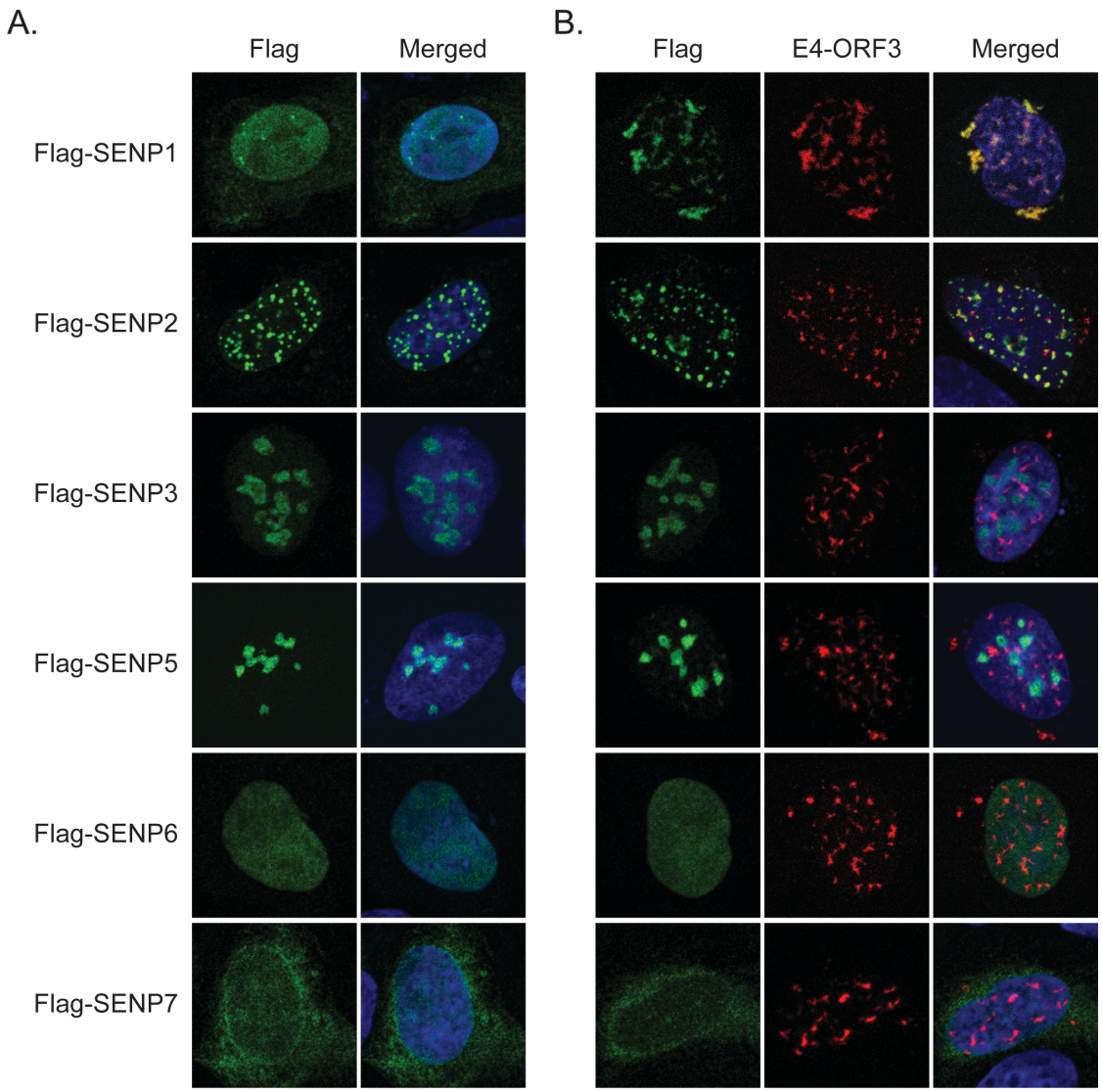

Figure 3.1. E4-ORF3 specifically targets SENP1 and SENP2 from the SENP SUMO protease family of proteins. (A) U2OS cells were transfected with Flag-tagged cDNA constructs of each SENP family member. Cells were then fixed 24 hours post transfection and immunostained for Flag (green). Nuclei were counterstained with Hoechst-33342. (B) Co-transfection of each SENP family member with E4-ORF3 under same conditions, and additionally stained for E4-ORF3 (red).

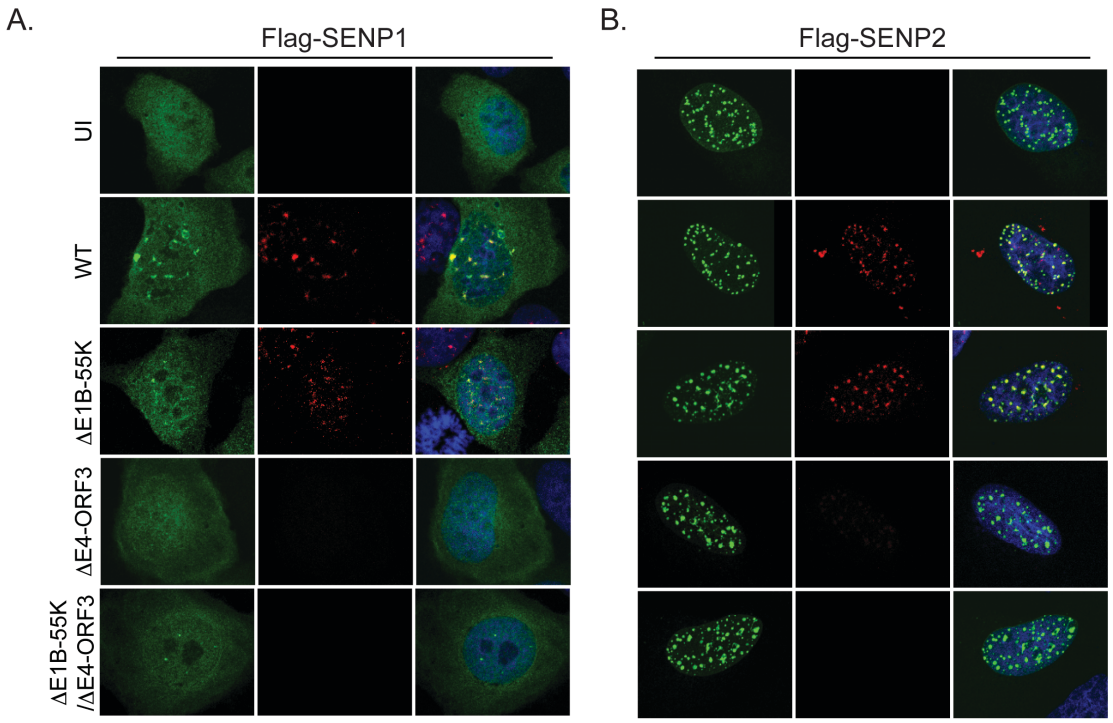

Figure 3.2. E4-ORF3 specifically targets SENP1 and SENP2 by adenovirus infection. U2OS cells were transfected with Flag-SENP1 (A) or Flag-SENP2 (B) then infected as indicated. Cells were fixed 36 h.p.i. and immunostained for Flag (green) and E4-ORF3 (red). Nuclei were counterstained with Hoechst-33342.

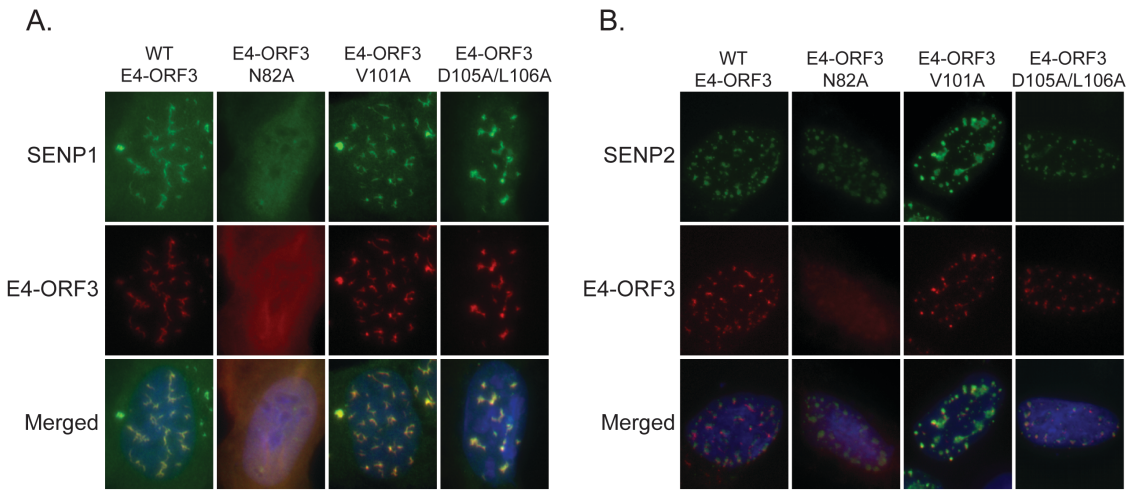

Figure 3.3. E4-ORF3 higher order assembly is required to mislocalize SENP1 and SENP2 and is independent of binding to MRN. U2OS cells were transfected with (A) Flag-SENP1 or (B) Flag-SENP2 (B) and wild type (WT) E4-ORF3, E4-ORF3 N82A, E4-ORF3 V101A, or E4-ORF3 D105A/L106A. Cells were fixed 24 hours post transfection and immunostained for Flag (green) or E4-ORF3 (red). Nuclei were counterstained with Hoechst-33342.

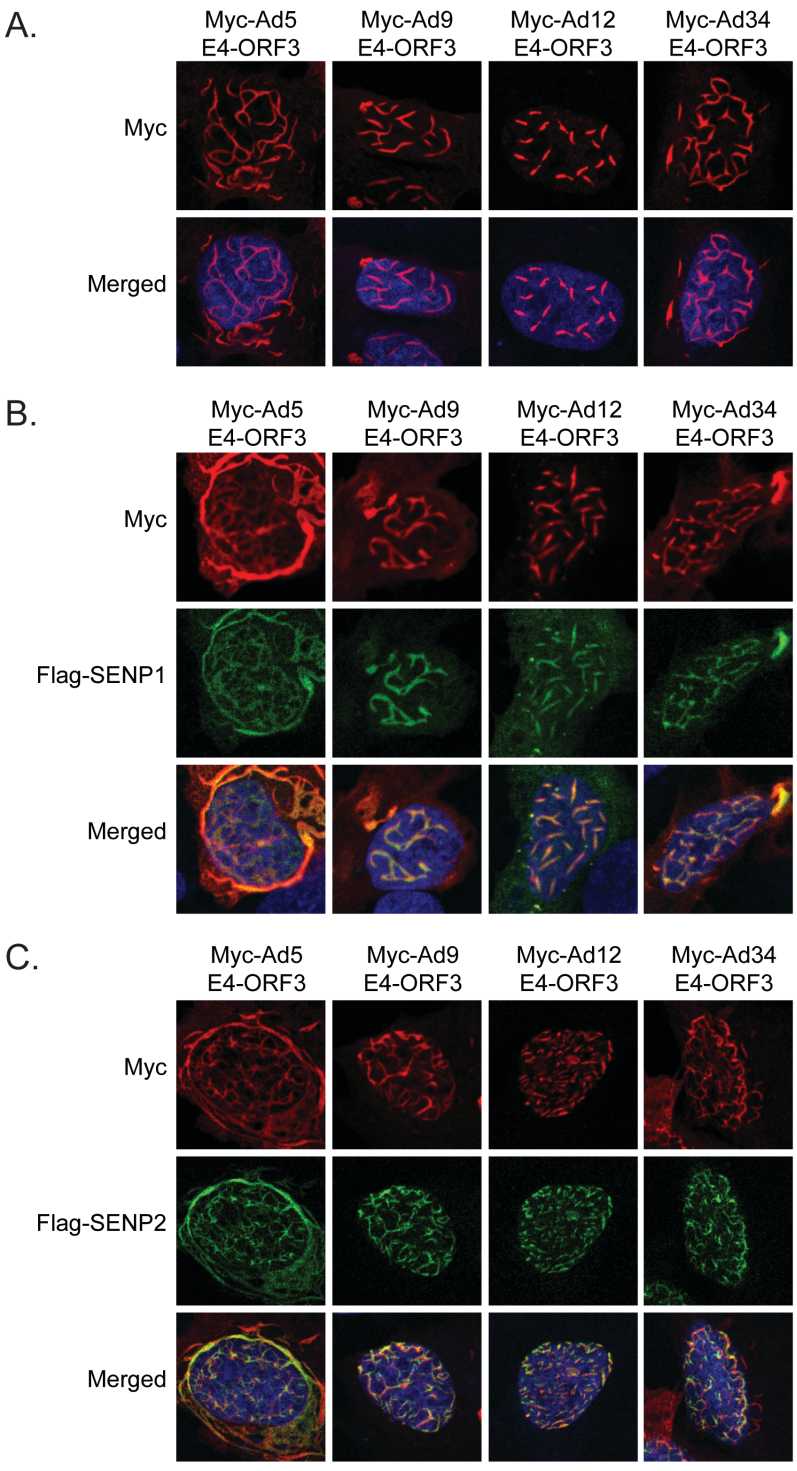

Figure 3.4. SENP1 and SENP2 are conserved targets of E4-ORF3 proteins from disparate human adenovirus subgroups. U2OS cells were transfected with Myc-tagged E4-ORF3 from Ad5, Ad9, Ad12, or Ad34 (A) alone or (B) with Flag-SENP1 or (C) Flag-SENP2. Cells were fixed 24 hours post transfection and immunostained for Flag (green) and Myc (red). Nuclei were counterstained with Hoechst-33342.

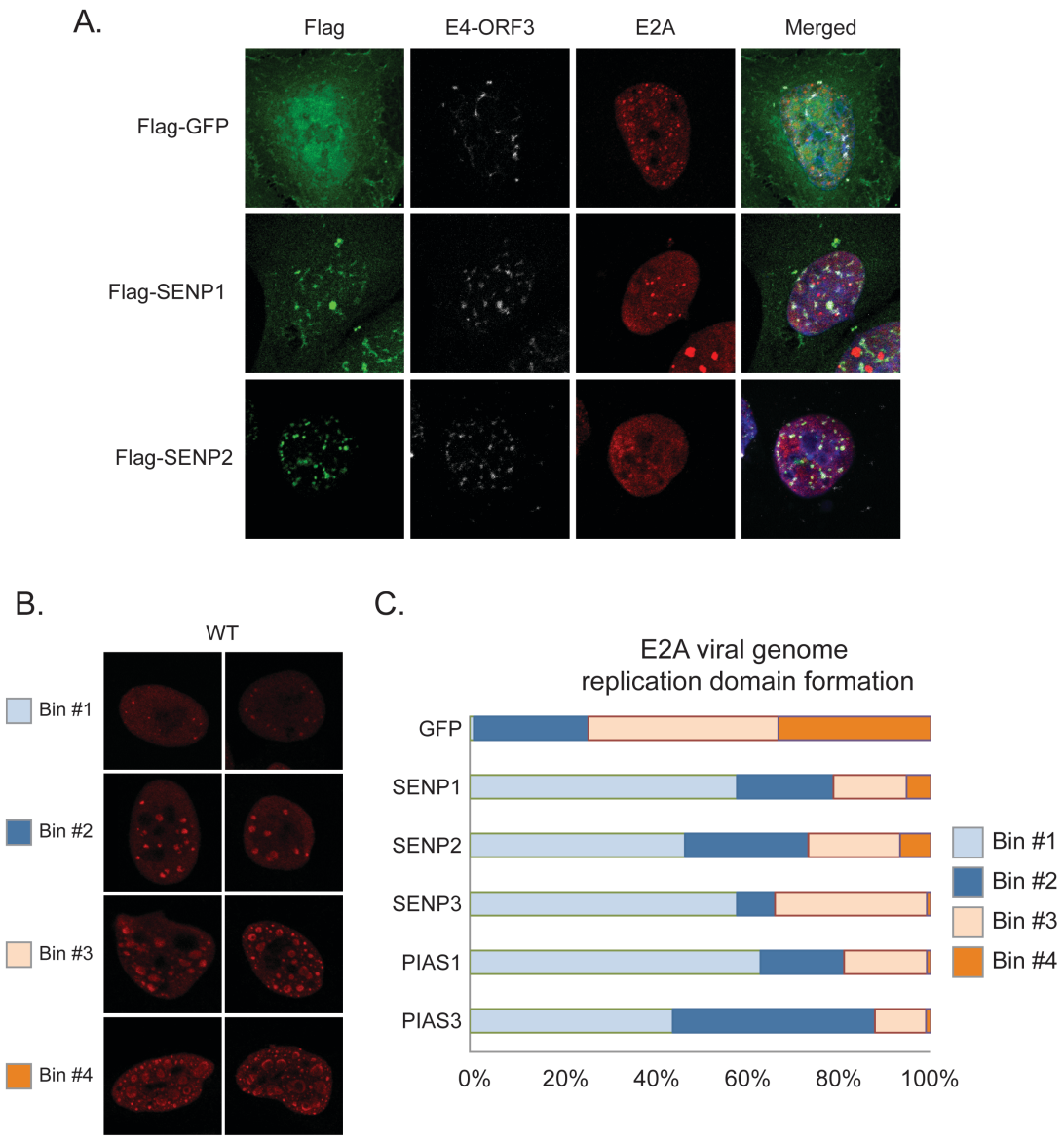

Figure 3.5. Overexpression of SUMO enzymes inhibits the formation of E2A viral replication domains. (A) U2OS cells were transfected with Flag-GFP, Flag-SENP1, or Flag-SENP2 and infected with wild-type (WT) Ad5. Cells were fixed 36 h.p.i. and immunostained for Flag (green), E4-ORF3 (white) and E2A (red). Nuclei were counterstained with Hoechst-33342. (B) Immunostaining of E2A of U2OS cells infected with WT Ad5. Two representative images of E2A viral genome replication domains from each "Bin" category are shown. (C) Distribution of each "Bin" category of E2A viral genome replication upon transfection of Flag-GFP, Flag-SENP1, Flag-SENP2, Flag-SENP3, Flag-PIAS1, or Flag-PIAS3.

Chapter 4

Sumoylation and SIMs of E2A DNA binding protein

4.1 Introduction.

Adenovirus infection induces a striking change in the nuclear distribution of SUMO2/3 at different stages in adenovirus infection. The assembly of viral genome replication domains is sufficient to induce the localization and recruitment of SUMO2/3 independently of early adenovirus proteins E1B-55K/E4-ORF3. SUMO2/3 can be recruited through non-covalent interactions with adenoviral/cellular macromolecules concentrated at E2A viral replication domains (92). However, the structural basis for E2A domains is poorly understood. E2A viral replication domains exhibit dramatic morphological differences and variations in size and number over the course of the viral lifecycle (58). One unexplored possibility is that viral proteins involved in genomåe replication, such

as E2A, contain sumoylation sites or SIMs. Therefore, SUMO-SIM interactions may explain the dynamic changes in nuclear architecture.

Early E2A DNA-binding protein (E2A) is a 1591 amino acid protein that is essential for adenovirus replication. E2A can bind both single-stranded DNA (96) and double-stranded DNA (97). In addition to DNA replication, E2A plays roles in RNA stability (98), transformation (99), and virion assembly (100). E2A is anisometric and is commonly divided into two domains. The N-terminus domain (residues 1-173) has a high proportion of proline as well as clusters of acidic and basic residues (101), and is highly phosphorylated (102). While no single phosphorylation site seems to be critical for viral growth, ablation of 8 or more sites leads to reduced viability (103), suggesting that the overall charge is more important than a particular modification. The C-terminal part of E2A (residues 174-529) is highly conserved among adenovirus subgroups (104) and is sufficient for viral DNA binding and DNA replication *in vitro* (105). The atomic structure of the E2A C-terminal DNA binding domain reveals that the C-terminal domain is mainly globular and has a C-terminal hook of 17 amino acid residues (106) that drives E2A to form protein filaments by multimerizing adjacent molecules.

Here we show that adenovirus protein E2A is itself sumoylated and has one or more SIMs that are involved in the formation of viral genome replication domains.

4.2 Results.

4.2.1 SUMO2 IP reveals sumoylation of adenovirus protein E2A.

Our previous work revealed that SUMO2/3 is recruited upon formation of E2A viral genome replication domains, and can occur independently of SUMO conjugation (Fig. 2.1)(92). We also observe that overexpression of SUMO ligases and proteases inhibits the formation of adenovirus genome replication domains (Fig. 3.5), suggesting that sumoylation is involved in their assembly. Therefore, we questioned whether proteins involved in the formation of viral genome replication domains, such as the E2A DNA binding protein, utilize sumoylation and/or protein-protein interactions via SIMs for assembly.

To determine if E2A associates with SUMO2/3, we performed immunoprecipitation analysis through SUMO2. To enrich for sumoylated proteins, we first transfected U2OS cells with Flag-SUMO2. Cells were left uninfected or infected with WT Ad5, lysed at 36 h.p.i., then subjected first to immunoprecipitation through Flag and then Western blot analysis. Blotting against Flag reveals an enrichment of sumoylated proteins in WT infection indicated by a high molecular weight smear, consistent with our previous results (92). The predicted molecular weight of E2A is 59 kDa, but runs on SDS-page gels at apparent weight of 72 kDa (101). The molecular weight of SUMO2 is 11 kDa; however the apparent size increase for each SUMO in SDS-PAGE is typically 15-17 kDa. Upon blotting against E2A, we find several bands that correspond with increases in MW of ~17 kDa, consistent with the predicted size of Flag-SUMO2 (Fig. 4.1). Multiple bands indicate that E2A has multiple sumoylation sites or has multiple SUMO proteins conjugated to a single lysine

residue.

4.2.2 Exogenously expressed Myc-E2A is sumoylated independently of Ad5 WT infection.

To determine whether E2A is sumoylated by a viral or cellular protein, we took advantage of a cDNA construct expressing a Myc-tagged E2A protein. U2OS cells were transfected with Flag-SUMO2 with and without Myc-E2A, then left uninfected or infected with WT Ad5. Lysates were harvested at 36 h.p.i. and Flag-SUMO2 immunoprecipitation was performed. We found that even in uninfected cells, multiple bands could be detected when blotting for E2A in Flag-immunoprecipitated samples, similar to WT (Fig. 4.2). We conclude that E2A can be sumoylated independently of adenovirus infection, and that a cellular, not viral, SUMO ligase is involved in sumoylating E2A.

4.2.3 Knockdown of E2 SUMO ligase UBC9 ablates sumoylation of Myc-E2A.

Our results indicate that E2A is constitutively sumoylated independently of adenovirus infection. This suggests that a cellular SUMO ligase mediates its sumoylation. To confirm this, we knocked down the central E2 SUMO ligase UBC9 by infecting U2OS cells with a lentivirus containing shRNA against UBC9. Western analyses confirm that protein levels of UBC9 are substantially decreased, and that sumoylation of Myc-E2A is ablated (Fig. 4.3). We conclude that UBC9 is required for sumoylation of E2A. However, we cannot conclude whether UBC9 itself sumoylates E2A or whether a downstream cellular E3

SUMO ligase targets E2A for sumoylation.

4.2.4. Overexpression of SENP1 and SENP2 ablates sumoylation of Myc-E2A.

We hypothesized that if E2A is in fact sumoylated, then overexpression of SENP1 and SENP2 would also inhibit sumoylation of E2A. This would be consistent with our immunofluorescence results, which show that SENP1 and SENP2 overexpression ablate proper E2A domain formation (Fig. 3.5). To test this, we co-transfected U2OS cells with Flag-SUMO2 and Myc-E2A and overexpressed SENP1 or SENP2 using GFP-tagged cDNA constructs. In cells overexpressing SENP1 or SENP2, overall sumoylation is decreased, as detected by staining for Flag. Importantly, E2A bands corresponding with an increase in molecular weight due to sumoylation are ablated (Fig. 4.4). These findings indicate that sumoylation of E2A is reversible by overexpression of a SUMO protease. Importantly, these results suggest that overexpressing SENP1 or SENP2 may inhibit the formation of E2A domains by inducing its desumoylation.

4.2.5. Adenovirus protein E2A is sumoylated on the C-terminus.

To predict if E2A is target of sumoylation we used an algorithm that identifies potentially sumoylated sites (107). We predicted dozens of possible lysines that could be sumoylated throughout the entire E2A protein (Table 4.1). To narrow down identification of the sumoylation sites on E2A, we cloned individual E2A domains into Myc tag expression plasmids: we generated E2A

containing the N-terminus alone (Myc-E2A N-term), the C-terminus alone (Myc-E2A C-term), and the C-terminus alone without the multimerizing 'hook' (Myc-E2A C-termΔHook) (Fig. 4.5). Transfection of these fragments into U2OS reveals that the Myc-E2A N-term is nuclear diffuse and both the Myc-E2A C-term and Myc-E2A C-termΔHook are mainly cytoplasmic due to the nuclear localization signals being on the N-terminus (Fig. 4.6A)(108). Strikingly, transfection of Myc-E2A fragments followed by infection of WT Ad5 reveals that expression of Myc-E2A N-term prevents the assembly of endogenous Ad5 E2A domains. This suggests that overexpression of the N-terminus of Ad5 E2A can act as a dominant negative, preventing assembly of adenovirus genome replication domains. Myc-E2A C-term, which contains the DNA binding domain, is able to assemble into domains indiscriminately from endogenous Ad5 E2A. Myc-E2A C-termΔHook fails to assemble due to lack of multimerization with endogenous Ad5 E2A (Fig. 4.6B).

To determine if N- and C-terminal fragments are sumoylated, we co-transfected Flag-SUMO2 with Myc-tagged E2A fragments and performed immunoprecipitation of Flag-SUMO2. We show that the E2A N-terminal domain is not sumoylated as it is not pulled down with Flag-SUMO2. In contrast, we demonstrate that the E2A C-terminus and E2A C-termΔHook are immunoprecipitated through Flag-SUMO2. We conclude that the E2A globular C-terminus is a target of sumoylation and does not require the C-terminal Hook domain (Fig. 4.7). These data demonstrate that sumoylation of the C-terminus could play an important role in the assembly of E2A domains in absence of the

multimerizing Hook.

4.2.6 Potential E2A SIM domains.

Our previous results show that even a conjugation-deficient 4x-SUMO2 construct is sufficient to be recruited to E2A viral genome replication domains (92). This indicates that SUMO is being recruited through other viral/cellular proteins in these domains. We hypothesized that E2A may not only be sumoylated but itself contain one or more SIMs that drive assembly for viral genome replication domains analogous to cellular bodies such as PML. For example, PML is conjugated to SUMO and contains SIM motifs that drive PML assembly into nuclear bodies (48). Sumoylation is critical for the assembly of PML nuclear bodies and the recruitment of additional SUMO-SIM proteins such as DAXX and Sp100 (49-51). Therefore, we used an algorithm similar to the one that identified sumoylation sites to identify potential SIMs on Ad5 E2A (109). Here, we identified six potential SIMs throughout E2A, with three on the unstructured N-terminus and three on the DNA-binding C-terminal domain (Fig. 4.8A and B).

4.2.7 Putative SIMs on adenovirus protein E2A are required for assembly into viral genome replication domains.

To determine if the putative SIMs of E2A are required for assembly of viral genome replication domains, we synthesized a construct of Ad5 E2A with mutations in each 4-residue SIM motif, changing each (i.e., VIVD) to alanine

residues (AAAA). We expressed a Myc-tagged WT and E2A 6xSIM mutant in the same plasmid as used for the WT Myc-E2A. Then we transfected U2OS with WT Myc-E2A E2A or Myc-E2A 6xSIM, infected with Ad5, and fixed at 36 h.p.i. to visualize viral genome replication domains. Immunostaining with both Myc and E2A reveals that cells with WT Myc-E2A can co-assemble into domains with the non-tagged endogenous Ad5 E2A protein. In contrast, Myc-E2A 6xSIM does not assemble into viral genome replication domains that are formed by the virus-encoded E2A protein. Instead, Myc-E2A 6xSIM is nuclear diffuse and is excluded from viral genome replication domains. These data indicate that mutation of these residues, identified as potential SIMs of E2A, are required for assembly of adenovirus genome replication domains.

4.3 Discussion.

Here, we show that E2A is constitutively sumoylated outside the context of viral infection (Fig. 4.2). Both knockdown of the central E2 SUMO ligase UBC9 (Fig. 4.3) and overexpression of SUMO proteases SENP1 and SENP2 (Fig. 4.4) ablate sumoylation of E2A. There are dozens of predicted sumoylation sites in the C-terminus of E2A, and six potential SIMs throughout the protein. Mutation of the potential SIMs prevent assembly of viral genome replication domains, suggesting a role of SUMO-SIM protein interactions for propagation of Ad5.

Here we reveal that early adenovirus proteins are not required for sumoylation of E2A, as Myc-tagged E2A in untreated cells is constitutively sumoylated (Fig. 4.2). However, immunofluorescence reveals that transfection of

Myc-E2A into untreated U2OS cells is nuclear diffuse. Therefore, sumoylation of E2A alone is not sufficient to form domains, which indicates a nucleating event must occur first. Others have shown that newly synthesized viral DNA genomes are displaced from replication domains and spread into the surrounding neoplasm, where they are used as templates for transcription (79). The C-terminal Hook may be required for nucleating E2A on single strand DNA, but upon dissociation, the E2A domains are stabilized through SUMO-SIM interactions. Therefore, SUMO-SIM interactions may be necessary for maintaining late E2A domains and/or regulating transcription and splicing.

Our previous results revealed that E1B-55K and E4-ORF3 have novel roles in determining the structure and nuclear compartmentalization of E2A viral replication domains. While E1B-55K and E4-ORF3 are not required for sumoylation of E2A directly, E1B-55K and E4-ORF3 may help modulate SUMO-SIM interactions and recruit other sumoylated proteins to specify the function and dynamic structural re-organization of viral replication and transcription/splicing centers. This could play an important role in compartmentalizing and catalyzing different activities in the course of the viral lifecycle.

We have shown that SUMO2 can be recruited to E2A viral genome replication domains though non-covalent interactions with cellular and/or viral proteins (92) and have identified six potential SIMs on E2A (Fig. 4.8A). With which sumoylated protein(s) the SIMs of E2A interact remains to be determined. One likelihood is that the SIMs of one E2A molecule interact with sumoylated sites on adjacent E2A molecules to drive subnuclear body assembly, similar to

how PML nuclear bodies form (48). This model is consistent with our results that both removal of SUMO (by overexpressing SENPs) from E2A and ablation of SIMs (by mutagenesis) inhibit assembly of E2A bodies (Fig. 3.5C and Fig. 4.9).

E2A viral replication domains exhibit dramatic morphological differences and variations in size and number over the course of the viral lifecycle (58). The structural basis for these differences in E2A domains and functional consequences is poorly understood. Early confocal microscopy studies indicate that the morphologies of E2A domains associated with sites of single strand and double strand viral genome accumulation are distinct (79). In addition, these studies suggested that viral DNA replication and transcription/splicing are spatially and functionally separated by distinct E2A domains at specific sites in the nucleus (79). SUMO-SIM interactions between E2A and other proteins involved in replication could play an important role in compartmentalizing and catalyzing different activities in the course of the viral lifecycle. Defining what these interactions are may determine how the morphology and function of various E2A viral genome replication domains is determined. Creating an adenovirus with point SUMO mutants and SIM mutants in E2A could help reveal how adenovirus genome domains are formed morphologically, and how structure dictates function.

4.4 Materials and methods.

4.4.1 Cells, culturing conditions, and viral infections.

U2OS cells were cultured in DMEM supplemented in 10% heat-inactivated

FBS without antibiotics. Infection was performed at an experimentally determined multiplicity of infection (MOI) of 30 plaque-forming units (PFU) in DMEM containing 2% heat inactivated FBS.

4.4.2 Viruses.

Viruses were titered on 293/E4/pIX cells, as described previously (24). Wild type (WT) virus is Ad5. The ΔE1B-55K virus (AdSyn-CO124) was created by mutating the start codon of E1B-55K (ATG to GTG) and I90 of E1B-55K to a stop codon (ATT to TAG). The ΔE4-ORF3 virus (AdSyn-CO118) was created by deleting the coding region of E4-ORF3. The ΔE1B-55K/ΔE4-ORF3 virus (AdSyn-CO140) is the same as ΔE1B-55K except the E4-ORF3 coding region is also deleted (26).

4.4.3 Plasmids and transfections.

WT Ad5 E2A and Ad5 E2A fragments were first cloned into pDONR221 and then recombined into a CMV expression vector with an N-terminal tag using the Gateway Cloning System (Invitrogen). Ad5 E2A 6xSIM was synthesized by Integrated DNA Technologies before being cloned into pDONR221. Lipofectamine 2000 (Invitrogen) was used for transfection of U2OS cells according to manufacturer's instructions.

4.4.4 Immunofluorescence.

Cells were fixed in 4% paraformaldehyde for 30 minutes at room

temperature, permeabilized in 0.1% TritonX-100 PBS-/-, and stained as described previously (24, 25). Primary antibodies were E4-ORF3 (6A11), Myc (71D10 from Cell Signaling Technology), and E2A (B6-8). Alexa 488-, 555- and 633-conjugated secondary antibodies (Molecular Probes) were used for detection of primary antibodies. Hoechst-33342 was used to stain DNA. Images were acquired with a Zeiss LSM780 imaging system with a 63x objective. Images are single z-planes.

4.4.5 Protein lysates, immunoprecipitation, and Western analysis.

Protein lysates were harvested in sample buffer containing 50mM Tris pH 8, 2% SDS, 10% glycerol, 100mM dithiothreitol, and 0.1% Bromophenol Blue. Lysates were boiled for 10 minutes and sonicated. For immunoprecipitation, lysates were prepared in TBS (50 mM Tris HCl pH 8.0, 15 mM NaCl, 2 mM Na_3VO_4, 100 mM NaF, 1 mM PMSF, 10 mM NEM) with 1% SDS. Lysates were boiled for 10 minutes and sonicated. Immunoprecipitation was performed in TBS containing 0.1% SDS and 1% Triton-X by adding 20 ml M2 Flag magnetic beads (Sigma) and rocking overnight. Beads were washed with TBS + 1% Triton-X + 0.1% SDS, then TBS + 1% Triton-X + 0.5 mM LiCl, then TBS + 1% Triton-X. Immunoprecipitation was eluted in sample buffer. For Western blot, samples were analyzed by SDS-PAGE and transferred to nitrocellulose membranes. The membranes were blocked using 5% milk. Primary antibodies were Flag (F742 from Sigma), Myc (9E10 from Roche), E2A (B6-8), GFP (FL from Santa Cruz Biotechnology), and β-Actin (AC-15 from Sigma). β-Actin expression was used

as a loading control. Primary antibodies were detected with secondary antibodies labeled with either IRDye800 (Rockland), or Alexa Fluor 680 (Molecular Probes). Fluorescent antibodies were visualized using a LI-COR-Odyssey scanner.

4.4.6 Prediction of SUMO binding sites and SIMs.

To predict potential sumoylation residues and SIMs, we utilized the prediction algorithm GPS-SUMO 1.0 with the lowest possible threshold for each (107).

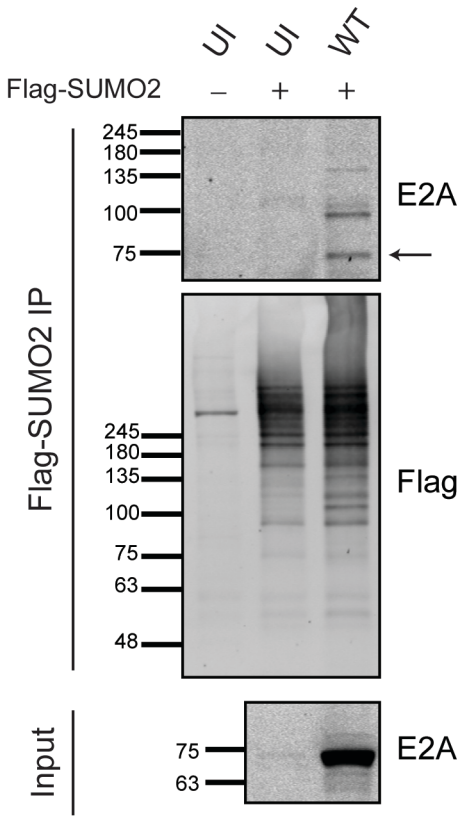

Figure 4.1. Adenovirus protein E2A associates with SUMO2 by immunoprecipitation. U2OS cells were transfected with Flag-SUMO2 as indicated then left uninfected (UI) or infected with wild-type (WT) Ad5. Cells were lysed at 36 h.p.i. and immunoprecipitation for Flag was performed. Western analysis for E2A reveals association with Flag-SUMO2 at distinct bands above where E2A normally runs at 72 kDa. Arrow indicates non-specific band.

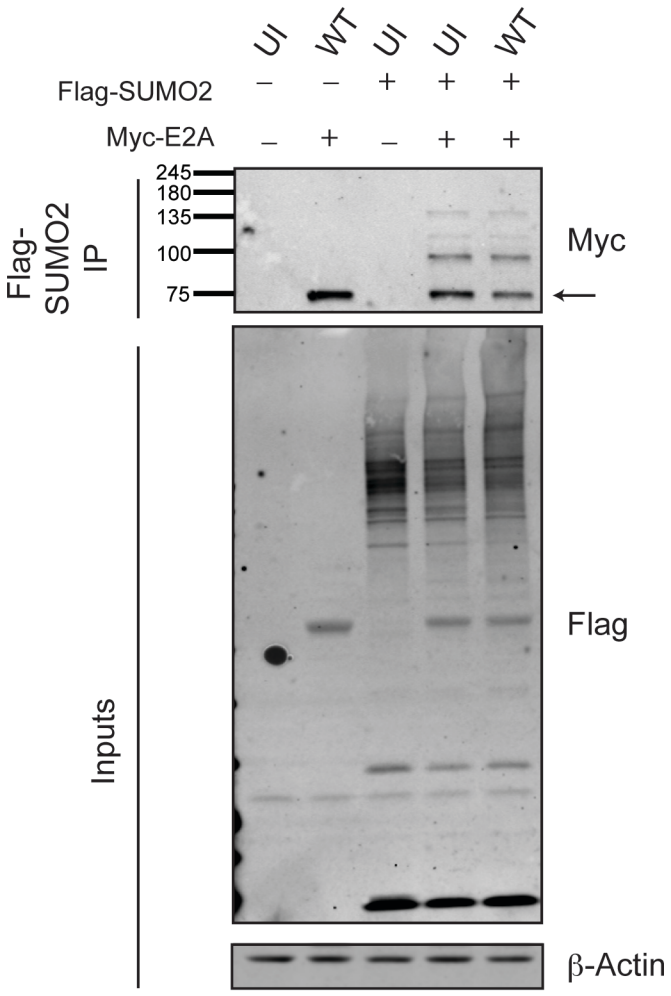

Figure 4.2. Exogenously expressed Myc-E2A associates with SUMO2 independently of adenovirus infection. U2OS cells were transfected with Flag-SUMO2 and Myc-E2A as indicated then left uninfected or infected with WT Ad5. Cells were lysed at 36 h.p.i. then immunoprecipitation for Flag was performed and subjected to immunoblot for Myc and Flag. β-Actin is a loading control. Arrow indicates non-specific band.

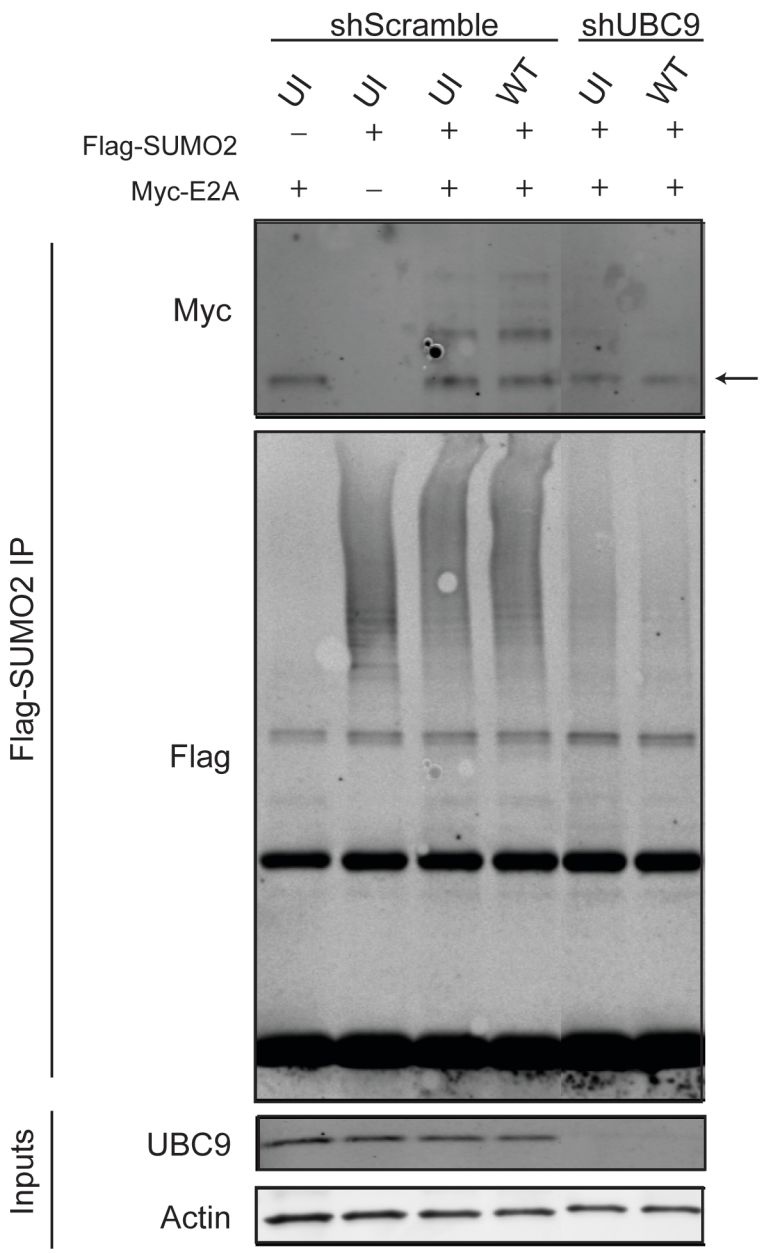

Figure 4.3. Knockdown of UBC9 ablates sumoylation of Myc-E2A. U2OS cells infected with lentiviruses containing either shRNA against a Scramble sequence or UBC9. Cells were then transfected with Flag-SUMO2 and Myc-E2A as indicated. Cells were then left uninfected or infected with WT Ad5. Cells were lysed at 36 h.p.i. then immunoprecipitation for Flag was performed and subjected to immunoblot for Myc and Flag. β-Actin is a loading control. Arrow indicates non-specific band.

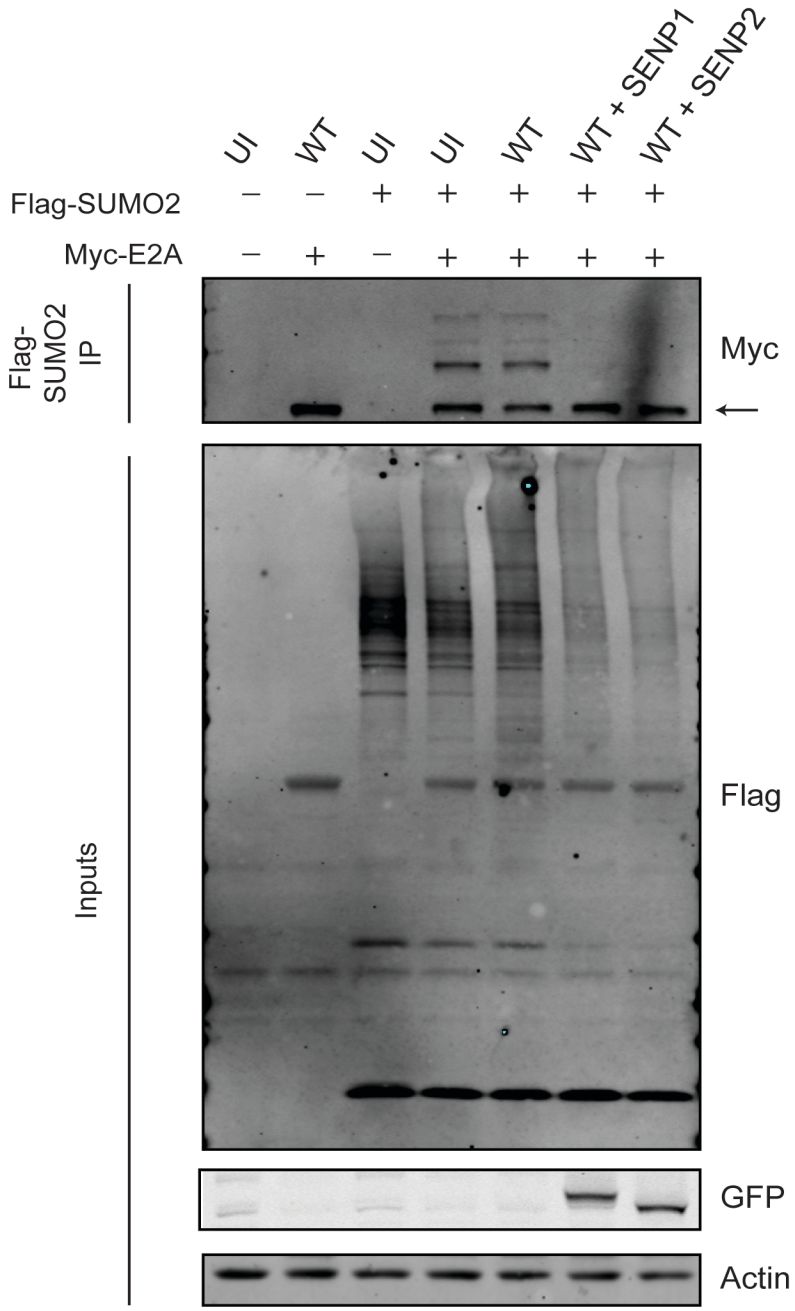

Figure. 4.4. Overexpression of SENP1 or SENP2 ablates sumoylation of Myc-E2A. U2OS cells were transfected with Flag-SUMO2, Myc-E2A, and GFP-SENP1 or GFP-SENP2 as indicated. Cells were then left uninfected or infected with WT Ad5. Cells were lysed at 36 h.p.i. then immunoprecipitation for Flag was performed and subjected to immunoblot for Myc and Flag. GFP confirms expression of GFP-SENP1 and GFP-SENP2; β-Actin is a loading control. Arrow indicates non-specific band.

Table 4.1. Predicted sumoylation sites of Ad5 E2A protein. SUMOsp software was used to utilize an algorithm to predict potential sumoylation sites of adenovirus 5 E2A. Table includes all of the amino acid residues predicted to be a sumoylation site.

Position	Peptide	Score	Type
44	APPKKRM	1.853	TypeII: Non-consensus
45	PPKKRMR	2.397	TypeII: Non-consensus
85	IAPKKKK	1.485	TypeII: Non-consensus
86	APKKKKK	2.015	TypeII: Non-consensus
87	PKKKKKR	2.515	TypeII: Non-consensus
88	KKKKKRP	1.882	TypeII: Non-consensus
89	KKKKRPS	2.147	TypeII: Non-consensus
94	PSPKPER	0.9	TypeI: Ψ-K-X-E
129	VLIKHGK	1.029	TypeII: Non-consensus
132	KHGKGGK	1.103	TypeII: Non-consensus
135	KGGKRTV	1.412	TypeII: Non-consensus
183	AWEKGME	0.706	TypeII: Non-consensus
194	LMDKYHV	0.676	TypeII: Non-consensus
202	NDLKANF	2.721	TypeII: Non-consensus
206	ANFKLLP	1.412	TypeII: Non-consensus
220	AVCKTWL	0.676	TypeII: Non-consensus
238	TSNKTFV	1.5	TypeII: Non-consensus
261	VTYKHHE	1.074	TypeII: Non-consensus
283	GELKCLH	1.5	TypeII: Non-consensus
293	MINKEHV	1.75	TypeII: Non-consensus
311	RALKEQS	2.279	TypeII: Non-consensus
316	QSSKAKI	1.412	TypeII: Non-consensus
318	SKAKIVK	1.103	TypeII: Non-consensus
321	KIVKNRW	1.132	TypeII: Non-consensus
353	FSGKSCG	0.25	TypeII: Non-consensus
364	EGAKAQV	1.691	TypeII: Non-consensus
370	VAFKQIK	1.397	TypeII: Non-consensus
373	KQIKAFM	2.794	TypeII: Non-consensus
401	CNSKPGH	0.75	TypeII: Non-consensus
414	QLPKLTP	1.162	TypeII: Non-consensus
434	ISDKSVL	0.926	TypeII: Non-consensus
470	CDFKISA	1.015	TypeII: Non-consensus
503	PEFKWST	1.25	TypeII: Non-consensus
507	WSTKHQY	0.868	TypeII: Non-consensus

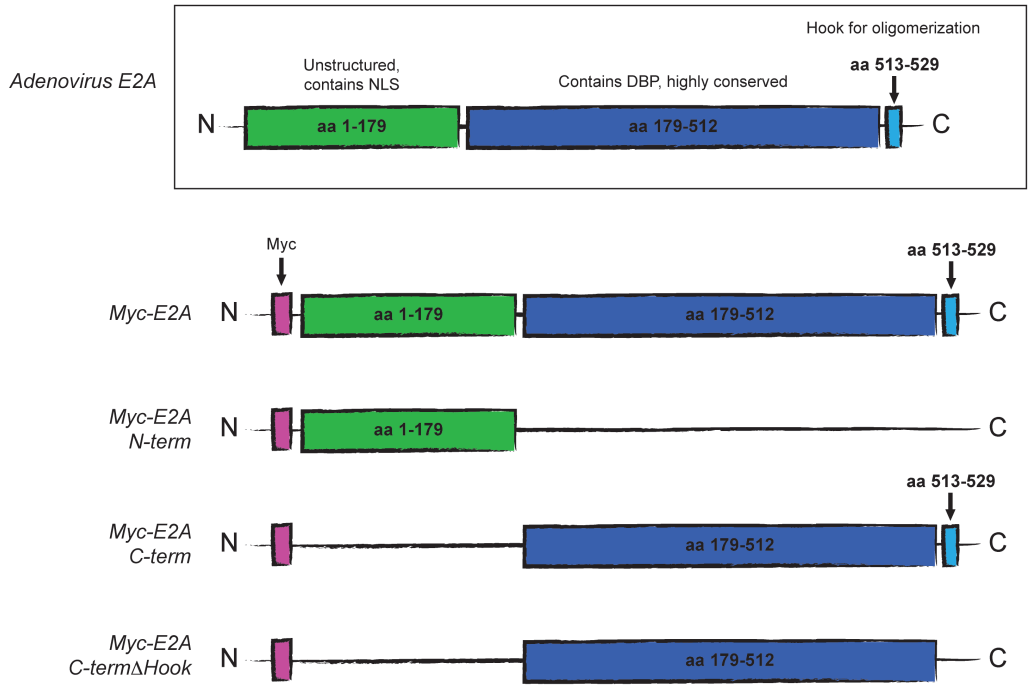

Figure. 4.5. Schematic of Ad5 Myc-E2A fragments.

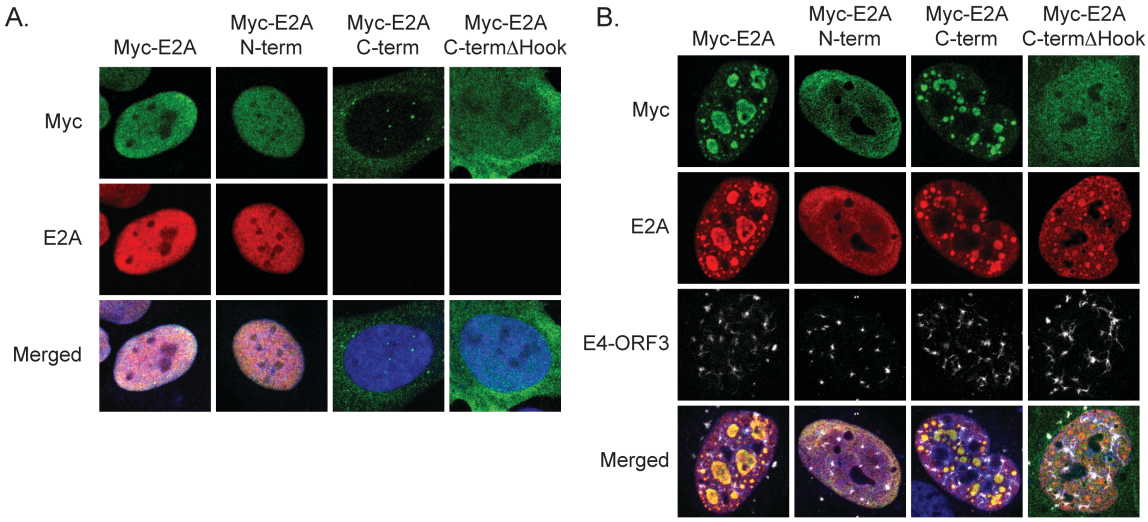

Figure 4.6. C-terminus with multimerizing 'hook' is sufficient for adenovirus genome replication domain assembly. U2OS cells were transfected with Myc-E2A fragments as indicated and (A) left uninfected or (B) infected with WT Ad5. Cells were then fixed 36 h.p.i. and immunostained for Myc (green), E2A (red), or E4-ORF3 (white). Nuclei were counterstained with Hoechst-33342.

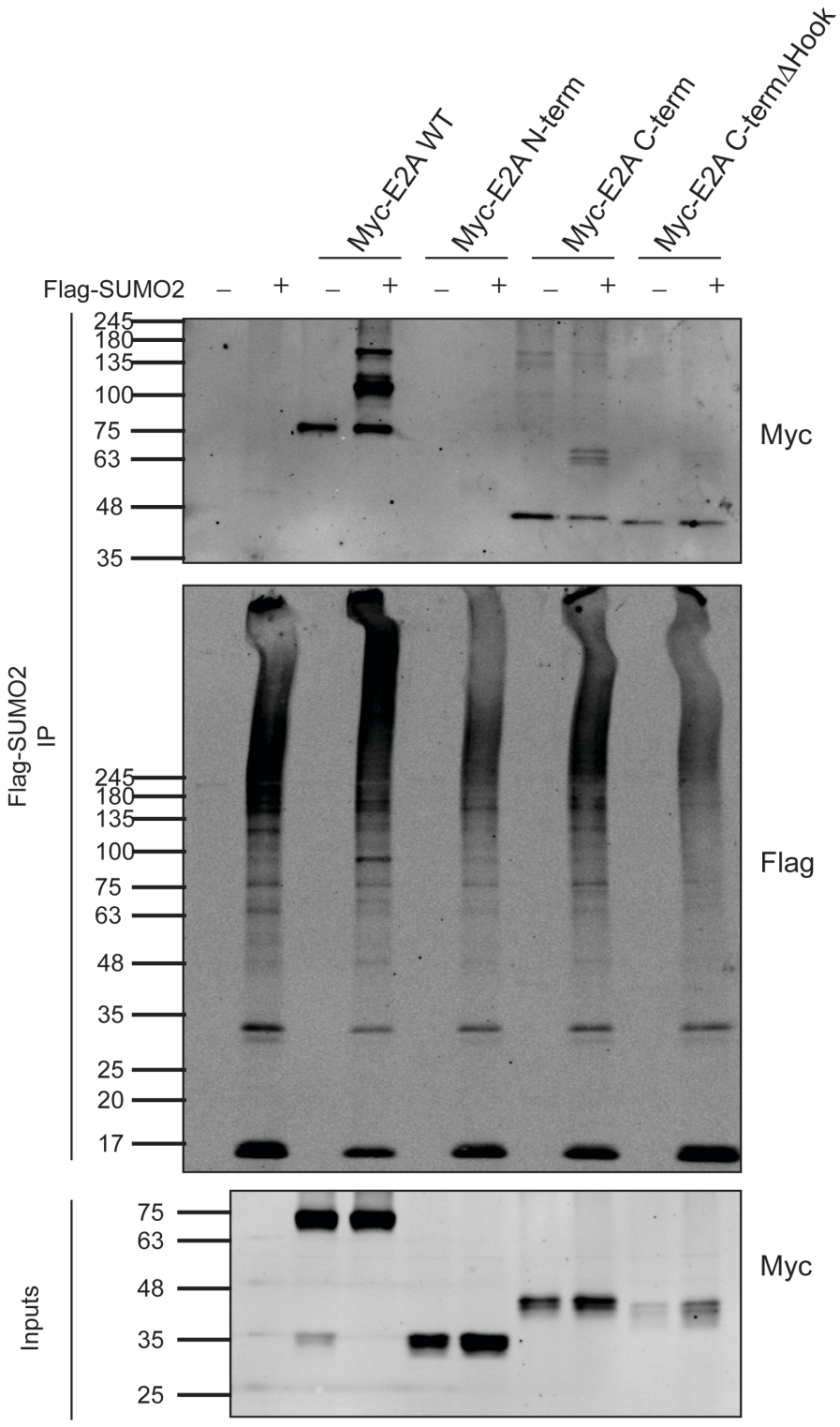

Figure 4.7. The C-terminus of Ad5 E2A is sumoylated. U2OS cells were transfected with Flag-SUMO2, and Myc-E2A fragments as indicated. Cells were lysed at 24 hours post transfection then immunoprecipitation for Flag was performed and subjected to immunoblot for Myc and Flag.

A.

Amino Acids	SIM sequence	Score
103 - 106	PPSPE **VIVD** SEEER	6.109
126 - 129	FSNPP **VLIK** HGKGG	2.609
175 - 178	MNPLS **VPIV** SAWEK	2.891
328 - 331	RWGRN **VVQI** SNTDA	3.935
445 - 448	VHHPA **LIVF** QCCNP	1.522
480 - 483	DLLNA **LVMV** RSLWS	1.391

B.

Figure 4.8. Predicted SIMs of Ad5 E2A protein. SUMOsp software was used to utilize an algorithm to predict potential SIMs of adenovirus 5 E2A. (A) Table includes all of the amino acid residues predicted to be a SIM, with SIMs in bold. (B) Schematic of the E2A protein, with asterisks indicating the location of predicted SIMs. Green indicates non-structured, high phosphorylated N-terminal domain, dark blue indicates DNA-binding domain, and light blue indicates C-terminal “hook” required for multimerization.

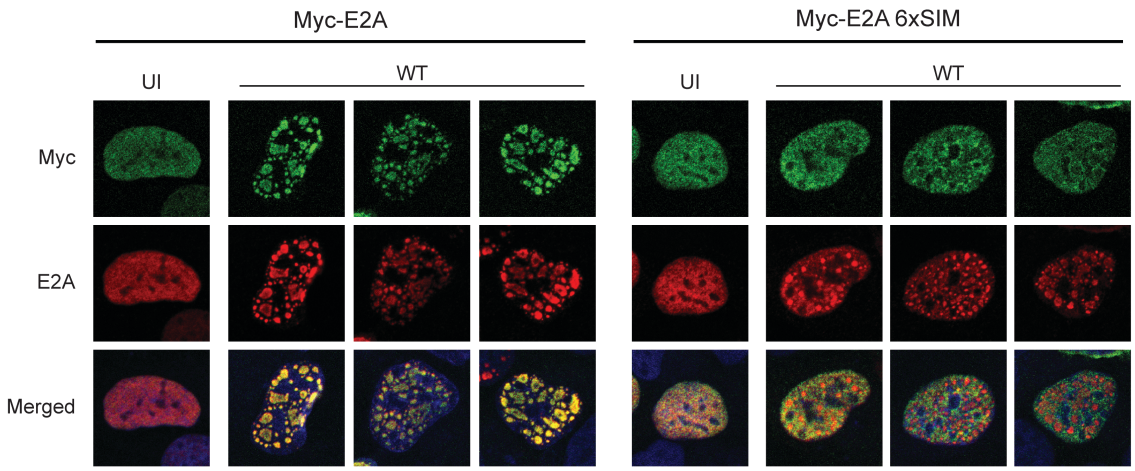

Figure 4.9. Mutation of predicted SIMs on E2A prevents its accumulation into viral genome replication domains in the nucleus. U2OS cells were transfected with Myc-E2A or mutant Myc-E2A 6xSIM then left uninfected (UI) or infected with wild-type (WT) Ad5. Cells were fixed 36 h.p.i. and immunostained for Myc (green) and E2A (red). Nuclei were counterstained with Hoechst-33342.

Chapter 5

Adenovirus mediates chromatin remodeling and gene silencing at antiviral promoters

5.1. Introduction.

During adenovirus infection, the nucleus undergoes drastic changes in nuclear architecture. As the virus replicates, E2A viral replication domains take over most of the space in the nucleus, and cellular subnuclear bodies such as PML are disrupted. Importantly, viral replication is also likely to have drastic effects on the 3D compartmentalization of the host genome. Our previous results reveal that adenovirus proteins E1B-55K and E4-ORF3 target the SUMO pathway (92). Usurping the SUMO pathway can be one way that E4-ORF3 and E1B-55K are able to disrupt cellular subnuclear bodies, assemble E2A viral replication domains, and regulate transcription. However, E4-ORF3 and E1B-55K converge on the other pathways as well to regulate transcriptional of cellular genes. E1B-55K and E4-ORF3 converge in disrupting the MRE11/RAD50/NBS1

(MRN) complex and preventing p53 activated transcription via independent mechanisms (28, 32). Here we will explore the role of epigenetics and chromatin compaction in modulating transcription during adenovirus infection.

Epigenetic gene regulation is a complex yet elegant system that is still in relatively early stages of exploration by the scientific community. Our current understanding of how epigenetic silencing is targeted in somatic human cells is limited as there is no dynamic system in which to study such a process or interrogate the key mechanisms and cellular targets that induce de novo epigenetic silencing. As such, we are left studying the aftermath of silencing in cancer and attempting to reverse a process of which we have very little knowledge. The significance of this is further underscored by the potential for translating such knowledge into novel and more effective cancer therapies. One promising cancer therapy is the development of adenoviruses that are engineered to specifically eradicate cancer cells. E1B-55K destroys p53 by inducing p53 degradation. It was proposed that an adenovirus mutant (ONYX-015) that does not have E1B-55K to inactivate p53 would only replicate in p53 deficient tumor cells, creating a tumor-selective virus. On this premise, ONYX-015 was tested in clinical trials as a p53 cancer therapy. However, we discovered that while the loss of E1B-55K induced high p53 levels and stability, p53 activity was still inhibited in adenoviral infected normal cells (32). This effect is due to the adenoviral protein E4-ORF3 that E4-ORF3 that prevents p53 activation irrespective of p53 protein levels by inducing heterochromatin formation at anti-viral target promoters, preventing binding of transcription factors to target genes

for activation. Using E4-ORF3 expression in somatic mammalian cells as a biochemical probe can enable the observation of heterochromatin formation in real time. This powerful and unique approach can overcome the previous limitation of deducing post hoc the mechanisms and processes of gene silencing and how changes in chromatin structure regulate transcription.

E4-ORF3 forms a nuclear structure that weaves throughout the nucleus and shows strong specificity to repressing p53 and anti-viral target genes. E4-ORF3 prevents transcriptional activation of 265 genes by a log-fold change of two or more in ΔE1B-55K cells (32). In addition to the p53 pathway, there is significant overrepresentation of genes associated with immune modulation and tissue remodeling, suggesting E4-ORF3 may target p53 promoters as part of a general anti-viral transcriptional silencing program. The distinctive web-like structure formed by E4-ORF3 is reminiscent of the nuclear matrix. This structure demarcates de novo heterochromatin domains, and is for the most part adjacent to H3K9me3, indicating that it may provide a platform to catalyze heterochromatin formation and epigenetic modifications through transient or long-range interactions.

E4-ORF3 induces de novo H3K9me3 heterochromatin formation at p53 target promoters, preventing p53-DNA binding (32). The causal relationship between chromatin remodeling and active transcription is not understood. The ability of E4-ORF3 to induce de novo H3K9me3 and heterochromatin compaction at a known set of targets makes it an ideal instrument for elucidating the initiating signals, histone modifiers, and chromatin remodeling complexes that orchestrate

heterochromatin formation and transcriptional regulation.

Polycomb group proteins are critical regulators of homeotic gene expression during development, and were first identified through genetic screens performed in *Drosophila* (110). The Polycomb Repressive Complex 1 (PRC1) has been shown to be required to maintain the transcriptionally repressive state of many genes, acting via both chromatin remodeling and modification of histones (111). Canonical PRC1 E3 ubiquitin ligase activity occurs through Ring1A/B heterodimer, paired with a PCGF member such as BMI1 (112). While the details of how the PRC1 complex represses genes, it appears that ubiquitination of H2A (H2Aub) is critical for at least a subset of PRC1 functions (113). Human PRC1 subunits each have multiple paralogues, resulting in a large number of potential combinations (111) (Fig. 5.1). PRC1 diversity largely depends on the presence of 5 different CBX proteins and different binding affinities to H3K9me3 and H3K27me3 chromatin. However, there is no clear insight into how many functional PRC1 complexes exist and what the biological relevance is for such diversification (114).

To establish how E4-ORF3 accomplishes such extensive yet specific inactivation of p53 and anti-viral genes, we invested a role for the PRC1 complex in adenovirus infection. Through a candidate screen approach, we have identified PRC1 complex members CBX2, CBX4, and Ring1b as novel cellular targets mislocalized with E4-ORF3 into the nuclear scaffold that specifies heterochromatin silencing of p53 and antiviral target genes. We identified the C-terminal “C-Box” domain of CBX2 and CBX4 to be both necessary and sufficient

for mislocalization by E4-ORF3. In contrast to MRN, we show that PRC1 components are targets of E4-ORF3 proteins from disparate human adenovirus subgroups, indicating that the PRC1 complex is an important and conserved target in virus evolution. Furthermore, we show that the enzymatic target of the PRC1 complex, H2Aub, associates remarkably close to E4-ORF3 nuclear tracks by super-resolution microscopy (SIM). Knockdown of CBX proteins in small airway epithelial cells (SAEC) reveal that CBX2 and CBX4 normally silence genes involved in differentiation and development, and show an overlap with anti-viral gene targets of E4-ORF3.

5.2 Results.

5.2.1 PRC1 complex members are mislocalized into E4-ORF3 tracks.

Previous work demonstrated that E4-ORF3 induces changes in chromatin structure to silence p53 and anti-viral target promoters (32). Therefore, we hypothesized that E4-ORF3 targets cellular chromatin remodeling factors that associate with chromatin. To test this, we conducted a candidate screen. HP1 proteins (CBX1, CBX3, and CBX5) have many important roles in chromatin architecture and can impact gene expression and silencing (115). Importantly, HP1 proteins are commonly associated with H3K9me3, which is enriched at p53 and antiviral target genes (32). We first investigated whether E4-ORF3 was mislocalizing HP1 into E4-ORF3 tracks by immunofluorescence. HP1 was found to associate with dense regions of DNA, but did not mislocalize to E4-ORF3 tracks by immunofluorescence (data not shown).

Chromodomain containing homologues of HP1, chromobox protein homologs known as CBXs, are interchangeable components of the Polycomb group multiprotein PRC1 complex (Fig. 5.1). We hypothesized that E4-ORF3 may be utilizing the CBX proteins to induce gene repression. To determine if the chromobox family of proteins is targeted by E4-ORF3, we created epitope tagged cDNA constructs of the five human CBX family members and co-transfected them with E4-ORF3. E4-ORF3 fails to mislocalize Flag-CBX6, Flag-CBX7, and Flag-CBX8 into nuclear track structures. In contrast, E4-ORF3 specifically targets and mislocalizes Flag-CBX2 and Flag-CBX4 (Fig. 5.2A and B).

5.2.2 The C-Box domain of CBX2 and CBX4 is necessary and sufficient for mislocalization by E4-ORF3.

Human CBX proteins have at least three conserved domains: an N-terminal chromodomain that binds to histones, an AT-hook (or AT-hook-like) domain that binds DNA adjacent to the chromodomain, and a C-terminal Polycomb Repressor domain known as the “C-Box” that has been shown to be required for repression (116)(Fig. 5.3). To determine whether one of these established domains is required for mislocalization by E4-ORF3, we deleted each of the three major domains of CBX2 that were conserved across chromobox proteins. Interestingly, deletion of the CBX2 chromodomain (amino acids 11-69), which is required for binding chromatin, had no effect on the ability of E4-ORF3 to mislocalize CBX2 (Flag-CBX2ΔChromo). Similarly, a CBX2 construct lacking the AT-Hook domain (amino acids 70-87) is mislocalized by E4-ORF3

indistinguishably from wild-type CBX2 (Flag-CBX2ΔAT-Hook). However, deletion of the C-terminal C-Box of CBX2 (amino acids 484-532) ablated mislocalization by E4-ORF3 (Fig. 5.4A and B).

The C-terminal C-box of the CBX proteins is involved in transcriptional silencing and required for their function and for associating with PRC1 complexes. There is 31.2% pairwise amino acid identity and 43.8% pairwise similarity between human CBX and *Drosophila* PC proteins (Fig. 5.5). We hypothesized that although these domains are quite distinct that the C-Box domain was also required for E4-ORF3 mislocalization of CBX4. Co-transfection of E4-ORF3 with a CBX4 construct lacking the C-terminal C-Box domain revealed that this same domain of CBX4 is required for mislocalization of E4-ORF3 (Fig. 5.6A and B). We conclude that E4-ORF3 targets CBX2 and CBX4 via the C-terminal C-Box domain.

Lastly, we wished to determine if the C-Box domains of CBX2 and CBX4 are sufficient to associate with E4-ORF3 tracks. Expression of the C-Box domain of CBX2 or CBX4 alone is not sufficient to associate with E4-ORF3 (data not shown). Therefore, we engineered CBX8, a protein that does not colocalize with E4-ORF3, to contain the C-Box domain of CBX2 instead of its own inherent C-Box domain (Flag-CBX8+CBX2 C-Box). Transfection of Flag-CBX8+CBX2 C-Box alone is nuclear diffuse, and has a staining pattern more similar to CBX2 than to CBX8 (Fig. 5.7A). Co-transfection of this construct with E4-ORF3 results in its mislocalization by E4-ORF3, similar to CBX2 (Fig. 5.7B). We conclude that the specificity of E4-ORF3 in targeting CBX2 and CBX4 lies within the C-Box domain.

5.2.3 PRC1 component Ring1b is mislocalized by E4-ORF3.

The C-Box domain of CBX proteins is required for binding to other PRC1 components such as Ring1b (117). Consistently, we found that deletion of the C-Box domain of CBX2 and CBX4 ablates association with Ring1b (Fig. 5.8A). To determine if E4-ORF3 also mislocalizes Ring1b when it mislocalizes CBX2 or CBX4, we transfected U2OS cells with Flag-CBX2 (data not shown) and Flag-CBX4 and stained for Ring1b with an endogenous antibody. As expected, Flag-CBX4 associates with endogenous Ring1b with and without E4-ORF3 (Fig. 5.8A and B). In addition, we show that E4-ORF3 can target Ring1b independently of the CBX proteins, as transfection of E4-ORF3 alone induces mislocalization of endogenous Ring1b (Fig. 5.8C). This suggests that E4-ORF3 may target specific subsets of PRC1 complexes that contain both Ring1b and CBX2 or CBX4.

5.2.4 Ring1b is a conserved target of E4-ORF3 proteins from disparate human adenovirus subgroups.

There are 68 human adenoviruses that are divided into 7 subgroups (A-G) based on sequence homology, biophysical, and biochemical criteria. There is 37.6% pairwise amino acid identity and 55.2% pairwise similarity between Ad5 E4-ORF3 (Subgroup C) and E4-ORF3 proteins from disparate adenoviral subgroups: Ad9 (Subgroup D), Ad12 (Subgroup A), and Ad34 (Subgroup B) (Fig. 2.8A). To determine if PRC1 components are conserved targets of E4-ORF3 proteins from disparate adenovirus subgroups, we transfected U2OS cells with

Myc-tagged Ad5, Ad9, Ad12, or Ad34 E4-ORF3 constructs. We show that E4-ORF3 proteins from Ad5, Ad9, Ad12, and Ad34 all target and mislocalize Flag-CBX2, Flag-CBX4 (data not shown), and endogenous Ring1b (Fig. 5.9). We conclude that the PRC1 component Ring1b is an evolutionarily conserved cellular target of E4-ORF3 proteins from disparate human adenovirus subgroups.

5.2.5 PRC1 enzymatic target H2Aub is enriched in E4-ORF3 tracks.

The PRC1 complex is required for ubiquitination of histone H2A at lysine 119 (118, 119), en epigenetic mark associated with repression of genes important in development. The enzymatic activity for this modification resides in the Ring1a/b subunit when paired with one of six PCGF partners such as PCGF4/BMI1 (Fig. 5.1). To determine if ubiquitination of H2A is involved in E4-ORF3 mediated silencing of p53 and anti-viral genes, we performed immunofluorescence on U2OS cells infected with WT Ad5. After fixing the cells at 36 h.p.i. and staining for H2A and E4-ORF3, we performed super-resolution structured illumination microscopy (SR-SIM) (120), which enables visualization of nuclear structure at resolutions of approximately 100 nm. SR-SIM reveals that E4-ORF3 mislocalizes H2Aub at remarkably specificity (Fig. 5.10A).

Our lab has previously shown that E4-ORF3 specifies heterochromatin assembly and H3K9me3 at p53 target promoters (32). High resolution confocal images reveal association of E4-ORF3 and H3K9me3 by immunofluorescence at 36 h.p.i. However, it is unknown whether this epigenetic modication is induced earlier or if another modification may initiate and induce H3K9me3 spreading. To

determine the principal epigenetic mark at early times in adenovirus infection, we infected U2OS cells with WT Ad5 and fixed at an early time point of 12 h.p.i., stained for E4-ORF3 and either H2Aub or H3K9me3, and imaged using SR-SIM. Surprisingly, we found that at 12 h.p.i., while H3K9me3 has not yet begun to associate with E4-ORF3 nuclear tracks, H2Aub is already mislocalized by E4-ORF3 (Fig. 5.10B). These results suggest that ubiquitination of H2A predicates p53 and anti-viral gene silencing by H3K9me3.

5.2.6 E4-ORF3 and CBX proteins repress developmental genes.

In our previously published microarray data, to define the genes specifically targeted by E4-ORF3, we compared ΔE1B-55K/ΔE4-ORF3- versus ΔE1B-55K-infected cells. In this way, we found that E4-ORF3 prevents the transcriptional activation of 265 genes by a log-fold change of two or more in ΔE1B-55K-infected cells. In addition to p53 genes, there is significant overrepresentation of genes associated with immune modulation and tissue remodeling, suggesting E4-ORF3 may target these promoters as part of a general anti-viral transcriptional silencing program. We further examined these data by analyzing the biological processes of these genes and categorizing them by Gene Ontology using Genomatix software. We found that the top functions of the genes that are repressed by E4-ORF3 are involved in differentiation and development of epidermal and epithelial cells (Table 5.1).

The PRC1 complex functions as transcriptional repressors with roles in development and stem cell biology (121, 122). Roles for proteins of the PRC1

complex have been implicated in somatic cells where a functional PRC1 complex would not seem required, but these roles are unclear (114). To determine the genes specifically regulated by CBX2 and CBX4 in quiescent small airway epithelial cells (SAECs), we performed genome-wide expression analyses in cells in which CBX2 or CBX4 had been knocked down using RNAi. The cells were infected with WT Ad5, ΔE1B-55K (015), and ΔE1B-55K/ΔE4-ORF3 (3112) viruses, harvested at 36 h.p.i., and microarray analysis was performed. Western analysis confirms that CBX2 and CBX4 are knocked down, but it is interesting to note that that CBX2 is undetectable in uninfected cells (Fig. 5.11). Knockdown of CBX2 or CBX4 does not affect p53 protein levels or the levels of p53 targets p21 and MDM2.

We next identified genes that are regulated by CBX2 or CBX4 in uninfected SAEC. CBX2 prevents the transcriptional activation of 316 genes by a log-fold change of two or more in uninfected SAEC. Similarly, CBX4 prevents the transcription of 357 genes by a log-fold change of two ore more (Fig. 5.12). We further examined these data by performing analyzing the biological processes of these genes and categorizing them by Gene Ontology using Genomatix software. We found that the function of the genes that are repressed by CBX2 or CBX4 are involved in differentiation and development of epidermal and epithelial cells, similar to E4-ORF3 (Table 5.2). We also found a substantial overlap in genes targeted by both CBX2 and CBX4: 65% of the genes repressed by CBX2 are also repressed by CBX4, and 57% of the genes repressed by CBX4 are also repressed by CBX2. This suggests that E4-ORF3 may specifically target CBX2

and CBX4 for their roles in transcriptional repressed of genes involved in differentiation and development as an anti-viral response.

We hypothesized that E4-ORF3 may be recruiting CBX2- and CBX4-containing PRC1 complexes to prevent cellular differentiation. Differentiation may be an anti-viral mechanism used by the cell to initiate programmed cell death through cornification and/or to create a physical barrier through keratinization to prevent viral spread. The switch from an undifferentiated state to a differentiated state requires the upregulation and actions of transcription factors such as grainy head-like 1 and 3 (GRHL1 and GRHL3), zinc finger protein (ZNF750), and kruppel-like factor 4 (KLF4) (123-125). To confirm the down-regulation of these genes in ΔE1B-55K-infected cells and to determine how these genes are regulated in other virus mutants, we compared mRNA levels of multiple transcription factors involved in differentiation in infected SAEC cells. GRHL3, KLF4, ZNF750, TGM1, and p63 are all down-regulated in virus-infected cells (WT, ΔE1B-55K, ΔE4-ORF3, and ΔE1B-55K/ΔE4-ORF3) (Fig. 5.13). These results indicate that adenovirus represses differentiation programs.

5.3 Discussion

Our studies demonstrate that adenovirus protein E4-ORF3 targets specific PRC1 components and mislocalizes CBX2 and CBX4 through their C-terminal C-Box domain. Furthermore, we identify CBX2, CBX4, and Ring1b as a novel target of E4-ORF3 proteins from disparate adenovirus subgroups, suggesting a conserved evolutionary role in adenovirus infection. We found that histone

modification H2Aub, which is modified by the PRC1 complex, is mislocalized into the E4-ORF3 nuclear matrix and that E4-ORF3 association with H2Aub precedes E4-ORF3 association with H3K9me3. Lastly, we reveal that E4-ORF3 and CBX2/CBX4 proteins targets a large subset of genes involved in cellular differentiation and development, and that critical transcription factors required for switching from an undifferentiated state to a differentiated state are down-regulated in adenovirus infection.

Our data reveal that the specificity of E4-ORF3 targeting CBX2 and CBX4 lies within the C-terminal C-Box domain, as domain deletions of CBX2 and CBX4 show that the C-Box domain as necessary (Fig. 5.4 and 5.6) and sufficient (Fig. 5.7) for mislocalization into E4-ORF3 track structures. It is known that the C-Box domain of CBX proteins is required for binding to Ring1b (117), which is also a target of E4-ORF3 (Fig. 5.8B and C). Interestingly, the crystal structure of the C-box domain reveals that it is mostly disordered in the absence of binding to the C-terminus of Ring1b, which is itself flexible and nonrigid (126). The use of intrinsically disordered regions for protein−protein interactions can expand the repertoire of binding partners by creating a discrete interaction surface for different binding partners, which a nonflexible protein is unable to do. Protein “hubs” are proteins that have many binding partners and frequently use unstructured protein regions in binding reactions (127). Our lab has shown that E4-ORF3 too forms a disordered protein superstructure that has multivalent binding sites to interact with many different cellular complexes. The flexible structures of the C-Box domain of CBX2 and CBX4, the C-terminus of Ring1b,

and E4-ORF3 could not only enhance associations between them, but also to be targeted to different genomic sites.

Interestingly, of the five CBX proteins, CBX4 is the only one known to have an enzymatic activity and is also a target of E4-ORF3 (Fig. 5.2B). CBX4 acts as an E3 SUMO ligase and this activity is dependent on its chromodomain and a C-terminal substrate binding domain (128). Our previous results (Chapters 2-4) indicate SUMO in nuclear organization, but SUMO is also well-established for roles in the regulation of many other cellular processes, including transcriptional repression, genome stability, chromatin organization, and DNA repair (45, 129). It will be interesting to determine if the E3 SUMO ligase activity is required for suppression of CBX4 target genes in differentiation and development; determining the role of CBX4 enzymatic activity may not only reveal a novel roles for sumoylation in CBX4-mediated transcriptional repression, but other SUMO enzymes as well.

Our immunofluorescence data indicates that E4-ORF3 usurps CBX2- and CBX4-containing PRC1 complexes, but not other CBX-containing PRC1 complexes. There is substantial overlap in genes targeted by both CBX2 and CBX4: 65% of the genes repressed by CBX2 are also repressed by CBX4, and 57% of the genes repressed by CBX4 are also repressed by CBX2 (Fig. 5.12). In hematopoietic stem cells (HSC), overexpression of CBX2 and CBX4 results in differentiation, while overexpression of CBX7 preserves HSC self-renewal and propagation (130). The roles of CBX2 and CBX4 for their roles in transcriptional

repressed of genes involved in differentiation and development may account for the differences in E4-ORF3 specificity in targeting the CBX family (Table 5.2).

Adenovirus infection induces repression of critical genes required for cellular differentiation and development (Fig. 5.13). Whether adenovirus infection suppresses this subset of genes involved as part of an anti-viral program still remains to be better elucidated. E1B-55K and E4-ORF3 both have roles in blocking cell cycle arrest and apoptosis, manipulating host cell proteins and DNA to turn on and off the appropriate pathways (3). Differentiation of epidermal and epithelial cells is another type of cell death: cell death by cornification. E1B-55K and E4-ORF3 may shut off this response to avoid premature nuclei breakdown or to prevent the formation of a cornified cell envelope that may prevent viral spread.

Our analysis of the role of the PRC1 complex during adenovirus infection demonstrates E4-ORF3 specifically targets a particular subset of PRC1 complexes, those that contain Ring1b, CBX2, and CBX4. These data indicate an important role for these PRC1 complexes in facilitating repression of an anti-viral response, particularly genes involved in differentiation and development. Our results reveal gene targets of the PRC1 complex SAEC cells and a new function for the PRC1 complex in pathological infection.

5.4 Materials and methods.

5.4.1 Cells, culturing conditions, and viral infections.

U2OS cells were cultured in DMEM supplemented in 10% heat-inactivated

FBS without antibiotics. Infection was performed at an experimentally determined multiplicity of infection (MOI) of 30 plaque-forming units (PFU) in DMEM containing 2% heat inactivated FBS. Primary human cells from multiple donors were obtained from Cambrex/Lonza, which were grown and infected as described previously (24, 25). SAECs were infected at an MOI of 10.

5.4.2 Viruses.

Viruses were titered on 293/E4/pIX cells, as described previously (24). Wild type (WT) virus is Ad5. The ΔE1B-55K virus (AdSyn-CO124) was created by mutating the start codon of E1B-55K (ATG to GTG) and I90 of E1B-55K to a stop codon (ATT to TAG). The ΔE4-ORF3 virus (AdSyn-CO118) was created by deleting the coding region of E4-ORF3. The ΔE1B-55K/ΔE4-ORF3 virus (AdSyn-CO140) is the same as ΔE1B-55K except the E4-ORF3 coding region is also deleted (26). For microarray analysis, wild-type virus is WtD18, ΔE1B-55k is dl1520/ONYX-015. The ΔE1B-55k/ΔE4-ORF3 (Δ55k/ΔORF3) virus, dl3112, has an identical genome backbone to dl1520/ONYX-015 but has a single base pair deletion (nucleotide 7143r) that ablates E4-ORF3 expression (32).

5.4.3 Plasmids and transfections.

PRC1 component plasmids were first cloned into pDONR221 and then recombined into a CMV expression vector with an N-terminal tag using the Gateway Cloning System (Invitrogen). E4-ORF3 constructs were generated as described previously (26). Lipofectamine 2000 (Invitrogen) was used for

transfection of U2OS cells according to manufacturer's instructions.

5.4.4 Immunofluorescence.

Cells were fixed in 4% paraformaldehyde for 30 minutes at room temperature, permeabilized in 0.1% TritonX-100 PBS-/-, and stained as described previously (24, 25). Primary antibodies were Flag (F742 from Sigma), Myc (9B11 from CST), E4-ORF3 (6A11), Ring1b (Active Motif), and H2Aub (E6C5 from EMD Millipore). Alexa 488-, 555- and 633-conjugated secondary antibodies (Molecular Probes) were used for detection of primary antibodies. Hoechst-33342 was used to stain DNA. Images were acquired with a Zeiss LSM780 imaging system with a 63x objective. Images are single z-planes.

5.4.5. Western analysis.

Protein lysates were harvested in reducing SDS-PAGE sample buffer containing 50mM Tris pH 8, 2% SDS, 10% glycerol, 100mM dithiothreitol, and 0.1% Bromophenol Blue. Lysates were boiled for 10 minutes and sonicated. For Western blot, samples were analyzed by SDS-PAGE and transferred to nitrocellulose membranes. The membranes were blocked using 5% milk. Primary antibodies were from Santa Cruz Biotechnology (p53 DO-1, MDM2 N20), Upstate (p21), and Sigma (CBX2 and CBX4). β-Actin (AC-15 from Sigma) expression was used as a loading control. Primary antibodies were detected with secondary antibodies labeled with either IRDye800 (Rockland), or Alexa Fluor 680 (Molecular Probes). Fluorescent antibodies were visualized using a LI-COR-

Odyssey scanner. Quantification of dot blots was performed using LI-COR-Odyssey Software (68).

5.4.6 Affymetrix expression arrays and data analysis.

Human primary quiescent SAECs were infected and harvested at 36 h.p.i. All samples were done in duplicate, and corresponding lysates were western-blotted. Total RNA was isolated and purified using TRIzol with the PureLink RNA Mini kit (Invitrogen), and treated with DNase I (Ambion). Total RNA (100 ng), spiked with Poly-A controls, was used to synthesize cDNA, according to recommended protocols using the Ambion WT Expression kit. Fragmentation and labeling of cDNA was performed as per the Affymetrix GeneChip WT Terminal Labeling standard protocol. Samples were hybridized to Affymetrix Human Exon 1.0ST arrays, washed, stained and scanned with the Affymetrix GCS 3000 7G and GeneChip Operating Software v1.3 to produce .CEL intensity files. Quality control analysis of all chips was performed with the Affymetrix expression console.

All array data were analyzed using tools in the Partek Genomic Suite of software (Partek). Exon-level data were imported and filtered to include only those probes that are in the 'Core Meta-probeset', which represents 17,800 RefSeq genes and full-length GenBank mRNAs. A pre-background adjustment was performed for GC content followed by robust multi-array analysis (RMA) background correction, quantile normalization and mean probeset summarization. Sources of variation due to random experimental factors, such as

scan date and experiment were batch-removed using analysis of variance (ANOVA). Differentially expressed genes were analyzed using the Genomatix Pathway System (GePS) and GeneRanker programs, which uses information extracted from public and proprietary databases. Over-representation of different biological terms (Gene Ontology categories, signal transduction pathways) within the input gene list are calculated and listed together with their respective *p*-value.

5.4.7 Real-Time Quantitative PCR analysis.

RT-qPCR quantification of GRHL3, KLF4, ZNF750, TGM1, and p63 mRNA was performed using the Bio-Rad CFX96 and analyzed using the Bio-Rad CFX Manager 3.0 software. RNA (1 μg) was reverse-transcribed with iScript cDNA synthesis kit (Bio-Rad). Taqman primers and probe sets for each gene were obtained from Life Technologies. RT-qPCR reactions were set up using Taqman Fast Mix (ABI) and run in triplicate. For 18S rRNA analysis, 10ng input cDNA was used; for GRHL3, KLF4, ZNF750, TGM1, and p63 analysis, 40 ng of input cDNA was used. Normalized gene expression (ΔΔCq) was determined using 18S rRNA as a reference gene and fold change was determined by setting gene expression levels of uninfected samples to 1. Error bars represent Standard Error of the Mean of triplicates.

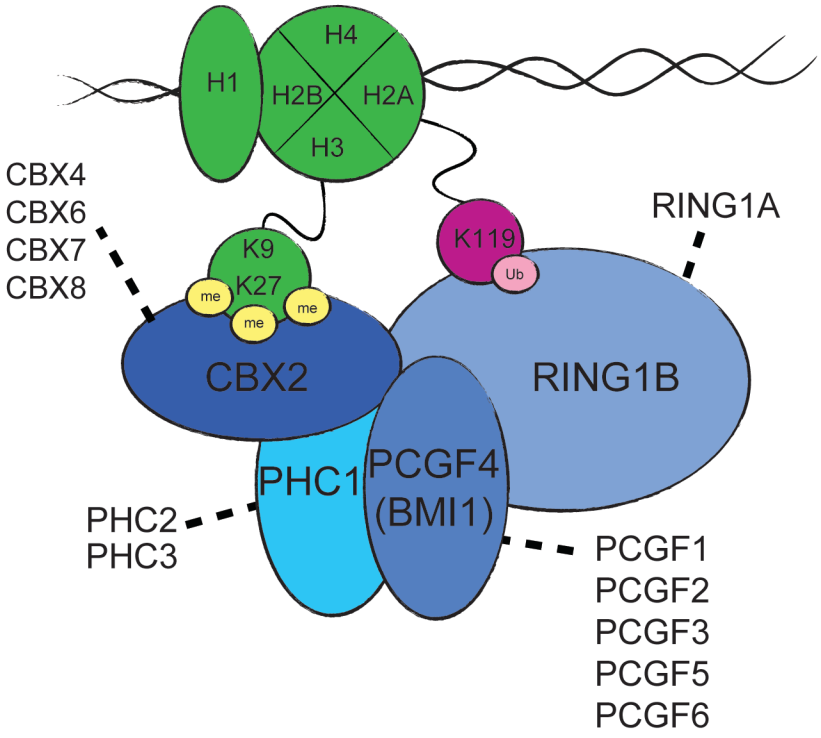

Figure 5.1. Schematic representation of the mammalian PRC1 complex. The PRC1 complex is made up of four subunits, each of which has at least one paralogue. The CBX proteins contain a chromodomain that can bind H3K27me3 and/or H3K9me3. Ring1a/b is key for the enzymatic activity of the complex, ubiquitination of histone H2A at K119.

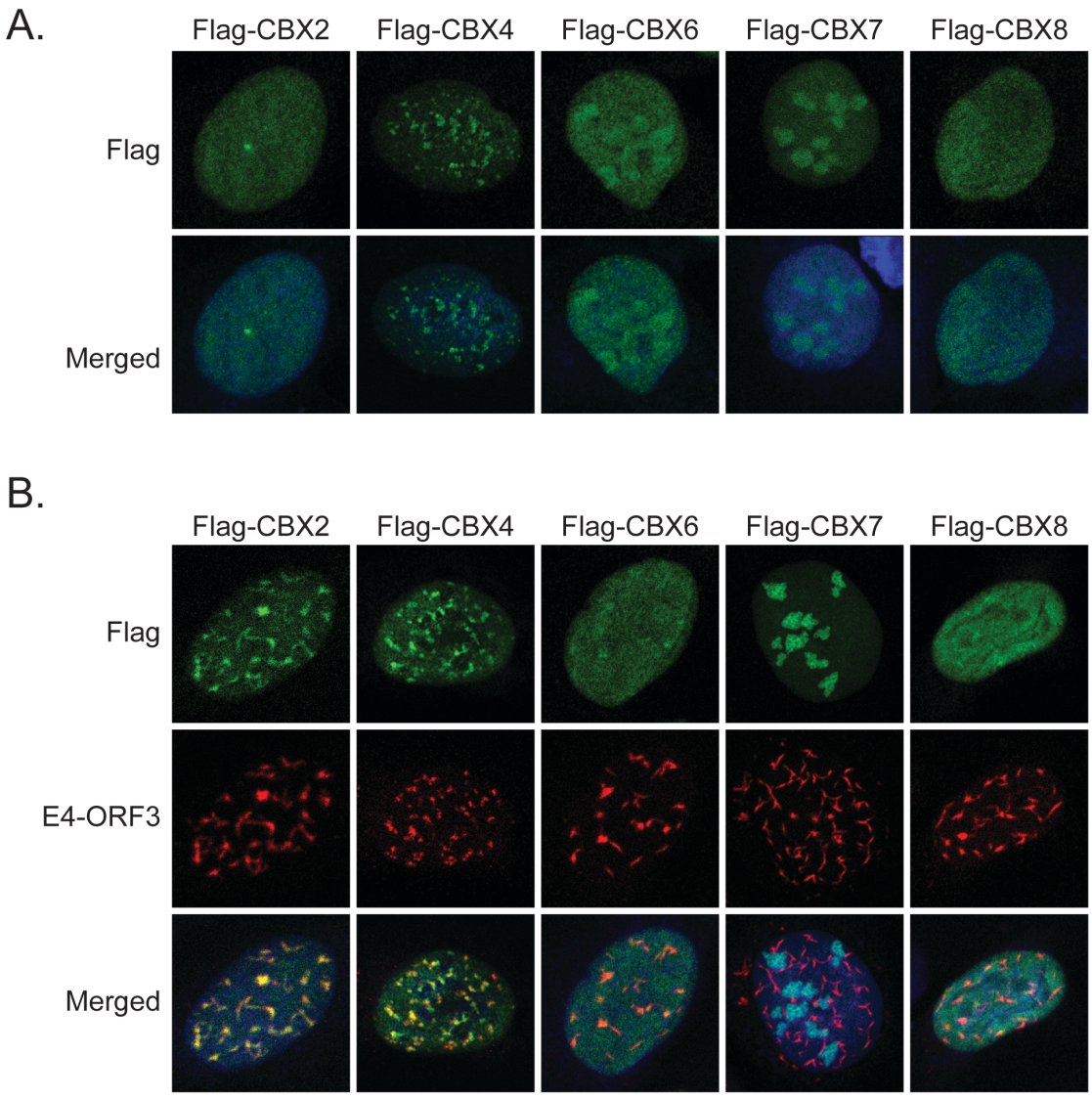

Figure 5.2. E4-ORF3 specifically targets CBX2 and CBX4 from the CBX family of proteins of the PRC1 complex. (A) U2OS cells were transfected with Flag-tagged cDNA constructs of each CBX family member. Cells were then fixed 24 hours post transfection and immunostained for Flag (green) and E4-ORF3 (red). Nuclei were counterstained with Hoechst-33342. (B) U2OS cells were co-transfected with E4-ORF3 and Flag-tagged cDNA constructs of each CBX family member. Cells were then fixed 24 hours post transfection and immunostained for Flag (green) and E4-ORF3 (red). Nuclei were counterstained with Hoechst-33342.

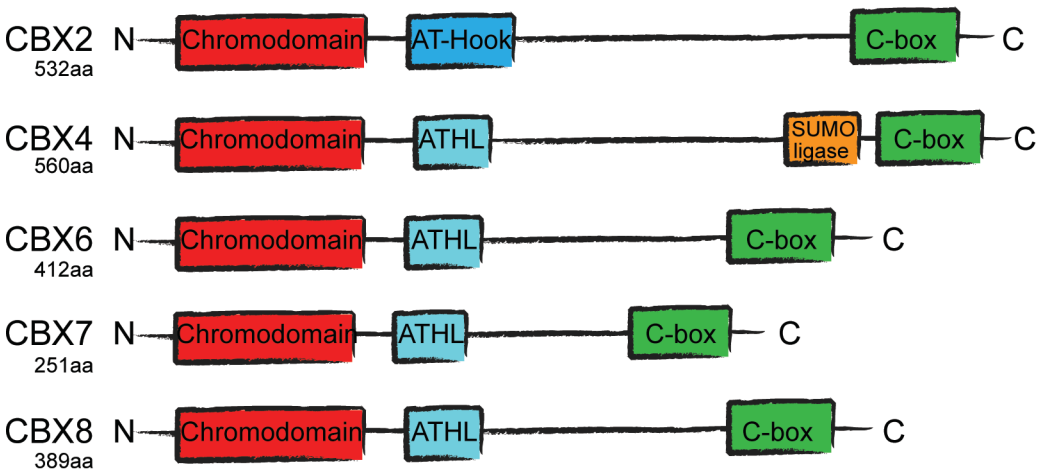

Figure 5.3. Schematic of the domain organization among CBX protein family members. "ATHL" indicates "AT-Hook like" domain.

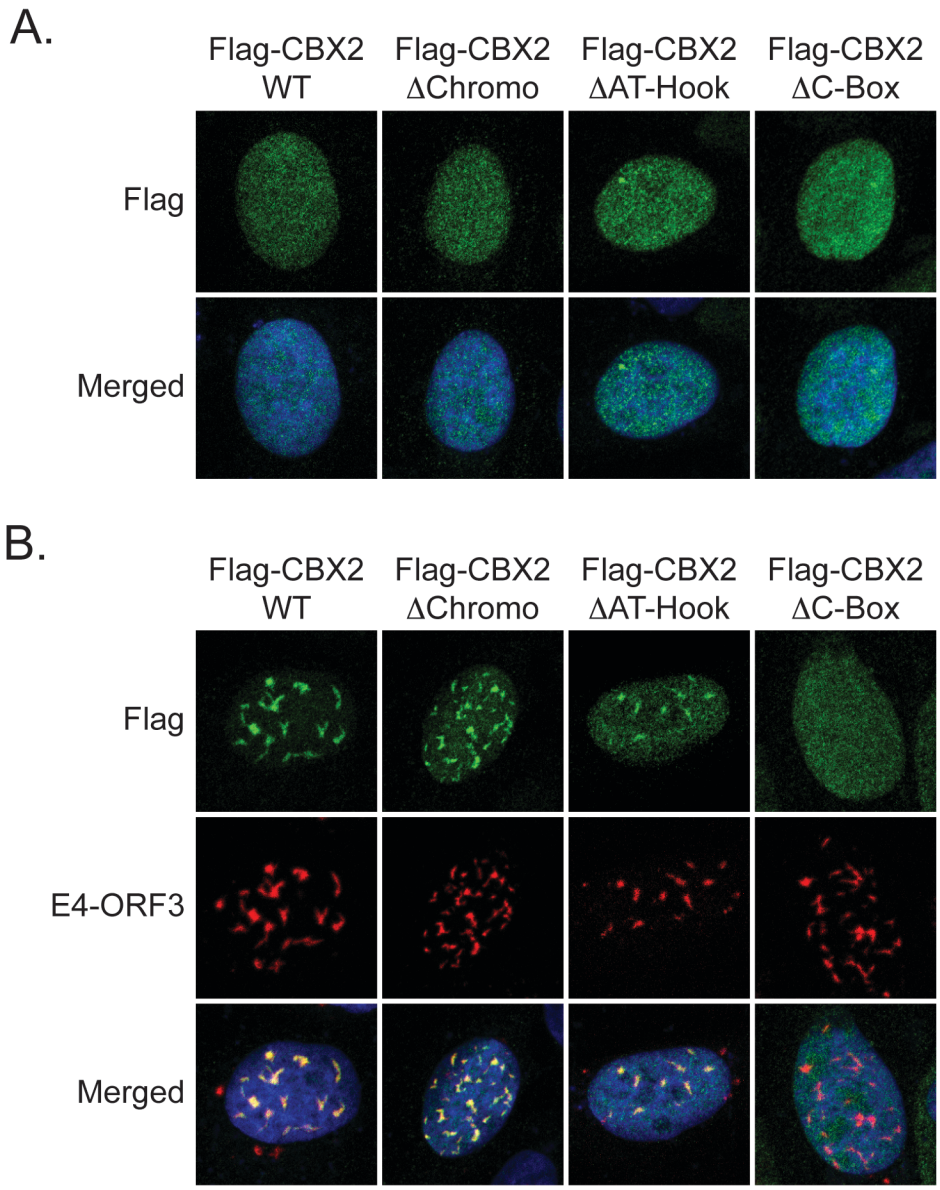

Figure 5.4. The C-Box domain of CBX2 is required for mislocalization into E4-ORF3 tracks. (A) U2OS cells were transfected with Flag-tagged cDNA constructs of each CBX2 mutant construct. Cells were then fixed 24 hours post transfection and immunostained for Flag (green). Nuclei were counterstained with Hoechst-33342. (B) U2OS cells were co-transfected with E4-ORF3 and Flag-tagged cDNA constructs of each CBX2 mutant construct. Cells were then fixed 24 hours post transfection and immunostained for Flag (green) and E4-ORF3 (red). Nuclei were counterstained with Hoechst-33342.

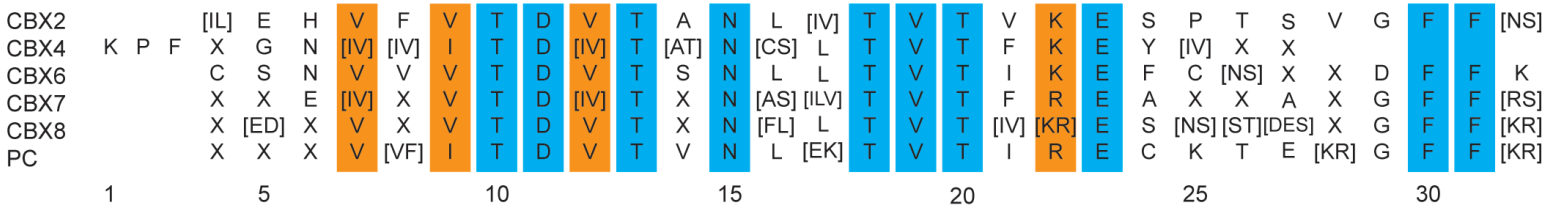

Figure 5.5. Alignment of human CBX and *Drosophila* PC family of proteins. Blue and orange denote conserved and semi-conserved residues, respectively.

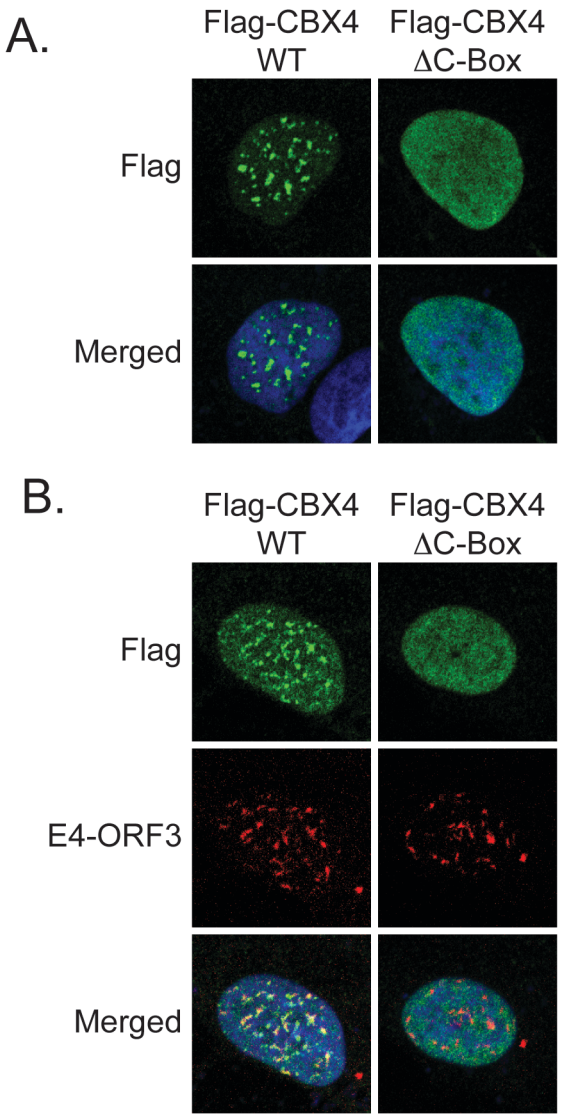

Figure 5.6. The C-Box domain of CBX4 is required for mislocalization into E4-ORF3 tracks. (A) U2OS cells were transfected with Flag-tagged cDNA constructs of WT or mutant CBX4 constructs. Cells were then fixed 24 hours post transfection and immunostained for Flag (green). Nuclei were counterstained with Hoechst-33342. (B) U2OS cells were co-transfected with E4-ORF3 and Flag-tagged cDNA constructs of WT or mutant CBX4 constructs. Cells were then fixed 24 hours post transfection and immunostained for Flag (green) and E4-ORF3 (red). Nuclei were counterstained with Hoechst-33342.

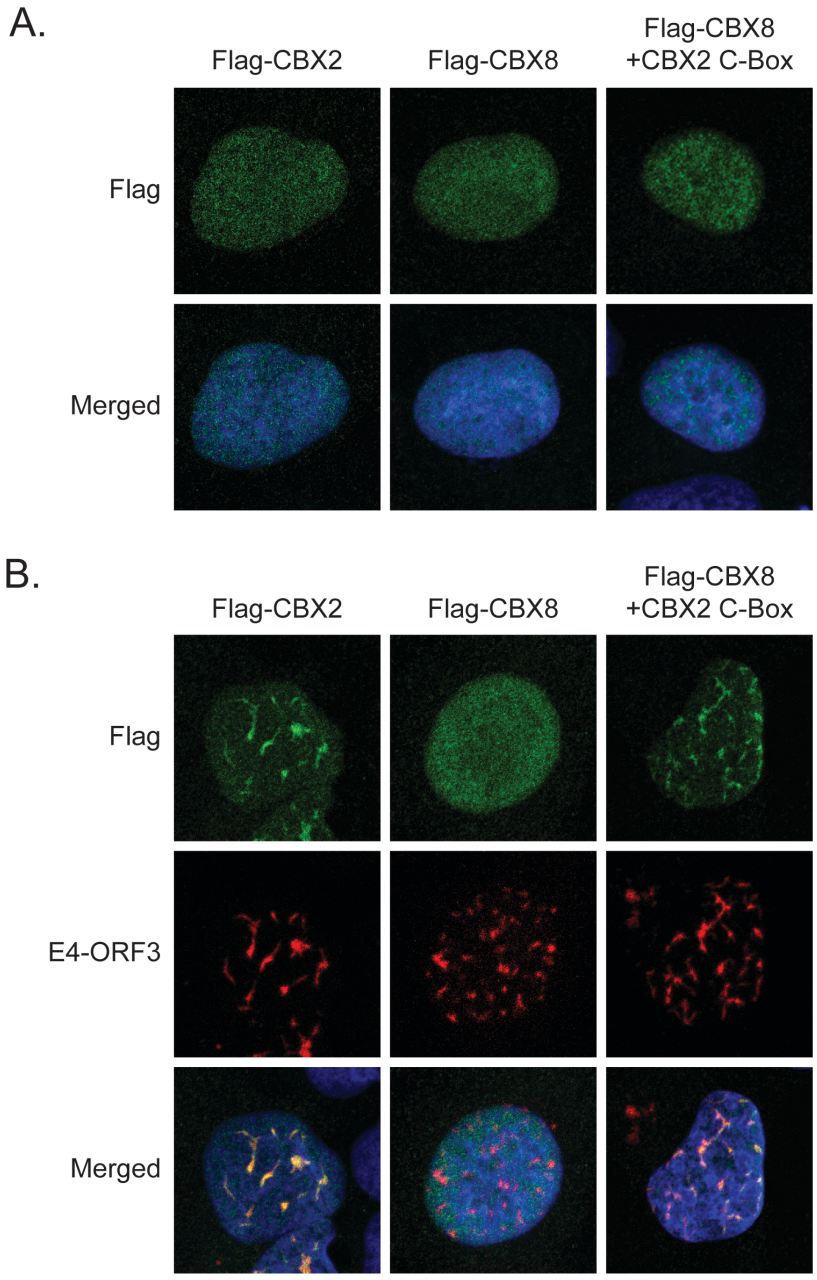

Figure 5.7. The C-Box domain of CBX2 is sufficient for CBX8 mislocalization into E4-ORF3 tracks. (A) U2OS cells were transfected with Flag-tagged cDNA constructs as indicated. Cells were then fixed 24 hours post transfection and immunostained for Flag (green). Nuclei were counterstained with Hoechst-33342. (B) U2OS cells were co-transfected with E4-ORF3 and Flag-tagged cDNA constructs as indicated. Cells were then fixed 24 hours post transfection and immunostained for Flag (green) and E4-ORF3 (red). Nuclei were counterstained with Hoechst-33342.

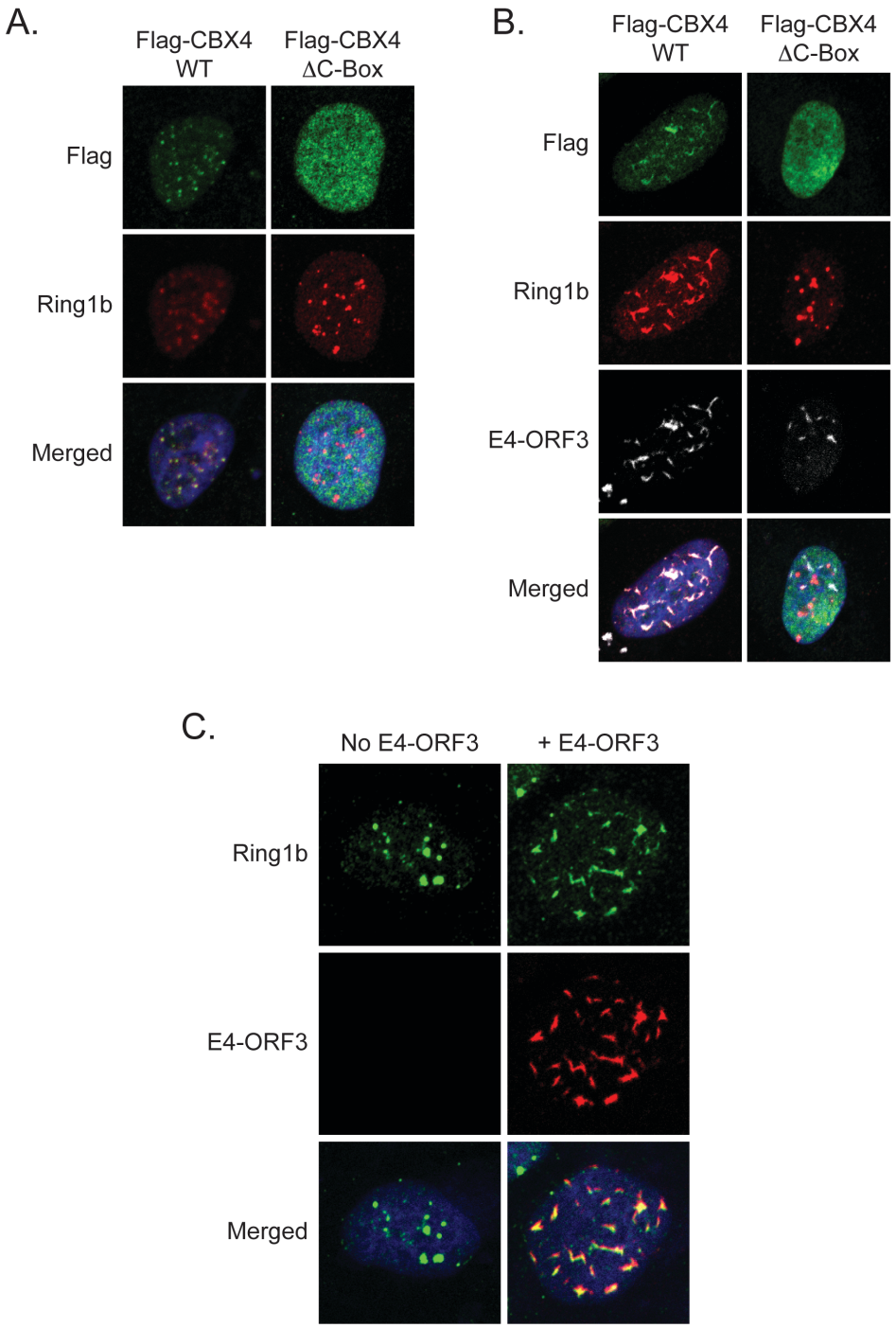

Figure 5.8. E4-ORF3 targets Ring1b independently of CBX proteins. (A) U2OS cells were transfected with Flag-tagged cDNA constructs as indicated. Cells were then fixed 24 hours post transfection and immunostained for Flag (green). Nuclei were counterstained with Hoechst-33342. (B) U2OS cells were co-transfected with E4-ORF3 and Flag-tagged cDNA constructs as indicated. Cells were then fixed 24 hours post transfection and immunostained for Flag (green) and E4-ORF3 (red). Nuclei were counterstained with Hoechst-33342.

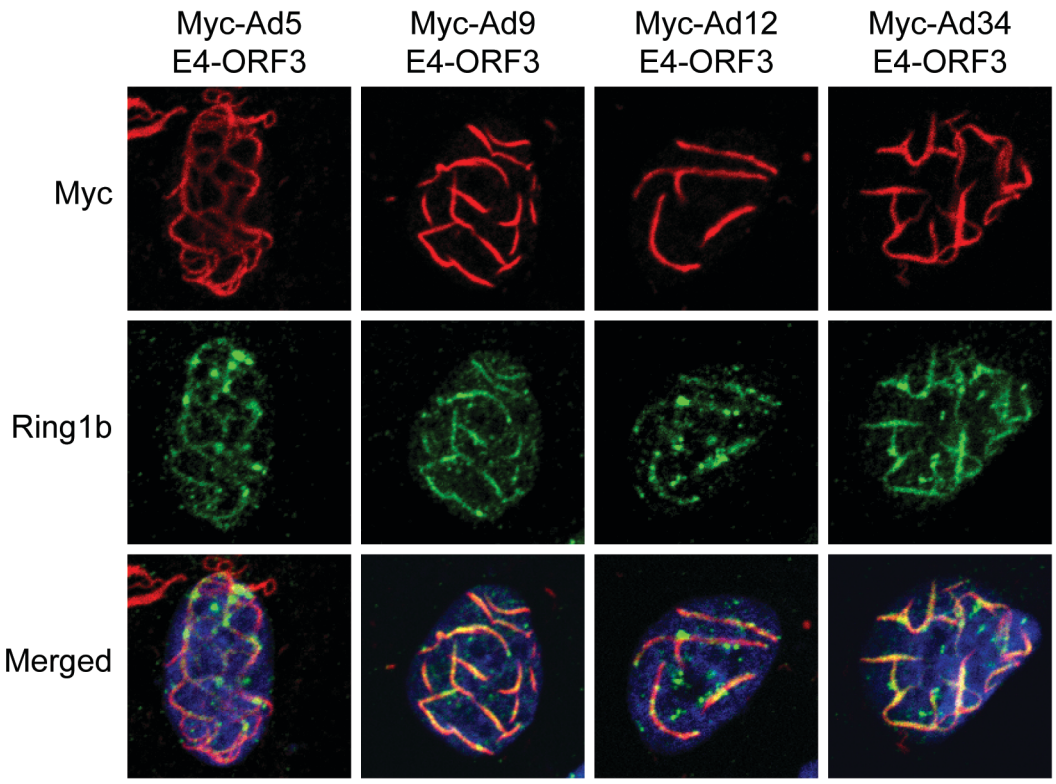

Figure 5.9. Ring1b is a conserved target of E4-ORF3 proteins from disparate human adenovirus subgroups. U2OS cells were transfected with Myc-tagged E4-ORF3 from Ad5, Ad9, Ad12, or Ad34. Cells were fixed 24 hours post transfection and immunostained for Myc (red) and Ring1b (green). Nuclei were counterstained with Hoechst-33342.

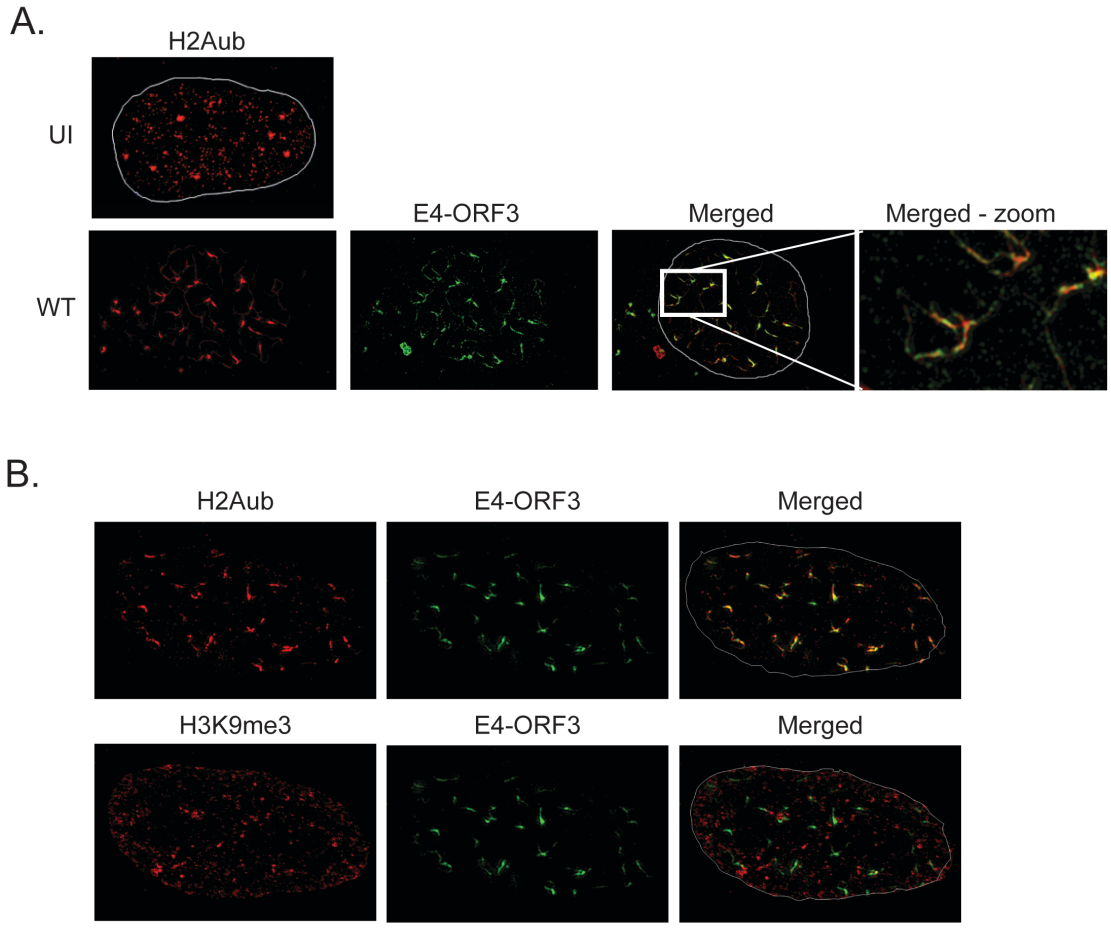

Figure 5.10. H2Aub is mislocalized into E4-ORF3 nuclear matrix. (A) U2OS cells were left uninfected (UI) or infected with wild-type (WT) Ad5. Cells were then fixed 36 h.p.i. and immunostained for H2Aub (red) and E4-ORF3 (green) and imaged by structure-illumination microscopy. White box indicates zoom. (B) U2OS cells were infected with WT Ad5 and fixed 12 h.p.i. Cells were immunostained for H2Aub or H3K9me3 (red) and E4-ORF3 and imaged by structure-illumination microscopy.

Table 5.1. Gene ontology of genes repressed in ΔE1B-55K-infected cells compared to ΔE1B-55K/ΔE4-ORF3-infected cells.

Biological Processes	p-value
Epidermis development	1.03e-09
Tissue development	5.37e-09
Keratinocyte differentiation	2.53e-08
Epidermal cell differentiation	1.66e-07
Anatomical structure development	4.51e-07
Epithelial cell differentiation	4.55e-07

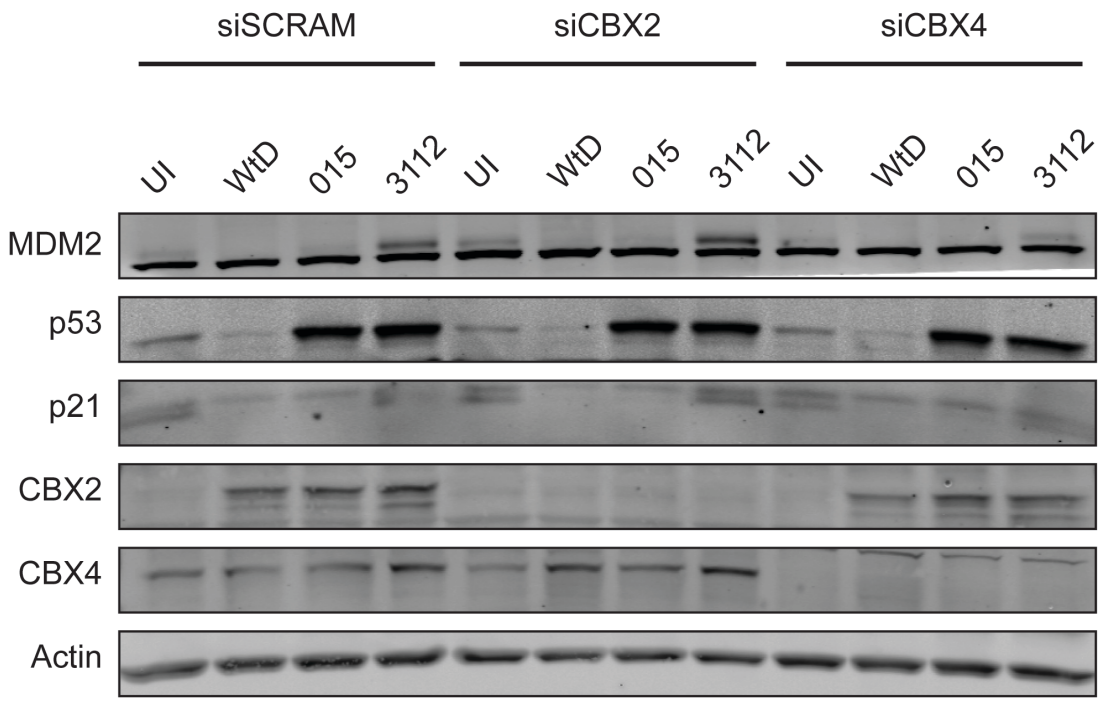

Figure 5.11. Knock down of CBX2 and CBX4 in SAEC. U2OS cells were infected as indicated. Protein lysates were collected at 36 h.p.i. and immunoblotted for CBX2 and CBX4 to confirm knockdown, and p53, p21, and MDM2 to confirm p53 activity of the infected cells. β-Actin is a loading control.

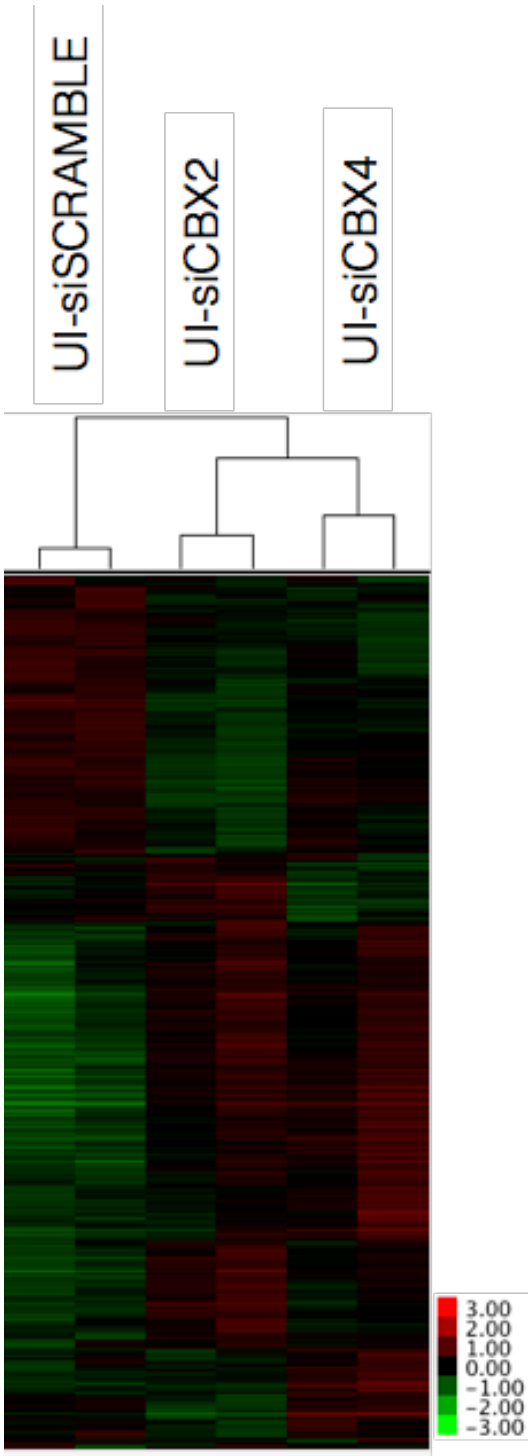

Figure 5.12. Transcriptional targets of CBX2 and CBX4 in SAEC. Affymetrix global gene expression analyses of SAECs; heat map of the differentially regulated genes (log-fold change >2 or <−2 with a false discovery rate (FDR) of 0.05) between SAEC containing siSCRAMBLE RNA, siCBX2 RNA, or siCBX4 RNA.

Table 5.2. Gene ontology of genes upregulated in siCBX2 and CBX4 SAEC compared to siSCRAMBLE.

CBX2 Biological Processes	p-value	**CBX4 Biological processes**	p-value
Epidermis development	1.19e-07	Epidermal cell differentiation	2.06e-09
Epidermal cell differentiation	3.30e-07	Keratinocyte differentiation	2.48e-09
Keratinocyte differentiation	5.92e-07	Tissue development	6.02e-09
Keratinization	5.08e-06	Epidermis development	6.49e-09
Tissue development	1.16e-05	Epithelial cell differentiation	1.67e-08
Triglyceride biosynthesis	2.89e-05	Epithelium development	2.04e-07

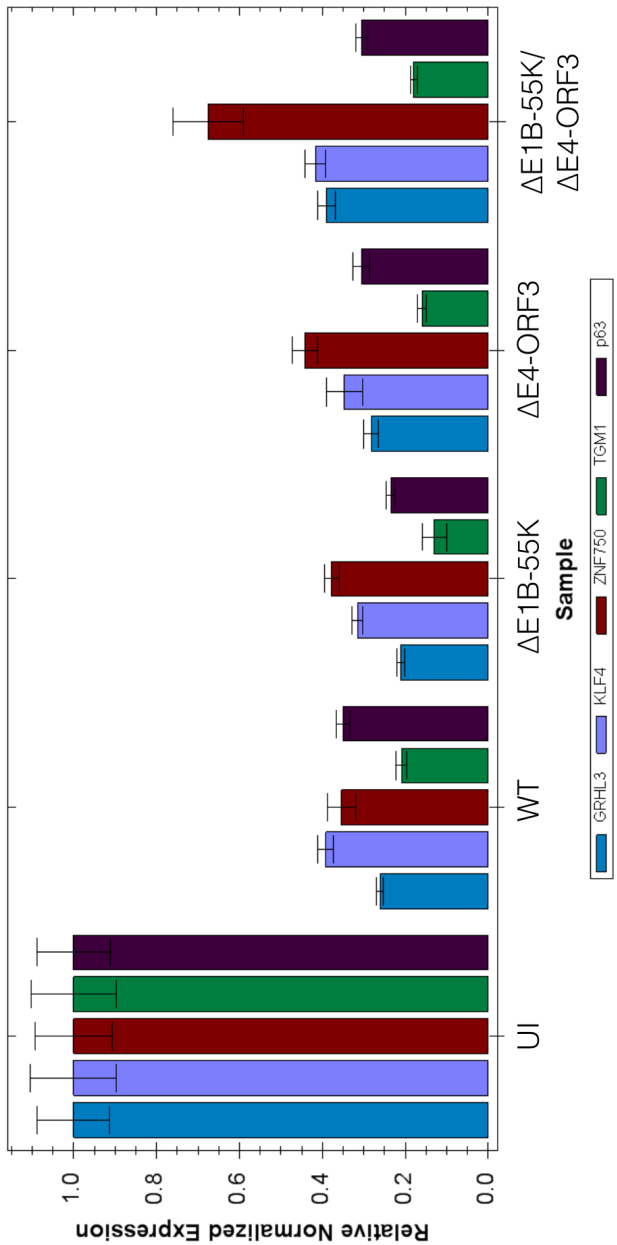

Figure 5.13 Differentiation transcription factors are downregulated during adenovirus infection. SAEC cells were infected as indicated and analyzed by RT-qPCR. GRHL3, KLF4, ZNF750, TGM1, and p63 transcripts were normalized relative to cellular 18S rRNA. Error bars indicate the Standard Error of the Mean of triplicates.

References

1. Gross L. 1951. Pathogenic properties, and "vertical" transmission of the mouse leukemia agent. Proc Soc Exp Biol Med 78:342-348.

2. Howley PM, Livingston DM. 2009. Small DNA tumor viruses: large contributors to biomedical sciences. Virology 384:256-259.

3. O'Shea CC. 2005. DNA tumor viruses -- the spies who lyse us. Curr Opin Genet Dev 15:18-26.

4. Zhang S, Huang W, Zhou X, Zhao Q, Wang Q, Jia B. 2013. Seroprevalence of neutralizing antibodies to human adenoviruses type-5 and type-26 and chimpanzee adenovirus type-68 in healthy Chinese adults. J Med Virol 85:1077-1084.

5. Greber UF, Willetts M, Webster P, Helenius A. 1993. Stepwise dismantling of adenovirus 2 during entry into cells. Cell 75:477-486.

6. Ben-Israel H, Kleinberger T. 2002. Adenovirus and cell cycle control. Front Biosci 7:d1369-1395.

7. Challberg MD, Kelly TJ, Jr. 1979. Adenovirus DNA replication in vitro. Proc Natl Acad Sci U S A 76:655-659.

8. de Jong RN, van der Vliet PC, Brenkman AB. 2003. Adenovirus DNA replication: protein priming, jumping back and the role of the DNA binding protein DBP. Curr Top Microbiol Immunol 272:187-211.

9. Wadell G. 1984. Molecular epidemiology of human adenoviruses. Curr Top Microbiol Immunol 110:191-220.

10. Wadell G, Hammarskjold ML, Winberg G, Varsanyi TM, Sundell G. 1980. Genetic variability of adenoviruses. Ann N Y Acad Sci 354:16-42.

11. Green M, Mackey JK, Wold WS, Rigden P. 1979. Thirty-one human adenovirus serotypes (Ad1-Ad31) form five groups (A-E) based upon DNA genome homologies. Virology 93:481-492.

12. Hierholzer JC. 1973. Further subgrouping of the human adenoviruses by differential hemagglutination. J Infect Dis 128:541-550.

13. Wadell G. 1979. Classification of human adenoviruses by SDS-polyacrylamide gel electrophoresis of structural polypeptides. Intervirology 11:47-57.

14. Berk AJ. 1986. Adenovirus promoters and E1A transactivation. Annu Rev Genet 20:45-79.

15. Whyte P, Buchkovich KJ, Horowitz JM, Friend SH, Raybuck M, Weinberg RA, Harlow E. 1988. Association between an oncogene and an anti-oncogene: the adenovirus E1A proteins bind to the retinoblastoma gene product. Nature 334:124-129.

16. Steegenga WT, Riteco N, Jochemsen AG, Fallaux FJ, Bos JL. 1998. The large E1B protein together with the E4orf6 protein target p53 for active degradation in adenovirus infected cells. Oncogene 16:349-357.

17. Dobbelstein M, Roth J, Kimberly WT, Levine AJ, Shenk T. 1997. Nuclear export of the E1B 55-kDa and E4 34-kDa adenoviral oncoproteins mediated by a rev-like signal sequence. Embo j 16:4276-4284.

18. Querido E, Marcellus RC, Lai A, Charbonneau R, Teodoro JG, Ketner G, Branton PE. 1997. Regulation of p53 levels by the E1B 55-kilodalton protein and E4orf6 in adenovirus-infected cells. J Virol 71:3788-3798.

19. Querido E, Blanchette P, Yan Q, Kamura T, Morrison M, Boivin D, Kaelin WG, Conaway RC, Conaway JW, Branton PE. 2001. Degradation of p53 by adenovirus E4orf6 and E1B55K proteins occurs via a novel mechanism involving a Cullin-containing complex. Genes Dev 15:3104-3117.

20. Harada JN, Shevchenko A, Shevchenko A, Pallas DC, Berk AJ. 2002. Analysis of the adenovirus E1B-55K-anchored proteome reveals its link to ubiquitination machinery. J Virol 76:9194-9206.

21. Muller S, Dobner T. 2008. The adenovirus E1B-55K oncoprotein induces SUMO modification of p53. Cell Cycle 7:754-758.

22. Pennella MA, Liu Y, Woo JL, Kim CA, Berk AJ. 2010. Adenovirus E1B 55-kilodalton protein is a p53-SUMO1 E3 ligase that represses p53 and

stimulates its nuclear export through interactions with promyelocytic leukemia nuclear bodies. J Virol 84:12210-12225.

23. Wimmer P, Blanchette P, Schreiner S, Ching W, Groitl P, Berscheminski J, Branton PE, Will H, Dobner T. 2013. Cross-talk between phosphorylation and SUMOylation regulates transforming activities of an adenoviral oncoprotein. Oncogene 32:1626-1637.

24. O'Shea CC, Johnson L, Bagus B, Choi S, Nicholas C, Shen A, Boyle L, Pandey K, Soria C, Kunich J, Shen Y, Habets G, Ginzinger D, McCormick F. 2004. Late viral RNA export, rather than p53 inactivation, determines ONYX-015 tumor selectivity. Cancer Cell 6:611-623.

25. O'Shea CC, Soria C, Bagus B, McCormick F. 2005. Heat shock phenocopies E1B-55K late functions and selectively sensitizes refractory tumor cells to ONYX-015 oncolytic viral therapy. Cancer Cell 8:61-74.

26. Ou HD, Kwiatkowski W, Deerinck TJ, Noske A, Blain KY, Land HS, Soria C, Powers CJ, May AP, Shu X, Tsien RY, Fitzpatrick JA, Long JA, Ellisman MH, Choe S, O'Shea CC. 2012. A structural basis for the assembly and functions of a viral polymer that inactivates multiple tumor suppressors. Cell 151:304-319.

27. Doucas V, Ishov AM, Romo A, Juguilon H, Weitzman MD, Evans RM, Maul GG. 1996. Adenovirus replication is coupled with the dynamic properties of the PML nuclear structure. Genes Dev 10:196-207.

28. Stracker TH, Carson CT, Weitzman MD. 2002. Adenovirus oncoproteins inactivate the Mre11-Rad50-NBS1 DNA repair complex. Nature 418:348-352.

29. Yondola MA, Hearing P. 2007. The adenovirus E4 ORF3 protein binds and reorganizes the TRIM family member transcriptional intermediary factor 1 alpha. J Virol 81:4264-4271.

30. Forrester NA, Patel RN, Speiseder T, Groitl P, Sedgwick GG, Shimwell NJ, Seed RI, Catnaigh PO, McCabe CJ, Stewart GS, Dobner T, Grand RJ, Martin A, Turnell AS. 2012. Adenovirus E4orf3 targets transcriptional intermediary factor 1gamma for proteasome-dependent degradation during infection. J Virol 86:3167-3179.

31. Evans JD, Hearing P. 2005. Relocalization of the Mre11-Rad50-Nbs1 complex by the adenovirus E4 ORF3 protein is required for viral replication. J Virol 79:6207-6215.

32. Soria C, Estermann FE, Espantman KC, O'Shea CC. 2010. Heterochromatin silencing of p53 target genes by a small viral protein. Nature 466:1076-1081.

33. Zhu L, Brangwynne CP. 2015. Nuclear bodies: the emerging biophysics of nucleoplasmic phases. Curr Opin Cell Biol 34:23-30.

34. Witte ON, Dasgupta A, Baltimore D. 1980. Abelson murine leukaemia virus protein is phosphorylated in vitro to form phosphotyrosine. Nature 283:826-831.

35. Hunter T, Sefton BM. 1980. Transforming gene product of Rous sarcoma virus phosphorylates tyrosine. Proc Natl Acad Sci U S A 77:1311-1315.

36. Reimand J, Wagih O, Bader GD. 2013. The mutational landscape of phosphorylation signaling in cancer. Sci Rep 3.

37. Skaug B, Chen ZJ. 2010. Emerging role of ISG15 in antiviral immunity. Cell 143:187-190.

38. Levy DE, Marie IJ, Durbin JE. 2011. Induction and function of type I and III interferon in response to viral infection. Curr Opin Virol 1:476-486.

39. Wimmer P, Schreiner S, Dobner T. 2012. Human pathogens and the host cell SUMOylation system. J Virol 86:642-654.

40. Everett RD, Boutell C, Hale BG. 2013. Interplay between viruses and host sumoylation pathways. Nat Rev Microbiol 11:400-411.

41. Rajsbaum R, Garcia-Sastre A. 2013. Viral evasion mechanisms of early antiviral responses involving regulation of ubiquitin pathways. Trends Microbiol 21:421-429.

42. Azuma Y, Tan SH, Cavenagh MM, Ainsztein AM, Saitoh H, Dasso M. 2001. Expression and regulation of the mammalian SUMO-1 E1 enzyme. FASEB J 15:1825-1827.

43. Talamillo A, Sanchez J, Barrio R. 2008. Functional analysis of the SUMOylation pathway in Drosophila. Biochem Soc Trans 36:868-873.

44. Golebiowski F, Matic I, Tatham MH, Cole C, Yin Y, Nakamura A, Cox J, Barton GJ, Mann M, Hay RT. 2009. System-wide changes to SUMO modifications in response to heat shock. Sci Signal 2:ra24.

45. Morris JR. 2010. SUMO in the mammalian response to DNA damage. Biochem Soc Trans 38:92-97.

46. Gareau JR, Lima CD. 2010. The SUMO pathway: emerging mechanisms that shape specificity, conjugation and recognition. Nat Rev Mol Cell Biol 11:861-871.

47. Saitoh H, Hinchey J. 2000. Functional heterogeneity of small ubiquitin-related protein modifiers SUMO-1 versus SUMO-2/3. J Biol Chem 275:6252-6258.

48. Bernardi R, Pandolfi PP. 2007. Structure, dynamics and functions of promyelocytic leukaemia nuclear bodies. Nat Rev Mol Cell Biol 8:1006-1016.

49. Ishov AM, Sotnikov AG, Negorev D, Vladimirova OV, Neff N, Kamitani T, Yeh ET, Strauss JF, 3rd, Maul GG. 1999. PML is critical for ND10 formation and recruits the PML-interacting protein daxx to this nuclear structure when modified by SUMO-1. J Cell Biol 147:221-234.

50. Zhong S, Muller S, Ronchetti S, Freemont PS, Dejean A, Pandolfi PP. 2000. Role of SUMO-1-modified PML in nuclear body formation. Blood 95:2748-2752.

51. Shen TH, Lin HK, Scaglioni PP, Yung TM, Pandolfi PP. 2006. The mechanisms of PML-nuclear body formation. Mol Cell 24:331-339.

52. Dundr M, Misteli T. 2010. Biogenesis of nuclear bodies. Cold Spring Harb Perspect Biol 2:a000711.

53. Shuai K, Liu B. 2005. Regulation of gene-activation pathways by PIAS proteins in the immune system. Nat Rev Immunol 5:593-605.

54. Mattoscio D, Segre CV, Chiocca S. 2013. Viral manipulation of cellular protein conjugation pathways: The SUMO lesson. World J Virol 2:79-90.

55. Novoa RR, Calderita G, Arranz R, Fontana J, Granzow H, Risco C. 2005. Virus factories: associations of cell organelles for viral replication and morphogenesis. Biol Cell 97:147-172.

56. Schmid M, Speiseder T, Dobner T, Gonzalez RA. 2014. DNA virus replication compartments. J Virol 88:1404-1420.

57. Hoeben RC, Uil TG. 2013. Adenovirus DNA replication. Cold Spring Harb Perspect Biol 5:a013003.

58. Boyer GS, Leuchtenberger C, Ginsberg HS. 1957. Cytological and cytochemical studies of HeLa cells infected with adeno-viruses. J Exp Med 105:195-216.

59. Sohn SY, Hearing P. 2012. Adenovirus regulates sumoylation of Mre11-Rad50-Nbs1 components through a paralog-specific mechanism. J Virol 86:9656-9665.

60. Sohn SY, R GB, Hearing P. 2014. Proteomic analysis of ubiquitin-like post-translational modifications induced by the adenovirus E4-ORF3 protein. J Virol doi:10.1128/JVI.02892-14.

61. O'Shea GASaCC. 2015. MRE11 and ATM activate distinct signaling responses to defend against DNA viruses versus DNA breaks. Cell.

62. Hickson I, Zhao Y, Richardson CJ, Green SJ, Martin NM, Orr AI, Reaper PM, Jackson SP, Curtin NJ, Smith GC. 2004. Identification and characterization of a novel and specific inhibitor of the ataxia-telangiectasia mutated kinase ATM. Cancer Res 64:9152-9159.

63. Shepard RN, Ornelles DA. 2004. Diverse roles for E4orf3 at late times of infection revealed in an E1B 55-kilodalton protein mutant background. J Virol 78:9924-9935.

64. Lakdawala SS, Schwartz RA, Ferenchak K, Carson CT, McSharry BP, Wilkinson GW, Weitzman MD. 2008. Differential Requirements of the C Terminus of Nbs1 in Suppressing Adenovirus DNA Replication and Promoting Concatemer Formation. Journal of Virology 82:8362-8372.

65. Gautam D, Bridge E. 2013. The kinase activity of ataxia-telangiectasia mutated interferes with adenovirus E4 mutant DNA replication. J Virol 87:8687-8696.

66. Watts FZ. 2013. Starting and stopping SUMOylation. What regulates the regulator? Chromosoma 122:451-463.

67. Sang J, Yang K, Sun Y, Han Y, Cang H, Chen Y, Shi G, Wang K, Zhou J, Wang X, Yi J. 2011. SUMO2 and SUMO3 transcription is differentially regulated by oxidative stress in an Sp1-dependent manner. Biochem J 435:489-498.

68. Castoralova M, Ruml T, Knejzlik Z. 2012. Using dot blot with immunochemical detection to evaluate global changes in SUMO-2/3 conjugation. BioTechniques doi:10.2144/000113925.

69. Boggio R, Colombo R, Hay RT, Draetta GF, Chiocca S. 2004. A mechanism for inhibiting the SUMO pathway. Mol Cell 16:549-561.

70. Jentsch S, Psakhye I. 2013. Control of nuclear activities by substrate-selective and protein-group SUMOylation. Annu Rev Genet 47:167-186.

71. Schmidt D, Muller S. 2003. PIAS/SUMO: new partners in transcriptional regulation. Cell Mol Life Sci 60:2561-2574.

72. Evans JD, Hearing P. 2003. Distinct roles of the Adenovirus E4 ORF3 protein in viral DNA replication and inhibition of genome concatenation. J Virol 77:5295-5304.

73. Hoppe A, Beech SJ, Dimmock J, Leppard KN. 2006. Interaction of the adenovirus type 5 E4 Orf3 protein with promyelocytic leukemia protein isoform II is required for ND10 disruption. J Virol 80:3042-3049.

74. Stracker TH, Lee DV, Carson CT, Araujo FD, Ornelles DA, Weitzman MD. 2005. Serotype-specific reorganization of the Mre11 complex by adenoviral E4orf3 proteins. J Virol 79:6664-6673.

75. Forrester NA, Sedgwick GG, Thomas A, Blackford AN, Speiseder T, Dobner T, Byrd PJ, Stewart GS, Turnell AS, Grand RJ. 2011. Serotype-specific inactivation of the cellular DNA damage response during adenovirus infection. J Virol 85:2201-2211.

76. Ullman AJ, Reich NC, Hearing P. 2007. Adenovirus E4 ORF3 protein inhibits the interferon-mediated antiviral response. J Virol 81:4744-4752.

77. Ullman AJ, Hearing P. 2008. Cellular proteins PML and Daxx mediate an innate antiviral defense antagonized by the adenovirus E4 ORF3 protein. J Virol 82:7325-7335.

78. Chahal JS, Qi J, Flint SJ. 2012. The human adenovirus type 5 E1B 55 kDa protein obstructs inhibition of viral replication by type I interferon in normal human cells. PLoS Pathog 8:e1002853.

79. Pombo A, Ferreira J, Bridge E, Carmo-Fonseca M. 1994. Adenovirus replication and transcription sites are spatially separated in the nucleus of infected cells. Embo j 13:5075-5085.

80. Nordqvist K, Ohman K, Akusjarvi G. 1994. Human adenovirus encodes two proteins which have opposite effects on accumulation of alternatively spliced mRNAs. Mol Cell Biol 14:437-445.

81. Gill G. 2003. Post-translational modification by the small ubiquitin-related modifier SUMO has big effects on transcription factor activity. Curr Opin Genet Dev 13:108-113.

82. Rytinki MM, Kaikkonen S, Pehkonen P, Jaaskelainen T, Palvimo JJ. 2009. PIAS proteins: pleiotropic interactors associated with SUMO. Cell Mol Life Sci 66:3029-3041.

83. Manders EMM, Verbeek FJ, Aten JA. 1993. Measurement of co-localization of objects in dual-colour confocal images. Journal of Microscopy 169:375-382.

84. Johnson L, Shen A, Boyle L, Kunich J, Pandey K, Lemmon M, Hermiston T, Giedlin M, McCormick F, Fattaey A. 2002. Selectively replicating adenoviruses targeting deregulated E2F activity are potent, systemic antitumor agents. Cancer Cell 1:325-337.

85. Livak KJ, Schmittgen TD. 2001. Analysis of relative gene expression data using real-time quantitative PCR and the 2(-Delta Delta C(T)) Method. Methods 25:402-408.

86. Felsenfeld G, Dekker J. 2012. Genome architecture and expression. Curr Opin Genet Dev 22:59-61.

87. Sleeman JE, Trinkle-Mulcahy L. 2014. Nuclear bodies: new insights into assembly/dynamics and disease relevance. Curr Opin Cell Biol 28:76-83.

88. Kang H, Kim ET, Lee HR, Park JJ, Go YY, Choi CY, Ahn JH. 2006. Inhibition of SUMO-independent PML oligomerization by the human cytomegalovirus IE1 protein. J Gen Virol 87:2181-2190.

89. Cimarosti H, Henley JM. 2008. Investigating the mechanisms underlying neuronal death in ischemia using in vitro oxygen-glucose deprivation: potential involvement of protein SUMOylation. Neuroscientist 14:626-636.

90. Guo C, Henley JM. 2014. Wrestling with stress: roles of protein SUMOylation and deSUMOylation in cell stress response. IUBMB Life 66:71-77.

91. Wimmer P, Schreiner S. 2015. Viral Mimicry to Usurp Ubiquitin and SUMO Host Pathways. Viruses 7:4854-4877.

92. Higginbotham JM, O'Shea CC. 2015. Adenovirus E4-ORF3 targets PIAS3 and together with E1B-55K remodels SUMO interactions in the nucleus and at virus genome replication domains. J Virol doi:10.1128/jvi.01091-15.

93. Hattersley N, Shen L, Jaffray EG, Hay RT. 2011. The SUMO protease SENP6 is a direct regulator of PML nuclear bodies. Mol Biol Cell 22:78-90.

94. Hickey CM, Wilson NR, Hochstrasser M. 2012. Function and regulation of SUMO proteases. Nat Rev Mol Cell Biol 13:755-766.

95. Jiang M, Chiu SY, Hsu W. 2011. SUMO-specific protease 2 in Mdm2-mediated regulation of p53. Cell Death Differ 18:1005-1015.

96. van der Vliet PC, Levine AJ. 1973. DNA-binding proteins specific for cells infected by adenovirus. Nat New Biol 246:170-174.

97. Fowlkes DM, Lord ST, Linne T, Pettersson U, Philipson L. 1979. Interaction between the adenovirus DNA-binding protein and double-stranded DNA. J Mol Biol 132:163-180.

98. Cleghon VG, Klessig DF. 1986. Association of the adenovirus DNA-binding protein with RNA both in vitro and in vivo. Proc Natl Acad Sci U S A 83:8947-8951.

99. Rubenstein FE, Ginsberg HS. 1974. Transformation characteristics of temperature-sensitive mutants of type 12 adenovirus. Intervirology 3:170-174.

100. Nicolas JC, Sarnow P, Girard M, Levine AJ. 1983. Host range temperature-conditional mutants in the adenovirus DNA binding protein are defective in the assembly of infectious virus. Virology 126:228-239.

101. Kruijer W, van Schaik FM, Sussenbach JS. 1981. Structure and organization of the gene coding for the DNA binding protein of adenovirus type 5. Nucleic Acids Res 9:4439-4457.

102. Cleghon V, Piderit A, Brough DE, Klessig DF. 1993. Phosphorylation of the adenovirus DNA-binding protein and epitope mapping of monoclonal antibodies against it. Virology 197:564-575.

103. Morin N, Delsert C, Klessig DF. 1989. Mutations that affect phosphorylation of the adenovirus DNA-binding protein alter its ability to enhance its own synthesis. J Virol 63:5228-5237.

104. Kitchingman GR. 1985. Sequence of the DNA-binding protein of a human subgroup E adenovirus (type 4): comparisons with subgroup A (type 12), subgroup B (type 7), and subgroup C (type 5). Virology 146:90-101.

105. Ariga H, Klein H, Levine AJ, Horwitz MS. 1980. A cleavage product of the adenovirus DNA binding protein is active in DNA replication in vitro. Virology 101:307-310.

106. Tucker PA, Tsernoglou D, Tucker AD, Coenjaerts FE, Leenders H, van der Vliet PC. 1994. Crystal structure of the adenovirus DNA binding protein reveals a hook-on model for cooperative DNA binding. Embo j 13:2994-3002.

107. Zhao Q, Xie Y, Zheng Y, Jiang S, Liu W, Mu W, Liu Z, Zhao Y, Xue Y, Ren J. 2014. GPS-SUMO: a tool for the prediction of sumoylation sites and SUMO-interaction motifs. Nucleic Acids Research 42:W325-W330.

108. Morin N, Delsert C, Klessig DF. 1989. Nuclear localization of the adenovirus DNA-binding protein: requirement for two signals and complementation during viral infection. Molecular and Cellular Biology 9:4372-4380.

109. Yang SH, Jaffray E, Hay RT, Sharrocks AD. 2003. Dynamic interplay of the SUMO and ERK pathways in regulating Elk-1 transcriptional activity. Mol Cell 12:63-74.

110. Simon J, Chiang A, Bender W. 1992. Ten different Polycomb group genes are required for spatial control of the abdA and AbdB homeotic products. Development 114:493-505.

111. Simon JA, Kingston RE. 2009. Mechanisms of polycomb gene silencing: knowns and unknowns. Nat Rev Mol Cell Biol 10:697-708.

112. Wang H, Wang L, Erdjument-Bromage H, Vidal M, Tempst P, Jones RS, Zhang Y. 2004. Role of histone H2A ubiquitination in Polycomb silencing. Nature 431:873-878.

113. Endoh M, Endo TA, Endoh T, Isono K, Sharif J, Ohara O, Toyoda T, Ito T, Eskeland R, Bickmore WA, Vidal M, Bernstein BE, Koseki H. 2012. Histone H2A mono-ubiquitination is a crucial step to mediate PRC1-dependent repression of developmental genes to maintain ES cell identity. PLoS Genet 8:e1002774.

114. Gil J, O'Loghlen A. 2014. PRC1 complex diversity: where is it taking us? Trends in Cell Biology 24:632-641.

115. Eissenberg JC, Elgin SC. 2014. HP1a: a structural chromosomal protein regulating transcription. Trends Genet 30:103-110.

116. Senthilkumar R, Mishra RK. 2009. Novel motifs distinguish multiple homologues of Polycomb in vertebrates: expansion and diversification of the epigenetic toolkit. BMC Genomics 10:549.

117. Muller J, Gaunt S, Lawrence PA. 1995. Function of the Polycomb protein is conserved in mice and flies. Development 121:2847-2852.

118. Buchwald G, van der Stoop P, Weichenrieder O, Perrakis A, van Lohuizen M, Sixma TK. 2006. Structure and E3-ligase activity of the Ring-Ring complex of polycomb proteins Bmi1 and Ring1b. Embo j 25:2465-2474.

119. Wang H, Wang L, Erdjument-Bromage H, Vidal M, Tempst P, Jones RS, Zhang Y. 2004. Role of histone H2A ubiquitination in Polycomb silencing. Nature 431:873-878.

120. Gustafsson MG. 2000. Surpassing the lateral resolution limit by a factor of two using structured illumination microscopy. J Microsc 198:82-87.

121. Di Croce L, Helin K. 2013. Transcriptional regulation by Polycomb group proteins. Nat Struct Mol Biol 20:1147-1155.

122. Schwartz YB, Pirrotta V. 2013. A new world of Polycombs: Unexpected partnerships and emerging functions. Nature Reviews Genetics 14:853-864.

123. Mlacki M, Darido C, Jane SM, Wilanowski T. 2014. Loss of Grainy head-like 1 is associated with disruption of the epidermal barrier and squamous cell carcinoma of the skin. PLoS One 9:e89247.

124. Segre JA, Bauer C, Fuchs E. 1999. Klf4 is a transcription factor required for establishing the barrier function of the skin. Nat Genet 22:356-360.

125. Sen GL, Boxer LD, Webster DE, Bussat RT, Qu K, Zarnegar BJ, Johnston D, Siprashvili Z, Khavari PA. 2012. ZNF750 is a p63 target gene that induces KLF4 to drive terminal epidermal differentiation. Dev Cell 22:669-677.

126. Wang R, Ilangovan U, Robinson AK, Schirf V, Schwarz PM, Lafer EM, Demeler B, Hinck AP, Kim CA. 2008. Structural Transitions of the RING1B C-Terminal Region upon Binding the Polycomb cbox Domain†. Biochemistry 47:8007-8015.

127. Dunker AK, Cortese MS, Romero P, Iakoucheva LM, Uversky VN. 2005. Flexible nets. The roles of intrinsic disorder in protein interaction networks. Febs j 272:5129-5148.

128. Kagey MH, Melhuish TA, Wotton D. 2003. The polycomb protein Pc2 is a SUMO E3. Cell 113:127-137.

129. Dou H, Huang C, Van Nguyen T, Lu LS, Yeh ET. 2011. SUMOylation and de-SUMOylation in response to DNA damage. FEBS Lett 585:2891-2896.

130. Klauke K, Radulović V, Broekhuis M, Weersing E, Zwart E, Olthof S, Ritsema M, Bruggeman S, Wu X, Helin K, Bystrykh L, de Haan G. 2013. Polycomb Cbx family members mediate the balance between haematopoietic stem cell self-renewal and differentiation. Nat Cell Biol 15:353-362.